Binghamton University
The Open Repository @ Binghamton (The ORB)

Graduate Dissertations and Theses | Dissertations, Theses and Capstones

1969

# Petrological and geochemical study of spilites and associated dike rocks from the Virgin Island core (Caribbean Island arc)

Roger Hékinian

Follow this and additional works at: https://orb.binghamton.edu/dissertation_and_theses

## Recommended Citation

Hékinian, Roger, "Petrological and geochemical study of spilites and associated dike rocks from the Virgin Island core (Caribbean Island arc)" (1969). *Graduate Dissertations and Theses*. 145.
https://orb.binghamton.edu/dissertation_and_theses/145

This Dissertation is brought to you for free and open access by the Dissertations, Theses and Capstones at The Open Repository @ Binghamton (The ORB). It has been accepted for inclusion in Graduate Dissertations and Theses by an authorized administrator of The Open Repository @ Binghamton (The ORB). For more information, please contact ORB@binghamton.edu.

* * *

This is an authorized facsimile and was produced by microfilm-xerography in 1971 by University Microfilms, A Xerox Company, Ann Arbor, Michigan, U.S.A.

* * *

70-11,471

HEKINIAN, Roger, 1935-
PETROLOGICAL AND GEOCHEMICAL STUDY OF SPILITES AND ASSOCIATED DIKE ROCKS FROM THE VIRGIN ISLAND CORE (CARIBBEAN ISLAND ARC).

State University of New York at Binghamton, Ph.D., 1969
Geology

University Microfilms, Inc., Ann Arbor, Michigan

© 1971

ROGER HEKINIAN

ALL RIGHTS RESERVED

# PETROLOGICAL AND GEOCHEMICAL STUDY OF SPILITES AND ASSOCIATED DIKE ROCKS FROM THE VIRGIN ISLAND CORE (CARIBBEAN ISLAND ARC)

BY

ROGER HEKINIAN

Submitted in partial fulfillment of the requirements
for the degree of Doctor of Philosophy
in State University of New York
at Binghamton
1969

AS
36
N55
no.2
cop.2




# PETROLOGICAL AND GEOCHEMICAL STUDY OF SPILITES AND ASSOCIATED DIKE ROCKS FROM THE VIRGIN ISLAND CORE (CARIBBEAN ISLAND ARC)

BY

ROGER HEKINIAN

Approved as to style and content by:

Thomas W. Donnelly
(Chairman of Committee)

Herman E. Rogerson
(Chairman of Dept.)

Marc W. Bodine, Jr.
(Member)

Reynold E. Stott
(Member)

(Member)

Nikolaas J. van der Merwe
(Member)

(Member)

May 1969
(Month) (Year)

343562

## ACKNOWLEDGMENT

This study was supported by the National Science Foundation under Contract G-A-588 awarded to Dr. H. H. Hess and Dr. T. W. Donnelly.

The writer is indebted to Dr. T. W. Donnelly who suggested this study and offered helpful criticism and advice. The writer is also grateful for the generous help given by Dr. R. E. Smith during the final stage of this study. Dr. H. E. Roberson and Dr. M. W. Bodine, Jr. kindly read the manuscript and made valuable suggestions for its improvement. The field work in the drilling areas fulfilled by G. Hinaman under the supervision of Dr. T. W. Donnelly is also gratefully acknowledged.

# CONTENTS

# PLATES

# FIGURES

# TABLES

# GLOSSARY

Albite-diabase - Coarse grained rock containing albite and having a diabasic texture.

Amphibole porphyry - Group name for porphyry dike rocks with phenocrysts of hornblende and generally containing feldspar.

Andesine-diabase - Coarse grained rock containing andesine-oligoclase-plagioclase with diabasic texture.

Biotite - Mixed-layer biotite.

Brecciated (zone, rock) - It means here a rock with a sheared textural feature, abundantly veined and with occasional angular fragments of other rock types.

FeO - Total iron content calculated from chemical analyses as ferrous oxide.

Green matrix - Chlorite rich green colored zone surrounding the dark patches included in the spilite flow.

Local - This term applies here to the distribution of elements and minerals within a limited distance from their original source, on the order of millimeters.

Magmatic or fluid solution - Aqueous fluid rich in volatiles concentrated into the last stage of magmatic crystallization and inherent in the parental magma itself.

Non-patchy - Spilite rocks containing diffuse patches or none.

Patchy - Spilite containing patches, darker in appearance than their immediate surroundings, with mineral associations characteristic of the spilite. The shape of the patches may be irregular, rounded, ellipsoidal, etc. with an average diameter of about 2 cm.

Spilite - Albitized extrusive mafic rock, containing epidote, calcite, plagioclase, and chlorite. Together with varying amounts of pyroxene and actinolite.

# A B S T R A C T

A continuous section of extrusive and intrusive rocks have been recovered through a drill core of about 2430 feet that was taken at St. John, U. S. Virgin Islands. The present study is confined to the upper 1180 feet and comprises a cummulative total of 950 feet of albitized mafic extrusive rocks (spilite). This portion of the core is also intruded by four dikes: two amphibole porphyryes (129-134 and 732-742 feet); an albite-diabase (177-226 feet) and an andesine-diabase (847-1003 feet).

The spilite is a fine-grained rock with pilotaxitic and intersertal textural features. Throughout the flow, the major mineralogical assemblages consist of partly albitized Ca-plagioclase, chlorite, epidote and quartz. The upper part of this flow shows a concentration of dark colored and fine-grained patches set in a green, fine-grained, and abundantly recrystallized matrix. This green matrix is characterized by glassy textural features and lower temperature assemblages (epidote, quartz, chlorite) than the dark patchy material. The patchiness decreases with depth and below 650 feet disappears, being replaced by a homogeneous, fine-grained spilite. Below the non-patchy spilite, there is a sheared and recrystallized spilitic zone which contains epidote, quartz, chlorite and breccia fragments.

After extrusion of the spilite flows onto the surface, the upper part of the core solidified faster than the underlying non-patchy zone. The dark patches represent centers of crystallization which solidified

before the surrounding green matrix. Once the lava flow solidified, it was intruded by several dikes and a later faulting gave rise to the bottom brecciated zone.

Alkali migrations occur throughout the rocks studied. The $K_2O$ content in the upper part of the spilite flow is higher and the $Na_2O$ content lower than the bottom of the flow. Local variations of alkalis show also that the dark patches are higher in $Na_2O$ than the surrounding green matrices. The alkali migration throughout the different lithological units of the core could have been caused by both magmatic and metamorphic processes. During the last stage of crystallization, hydrothermal solutions might have concentrated some of the $K_2O$ in the green matrix and the $Na_2O$ in the adjacent dark patches. Burial metamorphism also affected the core and caused the disappearance of prehnite and pumpellyite with depth.

The parental magma of the spilite is believed to be derived from the partial melting of amphibolite tapped in the lower Crust or upper Mantle (extrapolated from experimental data) beneath the Virgin Islands.

# INTRODUCTION

## Drilling Project

A deep drilling project directed by T. W. Donnelly was undertaken to penetrate and sample the Water Island Formation which is the oldest known basement formation in the Eastern Greater Antilles. Ram Head, St. John (U. S. Virgin Islands) was chosen as the drilling site as this promontory represents the lowest stratigraphic level of the formation.

The hole (completed February, 1967) penetrated 2345 feet of spilites and kerotophyres of the Water Island Formation, which is believed to be Mid-Cretaceous or older. The present study consists of a petrological and geochemical investigation of the upper half of the core (1180 feet) which is composed predominantly of spilites with subordinate minor intrusives of diabasic and amphibole porphyry rocks.

## Theories on the Origin of Spilites

Spilites and associated rocks are very abundant in the lower stratigraphic levels of the Virgin Islands. The survey of the literature on spilites shows environments with different associations and conditions which gave rise to the rocks called spilite, a name coined by Brongniart (1827).

Spilites are considered to be fine-grained mafic rocks with albite as the chief feldspar also with epidote chlorite, and calcite minerals.

Although most investigators in the field of spilites usually agree that these rocks are of igneous derivation, there is still controversy regarding the processes by which these rocks acquired their present appearance. Several theories have been postulated for the origin of spilites. Although these theories will be discussed in a later chapter (Petrogenesis), they may be summarized as follows: 1) magmatic theory, 2) sea-water assimilation theory, 3) burial metamorphic theory.

1). The theory of magmatic origin deals with the production of low temperature hydrous mineralogy (albite-chlorite-epidote) together with the redistribution of the principal chemical compounds due to deuteric alteration occurring simultaneously with consolidation (Wilshire, 1959; Hentschel, 1961; Vuagnat, 1946; Burri and Niggli, 1945). Another aspect of this theory involves autometasomatism (Van Overreem, 1948; Amstutz, 1954; Donnelly, 1959, 1960, 1963; Routhier, 1963).

2). The sea-water alteration theory postulates the reaction with sea water or wet sediment at the time of extrusion (Park, 1946; Gjelsvik, 1958; Szadeczky-Kardos, 1958; Rittman, 1958).

3). Recent workers have shown that burial-metamorphism of basic lavas results in rocks of spilitic mineralogy (Coombs et. al., 1959; Vallance, 1960 in part; Smith, 1968).

## Geological Setting

The Island of St. John is part of the U. S. Virgin Islands located

between the Caribbean Sea and the Atlantic Ocean, longitude 64°44' and latitude 18°20' North (Fig. 1). No evidence from field studies has yet supported the existence of a sialic layer beneath the Caribbean Island Arc System. Seismic refractions survey (Officer et. al., 1959) and gravity observations (Shurbert and Worzel, 1956; Talwani et. al., 1959) indicate that the Crust under the Caribbean Sea (Venezuela Basin) is very similar to the Atlantic crust. The Caribbean area existed during the whole of the Tertiary period more or less with its present outlines (Hess, 1966). Most of the major islands in the Caribbean, lesser Antilles, Dominican Republic, Virgin Islands and Puerto Rico, were centers of basic and intermediate (andesite) types of volcanism (Tomblin, in press; Bowin, 1966; Donnelly, 1966; Berryhill, 1960).

Cleve (1881) studied the geology of the Virgin Islands. However, the only detailed mapping and petrographic work in the Virgin Islands was made by Donnelly (1959, 1962, 1963, 1966). The lithology of St. John varies from north (Mary Point) to south (Ram Head) in five units. (1) Dioritic rocks from the Virgin Island batholith contain 65% tonalite, 25% granodiorite, and 10% gabbro (Longshore, 1965). (2) Tuffaceous wacke (called the Tutu Formation) with a thickness of 6000 feet. This formation consists of weathered fragments and plagioclase grains set in a matrix of chloritic material and calcite cement (Donnelly, 1966). The Tutu Formation also consists of limestone and some submarine mudflows. This limestone shows plastic deformation and contains fossilized fauna of the middle Cretaceous period (Donnelly, 1966).

Figure 1. Caribbean Island Arc System showing the island of St. John (arrow). The location of the drill core on St. John is shown in the upper right inset with the general geology of the island.

■ - Virgin Island Batholith

Kt - Volcanic wacke (Tutu Formation)

Kob - Thin bedded siliceous limestone (Outer Brass Ls.)

Kl - Augite andesite volcanic breccia (Lousenhoj Fm.)

Wl - Spilite and Keratophyre flows (Water Island Fm.)

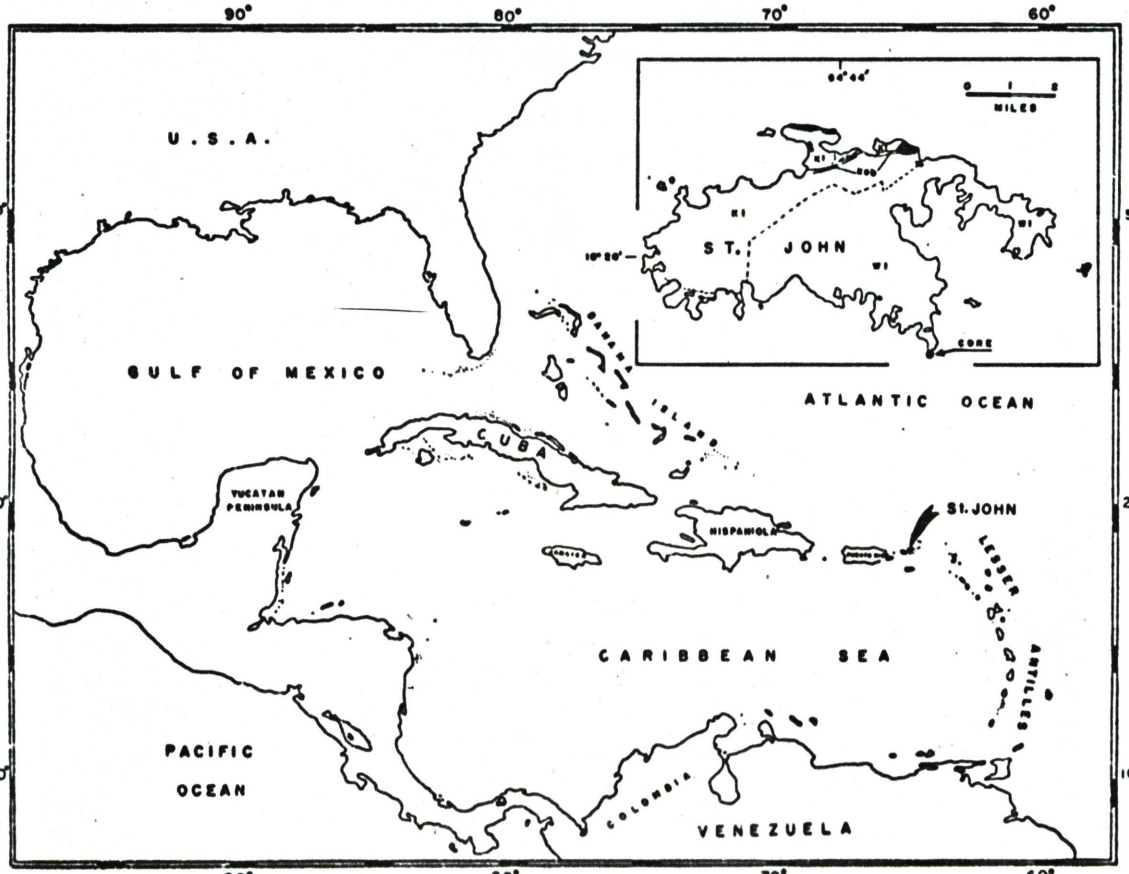
90°
80°
70°
60°
30°
20°
10°
U.S.A.
GULF OF MEXICO
YUCATAN PENINSULA
CUBA
HISPANIOLA
ATLANTIC OCEAN
ST. JOHN
LESSER ANTILLES
CARIBBEAN SEA
PACIFIC OCEAN
COLOMBIA
VENEZUELA
ST. JOHN
MILES
CORE

(3) A thin bedded siliceous limestone, Outer Brass Limestone, 200-600 feet thick with Globigerina and sponge spicules indicating an off-shore deposit (Donnelly, 1966). (4) Louisenhoj Formation, (7000 feet thick), which is composed of augite-andesite volcanic breccias and tuff with minor conglomerates. (5) Spilite and keratophyre flows with minor radiolarites intruded by dikes, set unconformably below the Louisenhoj Formation. The spilite-keratophyre association is called the Water Island Formation and has a total thickness of about 15,000 feet (Donnelly, 1966). Spilite, generally in the form of flows, comprise approximately one-fifth of the thickness of the Water Island Formation. Pillow structure is rare, but was found within a spilite flow at Elk Bay and Lagoon Point, St. John (Donnelly, 1966). Flow boundaries are commonly irregular and no chilled margins or baked zones were observed between each flow. The keratophyres associated with the spilites comprise about four-fifths of the Water Island Formation. This type of rock occurs usually as flows, but keratophyre intrusives are also present. One thick keratophyre flow, on Ram Head (St. John, near the core location), shows evidence of vertical differentiation (Donnelly, 1966). However, keratophyres are not studied here since this type of rock is concentrated in the lower half of the core. Donnelly (1966) in his study of the geology of the Virgin Island noticed also the appearance of pumpellyite in the Louisenhoj Formation, mostly pyroclastic, and the Water Island Formation.

The whole sequence, including the spilite flow, in the northern part of St. John, has undergone some contact metamorphism in the albite-

epidote-hornfels facies (Longshore, 1965). The commonest mineralogical association of these spilites is plagioclase ($An_0$-$An_{12}$)-pyroxene (relic)-chlorite-actinolite with minor amounts of biotite, calcite, quartz, epidote, and magnetite. Veinlets and veins and amygdules filled with epidote, quartz, chlorite, calcite and prehnite, or a combination of these minerals, were observed (Longshore, 1965). Metasomatic processes, accompanying the cooling of the Virgin Island Batholith, have locally altered the original composition of the wall rocks surrounding the Virgin Island batholith. However, most of the chemical exchange was confined within the hornblende-hornfels facies, which extended approximately one to one-and-one-half kilometers from the intrusive contacts (Longshore, 1965). The batholith was relatively enriched in sodium and depleted in potassium, while magnesium and calcium were gained by the wall rocks.

Donnelly (1966) suggested that the spilite-keratophyre association of the Water Island formation was extruded on a relatively flat sea bottom. His conclusion of flatness of surface of extrusion was based on the lack of terrigenous sediment, the paucity of slump structure in most tuffaceous units and the absence of bedding disturbances near the top of the Water Island Formation. There are evenly layered pyroclastic keratophyre beds (Donnelly, 1966).

## Present Work

The present study is primarily concerned with spilites, consisting of relatively low temperature mineral assemblages such as albite (low

temperature albite in spilite, stable below 700°C, Battey, 1956) pyroxene (variable temperature range) and chlorite. Minor intrusive rocks which also show low temperature associations intruded part of the core and are also studied. The adjustment of mafic flows to low temperature conditions and abundant water content may occur, as was suggested in previous studies, in any of several contrasted environments, such as late magmatic (Wilshire, 1959), hydrothermal (Burri and Niggli, 1945; Vuagnat, 1946; and Amstutz, 1958) and low-grade metamorphic (Coombs et. al., 1959).

In order to perceive a clearer view on the problem of the origin of the spilites, it is important to take into consideration all the advantages that could arise from the study of a continuous and unweathered lithological unit of such rocks. The core from the Virgin Island represents a unique continuous section through the spilite and associated rocks of this area of the Caribbean Island Arc. The importance of having an uninterrupted assemblage of rocks enables a better correlation between different zones within a single flow of spilites. The general stratigraphic section of the core consists mainly of several spilite flows and keratophyres (Fig. 2). The first half of the core shows about 950 feet of spilitic rocks intruded by dikes with chilled margins. The second half (not included in this study) is also composed of spilites, but they are inter-layered with keratophyres (Fig. 2).

The main purpose of the present study of the Virgin Island core is to attempt to determine if the spilites and associated rocks owe

Figure 2. General stratigraphy of the entire drill core.

S - Spilite

DK - Dike rocks

BS - Brecciated spilite rocks

K - Keratophyre

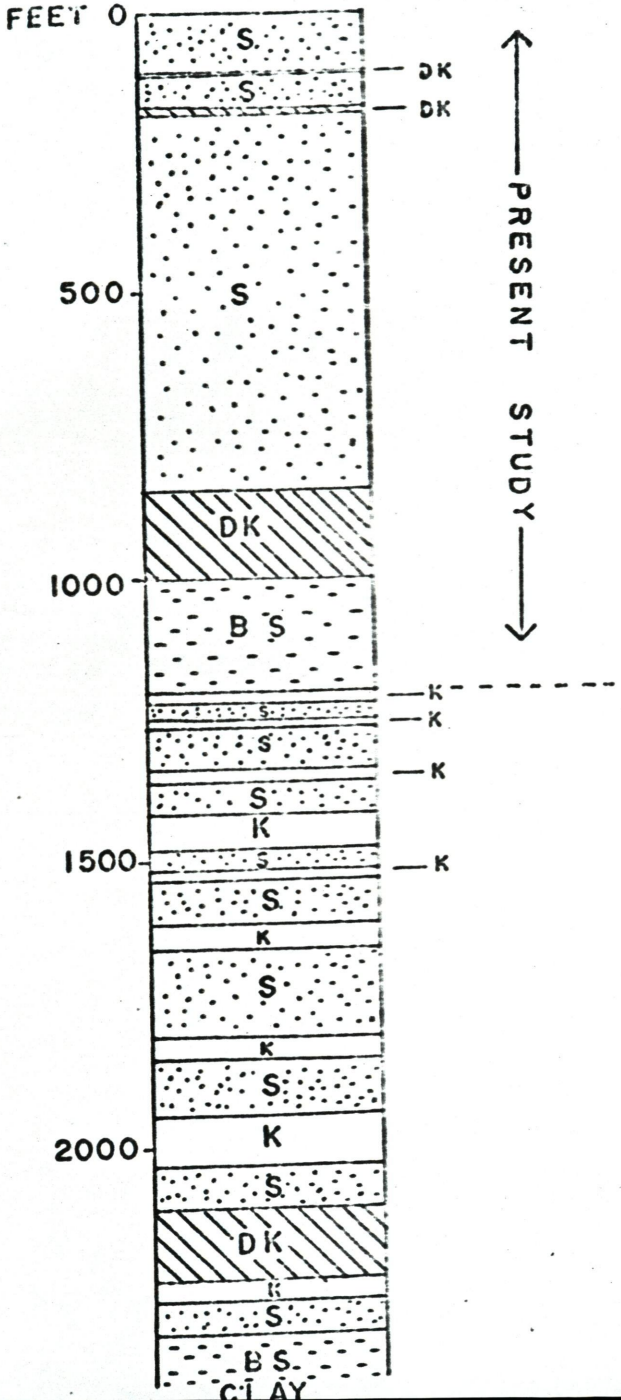
FEET 0
500
1000
1500
2000
S
DK
S
DK
S
DK
B S
K
S
K
S
K
S
K
S
K
S
K
S
K
S
K
S
K
S
K
S
DK
K
S
B S
CLAY
PRESENT STUDY

some of their present character to magmatic processes and others to metamorphic processes. Another aim of this study is to try to distinguish between the different processes such as metamorphism and autometasomatism which might have masked the original composition of the rocks from the core. The conclusions reached from this study primarily apply to the spilites of the Virgin Islands. However, it is hoped that this work will also help clarify a few points on spilites in general.

In order to reach the proposed goal, mineralogical and petrological investigations were made in the following order:

1. Detailed mineralogical and petrographical studies were made to recognize the minerals and the textural variations within the spilite flow and also among the different rock types encountered in the core.
2. Chemical analyses of major elements were made to show any systematic variation with depth and also between patch and matrix.

Certain assumptions were made before the study of this core began. These assumptions are as follows:

1. The core is a representative sample of a larger flow unit extending laterally.
2. Surface study in the area of the drilling site indicates intensive weathering (Donnelly, personnal communication).

As the first 20 feet of the core is weathered, it is assumed to be similar in mineralogy and chemistry to the rock sequence immediately below.

The age of the core was inferred from previous work (Donnelly, 1966) to be lower Cretaceous or older. Near the top of the core small reddish patches of microcrystalline hematite rich aggregates occur, and these were examined for traces of fossils; however, no fossils were found.

## Laboratory Techniques

This work consists exclusively of laboratory investigation, including thin section and X-ray diffraction study and chemical studies. Pyroxene compositional estimates were made also by determining indices of refraction on crushed samples and 2V measurements according to the method of Hess (1949). On the basis of X-ray data ($K_{\alpha}$ Fe radiation), compositions of eight pyroxene samples were also estimated by using Kuno and Hess (1953, 1955) curves between the relative d - spacings of certain reflections and chemical compositions of the clinopyroxene. The composition of chlorite was estimated in twenty-six samples taken from various depths in the core and using the methods of Schoen (1962) and Brindley and Gillery (1956) to determine the chemical compositions of this mineral by structural factor ratios and $d_{001}$ spacings. Determinations of anorthite content in plagioclase were made using a four-axis universal stage and the curves of Slemmons (1962). However, the samples were limited to twenty-eight because of the fine-grained texture

of the rocks and also the contamination of the grains which made any accurate determination difficult. The orthoclase content of some feldspars was determined using the method of Orville (1963) with $KBrO_3$ as an internal standard.

Partial chemical analyses of the rocks were made using the rapid method of Shapiro and Brannock (1962) modified by Donnelly (1966). One hundred thirty-three analyses have been made. These analyzed samples are comprised of thirty-six analyses of patches and corresponding matrices, sixty-three spilites, three amphibole porphyry dikes, four albite-diabase dikes, fifteen andesite-diabase dikes, and twelve brecciated type of rocks. These rocks were analyzed for nine components: $SiO_2$, $Al_2O_3$, $TiO_2$, total iron as FeO, MgO, CaO, $Na_2O$, $K_2O$ and MnO. The Beckman D-U flame photometer was used to determine $TiO_2$, total iron as FeO, $SiO_2$, and $Al_2O_3$, and the Perkin-Elmer atomic absorbtion spectrophotometer, Model 303, was used to determine MgO, CaO, $Na_2O$, $K_2O$ and MnO. Rock standards W-1 (basalt), G-2 (granite), GSP-1 (granodiorite), BCR-1 (basalt) and AGV-1 (andesite), were also prepared in conjunction with the samples to determine the weight oxide percent.

The precision achieved from the standard curve deviation was: $SiO_2 \pm$ .70 percent; $Al_2O_3 \pm$ .60 percent; $TiO_2 \pm$ .05 percent; total iron as FeO $\pm$ .20 percent; MgO $\pm$ .09 percent; CaO $\pm$ .15 percent; $Na_2O \pm$ .10 percent; $K_2O \pm$ .05 percent; and MnO $\pm$ 0.01 percent. Duplicate analyses of about ten rock samples were made to determine the accuracy of the method used. The reproducible values of the different oxides vary as follows: $SiO_2$ ranges from $\pm$ 2.3 - 1.0 percent; $Al_2O_3$

from ± 2.6 - 0.6 percent; $TiO_2$ from ± 1.8 - 0 percent; total iron as FeO from ± 2.2 - 0 percent; MgO from ± 2.4 - 0.5 percent; CaO from ± 4.8 - 1.3 percent; $Na_2O$ from ± 2.6 - 0.5 percent; $K_2O$ from ± 2.6 - 0 percent.

# MINERALOGY

The different lithologic units encountered in the upper part of the Virgin Island core contain more or less similar mineral associations, and they differ only in the distribution of minerals among these zones. The chief exception is biotite which occurs in minor amounts in the upper 650 feet and then disappears. The most common minerals of the core include plagioclase, chlorite, clinopyroxene, calcite, epidote, actinolite and opaque minerals.

## Mineralogy of the Spilite

Feldspar. The composition of the albite mineral was determined using the universal stage and the method of Slemmons (1962). Albite with an anorthite content varying between $An_2$ and $An_{11}$ is abundant in many spilitic rocks and occurs usually as tiny microlite laths (average .05 mm. in length), and microphenocrysts (average 0.1 mm. to 0.4 mm. in length). The twinning of some plagioclase, determined by Slemmons' (1962) method, is usually according to the albite-Carlsbad law, and less commonly Manebach and Carlsbad (Table 1). No evidence of perthitic texture was observed. The larger crystals of plagioclase are often clouded by sericite aggregates and may also show sieve structure in the core of the mineral or close to their edge. This makes optical determination of the plagioclase difficult. The outer rim of these coarser crystals of plagioclase represents an overgrowth of albite, while the core of the crystals is sometimes altered into sericite. These plagioclase crystals from the spilite plot on the Slemmons (1962) curve (Fig. 3).

Figure 3. Plagioclase determination from the spilite (●) and andesine diabase dike (Δ) plotted on Slemmon's curve. Thick line represents plutonic rocks; thin line represents volcanic rocks.

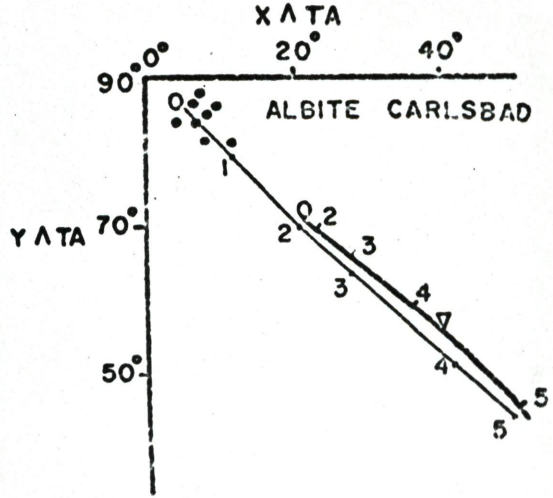
XATA
20°
40°
90°0°
ALBITE CARLSBAD
YATA 70°
50°
0
1
2
0,2
3
3
4
4
5
5

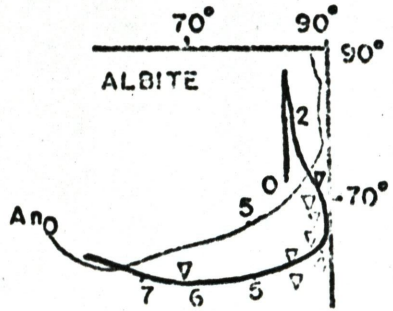
70°
90°
90°
ALBITE
2
5
0
70°
An0
7
6
5

The relative content of orthoclase in the feldspar was determined using Orville's (1963) X-ray methods. The difference in $2\theta$ for $CuK_{\alpha}$ radiation between (201) peak of $KBrO_3$ used as internal standard is plotted against the composition in terms of mol percent of Or (Orville, 1963). Table 2 shows that the content of orthoclase in the albite of these spilites is nil. Donnelly (1966) studied the composition of plagioclase in the spilite from the Virgin Islands and found a similar poverty of orthoclase.

Another type of feldspar less commonly encountered in the spilite flow consists of clear sodic plagioclase ($< An_{15}$). This type of plagioclase is determined with the universal stage method using Slemmons (1962) curve, is colorless, contains few alteration products, and appears limpid under the polarizing microscope. This clear sodic plagioclase is anhedral and assumes various forms such as radiating fibers with strong undulatory extinction and platy with simple twins. The characteristic twinning of the feldspar may sometimes be indistinguishable, and the mineral looks like quartz; however, the figure of interference is biaxial negative. The clear sodic plagioclase crystals are usually encountered in vesicles and veinlets (Plate 1, Fig. 1).

Calcic plagioclase was also encountered throughout the spilite flow. This type of plagioclase occurs as microphenocrysts and microlites associated usually with albite or partially replaced calcic plagioclase having albitic rims (Fig. 4). No systematic variation of calcic plagioclase occurs either with depth or between patches and matrices. An estimated calculation indicates that the calcic plagio-

PLATE 1, Figure 1 - Vesicles filled with a large quartz crystal (center) and "clear" plagioclase laths lining the edge in the non-patchy spilite zone (761 feet, X Nicol).

PLATE 1, Figure 2 - Pyroxene phenocrysts almost completely altered into chlorite and actinolite in the non-patchy spilite zone. The surrounding matrix is fine grained with microlites of plagioclase, chlorite and opaques. (673 feet, X Nicol).

PLATE 1, Figure 3 - Vesicles filled with chlorite and hydrogarnets (H) in the patchy spilite zone (251 feet). The groundmass shows intersertal texture (45° Nicol).

PLATE 1, Figure 4 - Very fine grained biotite (B) flakes in chlorite-filled vesicles in the patchy spilite flow (473 feet, 45° Nicol).

# PLATE 1


FIGURE 1


FIGURE 2

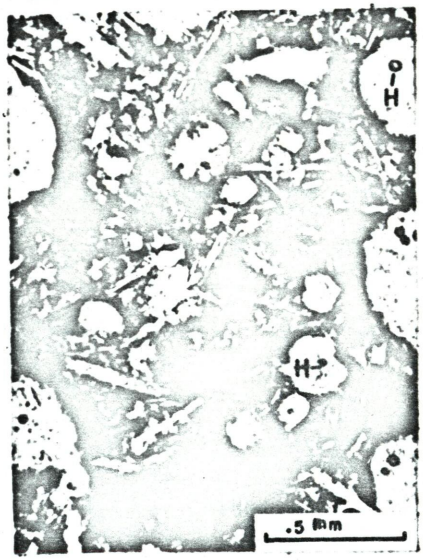


FIGURE 3


FIGURE 4

Figure 4. Features of the plagioclase of the spilite from the core.

1. Albite (Ab.) microlites associated with chlorite (Chl.) and magnetite (Mt.) against quartz (Qtz.).

2. Partially altered calcic plagioclase (C.P.) showing a narrow rim of albite (Ab.). Phyllosilicate (Phl.), probably sericite, has partially altered the core of the plagioclase.

3. Calcic plagioclase (C.P.) laths showing intersertal texture. The plagioclase is associated with fine-grained quartz (Qtz.), magnetite (Mt.), chlorite (Chl.), and phyllosilicates (Phl.).

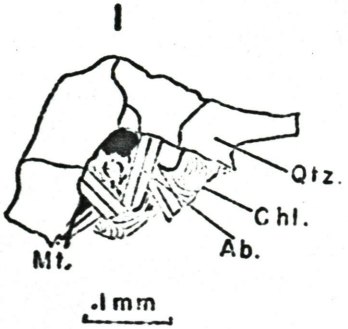
1
Qtz.
Chl.
Ab.
Mt.
.1mm

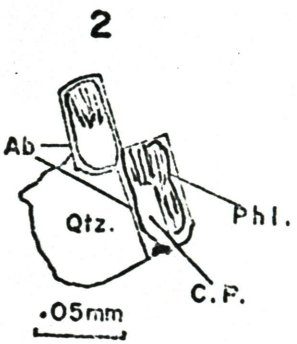
2
Ab
Qtz.
Phl.
C.P.
.05mm

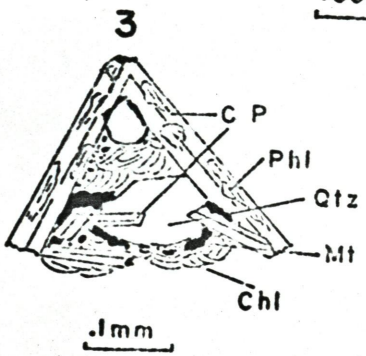
3
C P
Phl
Qtz
Mt
Chl
.1mm

clase content is usually less than albite. The determination of this calcic plagioclase was made by using the index of refraction against quartz.

Clinopyroxene. The clinopyroxene grains occur usually as euhedral to subhedral phenocrysts and microphenocrysts and they appear to be generally more altered towards the bottom of the spilitic flow. The optical index of refraction and 2V determination combined with the X-ray studies of pyroxene indicate the presence of a diopsidic clinopyroxene (Fig. 5). The composition of the clinopyroxene calculated according to the Hess (1949) method is close to $Ca_{50}Fe_9Mg_{41}$ for the spilite. The X-ray determination using the relative differences in Å of certain reflections ($FeK_\alpha$ radiations) d (220) and d (221)(Kuno and Hess, 1953) shows a value close to that of the optical methods (Fig. 5, Tables 2, 3).

The clinopyroxene of the spilitic flow is usually fresh near the top of the flow and is more altered toward the bottom where relics of pyroxene, replaced completely by chlorite (560 feet), occur (Plate 1, Fig. 2). Other less common alteration products of the pyroxene are calcite, epidote and amphibole. Pyroxene granules occur also in the groundmass, usually filling interstices between plagioclase laths. Within the patchy portions of the flow, clinopyroxene decreases usually towards the green matrix and disappears completely further away from the dark patches.

Chlorite. Chlorite is an abundant component of the spilite flow and averages around 22% in these rocks (Table 9). The chlorite occurs in

Figure 5. Left - Composition of clinopyroxene deduced from index of refraction and 2V.

Right - Composition of clinopyroxene from X-ray data.

• Spilite.

× Albite-Diabase dike.

▽ Andesine-Diabase dike.

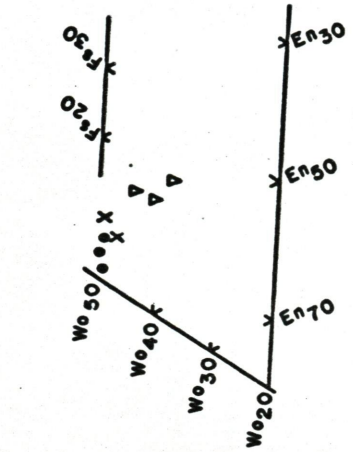
En30
En50
En70
Wo20
Wo30
Wo40
Wo50
Fs20
Fs30

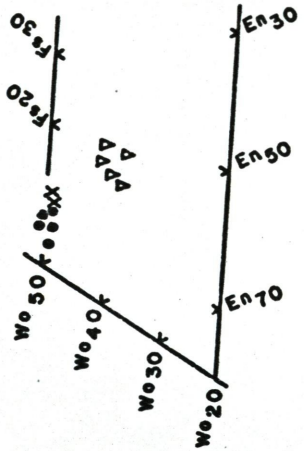
En30
En50
En70
Wo20
Wo30
Wo40
Wo50
Fs20
Fs30

tiny plates and fibrous aggregates filling irregular cavities, veins and vesicles. In the spilites, chlorite is commonly arranged radially between interstices of the plagioclase laths. The most patchy spilites near the top of the core (above 300 feet) show a greenish intermediate zone between the dark patches and the green matrix. This transitional zone is characterized by having plates of chlorite arranged in a parallel fashion along the patch boundaries. Chlorite also occurs abundantly in amygdules and it is often accompanied by calcite and quartz which form concentric rims around the chlorite.

X-ray methods were used to determine the chemical composition of chlorites using structure factor ratios and $d_{001}$ spacings (The structure factor (F) is related to the intensity of an X-ray peak). The use of $F_{003}/F_{001}$ ratios (Schoen, 1962) gives comparable results to a $F_{002}/F_{001}$ ratio (Brindley and Gillery, 1956). These ratios give the value of the "x" variable in the following formula:

$$(Mg,Al)_{12-x}Fe_x(Si_{8-y}Al_y)\ O_{20}(OH)_{16}$$

The "y" variable is found by measurement of the $d_{001}$ spacing and using the equation of Brindley and Gillery (1956).

The structure factor varies when elements of different scattering factors are substituted into the chlorite structure. Since the atomic scattering factors of silicon, aluminum and magnesium are about the same, the structure factors are unaffected by substitution of aluminum for silicon in tetrahedral sheets or aluminum for magnesium in the octahedral sheets. However, the atomic scattering factors for the iron - magnesium - chromium - titanium group are twice as large as

Figure 6. Diagramatic representation of chlorite composition (X-ray data) from the core.

(●) Spilite.

(◐) Amphibole porphyry dike.

(×) Albite diabase dike.

(▽) Andesine diabase dike.

(○) Brecciated spilite rocks.

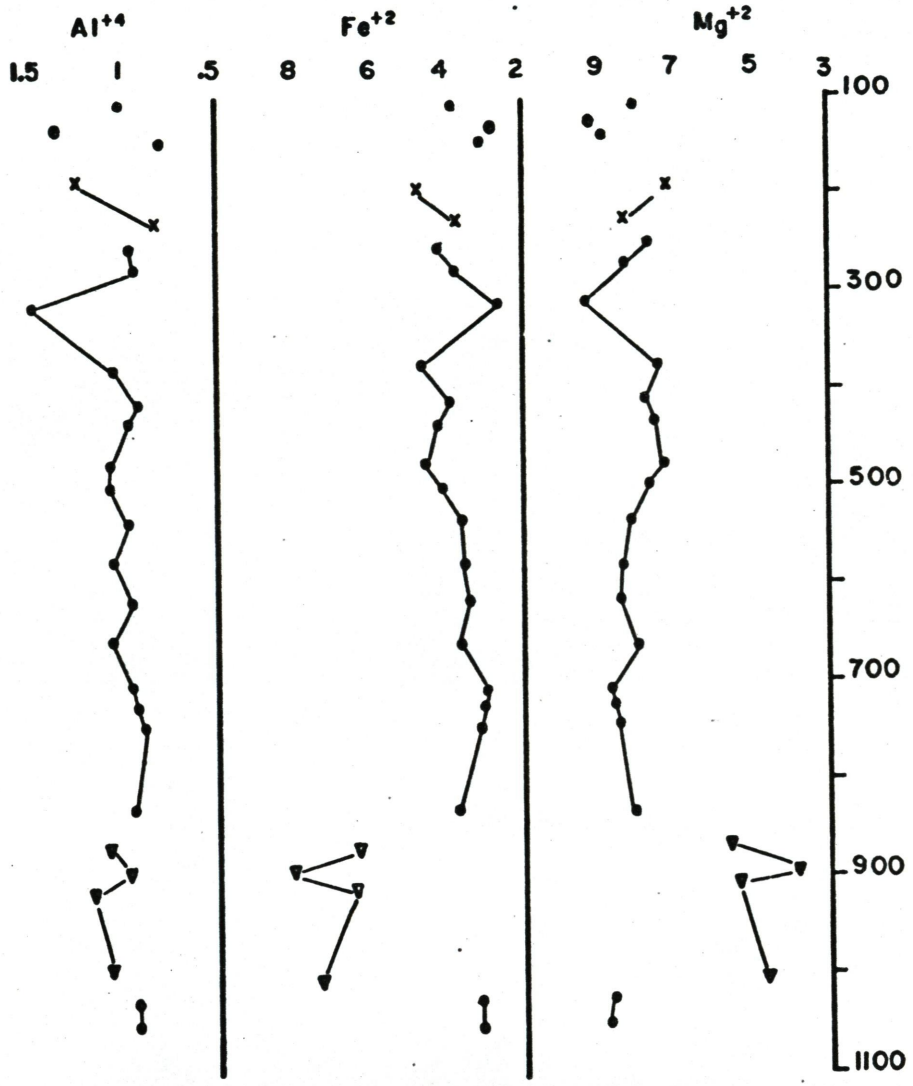
Al+4
1.5
1
.5
Fe+2
8
6
4
2
Mg+2
9
7
5
3
100
300
500
700
900
1100

those for the silicon - magnesium - aluminum group. X-ray intensities should distinguish the latter group of elements from the former.

The calculated $F_{003}/F_{001}$ and the calculated $F_{002}/F_{001}$ ratio are compared with theoretical values. The value for each ratio was added, and the average value represents the "x" variable for that particular chlorite (Table 5). Twenty samples taken at various depths in the spilite flow were studied by this method. For the application of the X-ray technique, it was not necessary to separate the chlorite from the bulk rock. However, a uniform fine fraction was oriented onto a glass slide for the purpose of enhancing the 001 peaks. The final ground material was put into a suspension in a 200 ml. graduated cylinder and allowed to settle. The fine fraction of the sample was pipetted from the suspension and transferred onto a preheated ($35^{o}C$) glass slide in the oven. The drying time took about 60 minutes. The slide was then scanned in a diffractometer, the peak areas estimated and the compositions calculated. The results are listed in Table 5, and then plotted in Figure 6. Internal quartz was used for $2\theta$ correction and estimation of the position (004) peak in the chlorite. These results, plotted in Figure 6, show that $Mg^{2+}$ in chlorite is the same throughout the spilite flow.

The $(Si,Al)_8$ distribution of the chlorite, the "y" variable in the formula:

$$(Mg,Al)_{12-x}(Fe,Mn,Gr,Ti)_x(Si_{8-y}Al_y)\ O_{20}(OH)_{16}$$

was determined by calculation of the $d_{001}$ spacing. The results of the Brindley and Gillery (1956) equation for chlorite are plotted in Figure 6.

Figure 7. Ternary plot of chlorite from the Virgin Island Core.

(●) Spilite.

(×) Albite diabase dike.

(▽) Andesine diabase dike.

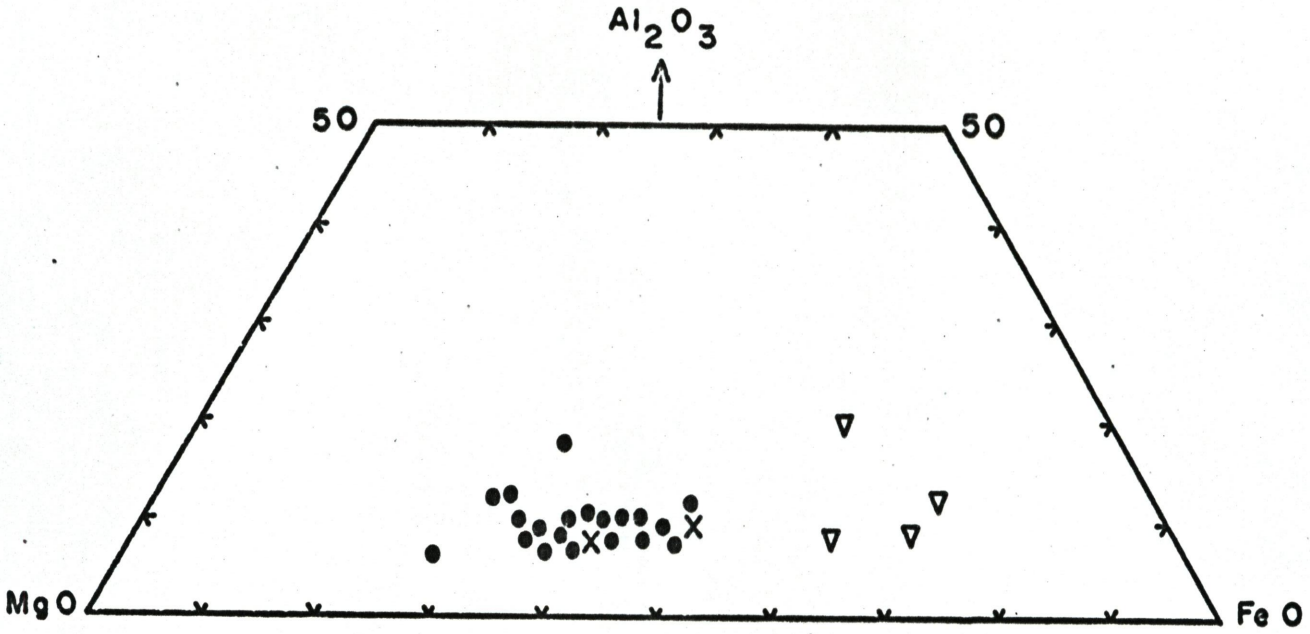
$Al_2O_3$
50
50
MgO
FeO

The number of $Al^{4+}$ replacing $Si^{4+}$ in the formula $(Si,Al)_4$ indicates that aluminum values in the chlorite are more or less constant throughout the core.

Glycolated samples were also studied with the use of an X-ray diffractometer, but no trace of expanding layers were noticed. The composition of chlorite, calculated from Schoen (1962), and from Brindley and Gillery (1956), was plotted in the iron/iron magnesium - iron - silicon diagram of Hey (1954). The type of chlorite of the spilite flow, according to Hey's classification, is diabantite.

The spilitic chlorite is variable in its optical properties. Chlorite shows color variations within the spilitic flow. This may be due to an oxidation state of the iron as mentioned also by Donnelly (1966). However, the composition of chlorite is not uniform throughout the core and sometimes this composition varies between the different rock types encountered in the core. The composition of chlorite plotted on a ternary diagram $Al_2O_3$-MgO-FeO (Fig. 7) indicates similarities between the chlorite of the greenstone (Melson and Van Andel, 1966) dredged from the North Atlantic and the chlorite of the spilite flow from the core (Fig. 7). Lehmann (1965) studied chlorite minerals from spilitic igneous rocks and indicated that diabantite is the commonest chlorite found.

Amphibole. Amphibole of the spilite flow was recognized by optical and X-ray methods. No chemical analyses or index of refraction measurements were attempted because of the small size, and the close association with chlorite. The name of actinolite given to this amphibole is based upon

its occurrence, since the optical properties provided in Winchell and Winchell (1951) and Deer, Howie, and Zussman (1966) are broad and overlapping in their variation properties. Amphibole occurs as fibrous aggregates and pleochroic in green or yellow (x = pale yellow, y = greenish yellow, and z = dark green). The cleavage traces are parallel to the length of the crystal. The elongated sections are length-slow and the maximum extinction angle $Z \wedge c$ varies between $12^{\circ}$ and $15^{\circ}$ with 2V around $80^{\circ}$. Amphibole occurs mainly as a marginal alteration product of clinopyroxene. From these optical data it is probable that the type of amphibole encountered in the spilite flow is an actinolite.

Calcium Bearing Minerals. Most of the calcium bearing minerals such as epidote, calcite, pumpellyite, prehnite, and hydrogarnet occur as inclusions in vesicles, veins, and veinlets in the groundmass of the spilite flow and also in the form of irregular patches, which are probably replacement products of an original plagioclase or pyroxene. However, they rarely occur in contact with each other. Usually where calcite occurs as a major replacement product of an original plagioclase or pyroxene, epidote has disappeared or is rare.

1. Pumpellyite. Pumpellyite was identified with the use of a polarizing microscope. This mineral is characterized by an anomalous interference color, moderate relief, strong dichroism in blue-green and it occurs as very fine grained crystals usually associated with chlorite. Pumpellyite occurs also as isolated anhedral crystals with relief higher than the chlorite. Pumpellyite is occasionally encountered

in the spilite flow at depths of about 200-300 and 400-500 feet (Fig. 8). Pumpellyite has been reported from many parts of the world in rocks which have undergone low grades of metamorphism, as in the upper Water Island Formation of the Virgin Islands (Donnelly, 1966).

2. Prehnite. Prehnite is also an occasional constituent found in the spilite flow. This mineral occurs usually as small colorless aggregates that are sheaf-like and commonly associated with pyroxene. Prehnite shows a moderate relief with moderately strong birefringence of the upper second order and wavy extinction. This mineral was recognized under the microscope at 173, 242, and 542 feet.

3. Hydrogarnet. Hydrogarnet is also an accessory mineral encountered at 406 and 473 feet. Hydrogarnet occurs in small rounded isotropic crystals with a weak birefringence at their edge due probably to the presence of water molecules. The hydrogarnet, usually associated with chlorite (Plate 1, Fig. 3), was also identified by standard X-ray diffraction methods. This hydrogarnet is characterized by d - spacings of 3.0 Å (Table 6). Table 6 also shows the X-ray diffraction pattern of hydrogarnet with impurities, chlorite, quartz, albite, and sphene.

Experimental studies on the system $CaO-Al_2O_3-SiO_2-H_2O$ (Roy and Roy, 1957) shows that with pressure up to 4 kbs., the maximum stability temperature of the hydrogarnet phase is around 300-400°C. It is believed that the occurrence of hydrogarnet in the spilite flow of the core is due to the alteration of calcium bearing minerals.

Micas. The mica content of the spilite flow decreases with depth. Two

Figure 8. Diagram showing the variation of minerals and amygdules with depth in the spilite and brecciated spilite rocks. (B) biotite.

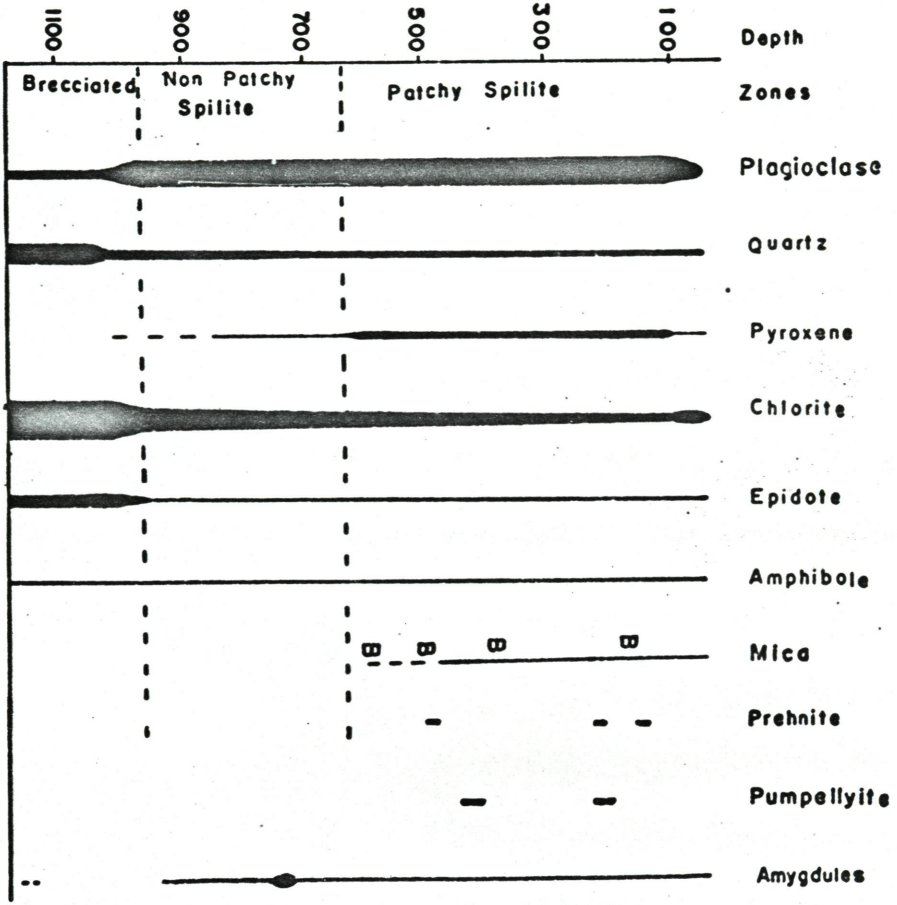
1100
900
700
500
300
100
Depth
Brecciated
Non Patchy Spilite
Patchy Spilite
Zones
Plagioclase
Quartz
Pyroxene
Chlorite
Epidote
Amphibole
Mica
Prehnite
Pumpellyite
Amygdules

types of micas are recognized in these rocks. One is a fine-grained white mica generally included within feldspar. This "sericite" occurs as tiny colorless flakes with parallel birefringence of the upper second order. This mineral was identified as muscovite 10.3 Å by X-ray diffraction (Table 7) and by microscopic determinations.

The other, less common, type of mica is apparently biotite. It is pleochroic in green, and the extinction is almost parallel to the cleavage traces of the mineral. The direction of these cleavage traces is the slower ray. This mica optically appears to be a green biotite, occurring as very fine-grained short, prismatic to columnar crystals with no traces of resorption (or embayment). The biotite (3-5%) of the rock is mainly associated with chlorite filling vesicles (Plate 1, Fig. 4) in the patchy spilite zone near 110, 163, 417-446, 473-542, and 569-581 feet.

The identification of this mineral was confirmed by X-ray powder camera techniques. The material analyzed was collected from a thin section by hand-picking with a needle. The sample was then exposed for approximately twelve hours in a 9 cm. camera to $CuK_{\alpha}$ radiation. The X-ray diffraction of this mica shows a broad 10.5 Å spacing for (001) and is reported in Table 8. After heating the sample at 400°C for three hours, the lines of the X-ray powder photograph sharpened and the d-spacings decreased to 10.1 Å. This latter experiment may indicate that the phase diffractive at 10 Å is a mixed-layer structure (probably biotite-vermiculite).

Accessory and Opaque Minerals. The other accessory minerals consist

of sphene, magnetite, hematite, and pyrite. Fine grains and granules of sphene occur in amygdules and are primarily associated with chlorite in the spilite flow. In the spilite flow, the amount of sphene increases with the decrease of clinopyroxene. This may indicate that pyroxene alteration has contributed to the formation of sphene crystals. Magnetite, hematite and pyrite are the most common opaque minerals encountered in the core. Magnetite occurs as small granules mainly concentrated in the groundmass of the dark patches and also may be found concentrated around the edge of amygdules in the spilite flow. Hematite seems also to be concentrated in reddish patches in the upper part of the spilite flow. Minute crystals of hematite occur also in veins associated with chlorite and other micro-crystalline aggregates showing a flow textural feature.

## Mineralogy of the Brecciated Spilitic Rocks

Feldspar. The feldspar (<15%) of the brecciated zone is an albite and varies in size from microlitic to occasional phenocrysts (at 1127 feet). The fine-grained feldspars do not usually contain any inclusions, are anhedral, have undulatory extinction, and show polysynthetic twins. The phenocrysts are euhedral to subhedral and are enriched with epidote inclusions.

Chlorite. The chlorite content of this zone varies between 10 and 30 percent (Table 9). Chlorite may occur either as fibrous aggregates scattered in the form of irregular patches, or as elongated flakes surrounding quartz crystals. The composition of this chlorite was

determined by the X-ray method (Schoen, 1962) and shows the chlorite to be a diabantite, similar to the composition of the chlorite from the spilite flow.

Epidote. This mineral averages about 20 percent and occurs as radiating clusters or granular crystals in veins, as irregular patches, or scattered in the groundmass. Epidote is usually yellowish-green with an interference color of the upper third order and has a parallel extinction in elongated sections. The figure of interference is biaxial negative.

Quartz. Quartz is a major constituent (about 35%) of the brecciated zone. It occurs usually as fine-grained aggregates scattered throughout the groundmass. Rounded crystals of quartz showing sutured boundaries with strong undulatory extinction were also commonly seen. The quartz is colorless and usually does not contain inclusions.

Accessory and Opaque Minerals. The accessory and opaque minerals comprise less than 10 percent of the rocks with the exception of the veins. These veins are entirely formed by calcite, quartz, or epidote, or a combination of these mineral assemblages. Gypsum was also seen in veins at 1060 feet. Sodic plagioclase, Sphene, Actinolite, and Calcite constitute the accessory anisotropic minerals and hematite granules, magnetite and pyrite are among the opaque minerals encountered in the brecciated zone.

## Mineralogy of the Amphibole Porphyry Dikes

Feldspar. The feldspar of the amphibole porphyry dike is an albite

($Or_5Ab_{95}Or_5Ab_{95}$) and averages around 40 percent. This feldspar is usually cloudy due to inclusions of sericite and small needles of amphiboles. The form varies from platy in the phenocrysts to lath-shaped in the matrix.

Amphibole. The amphiboles of these rocks occur usually as subhedral phenocrysts with strong pleochroism towards green. These amphiboles show a negative interference figure with a 2V varying between 81° and 89°. The extinction angle $z\wedge c$ in a longitudinal section varies from 15° to 19° and the cleavages in two directions form an angle of about 124°. The main alteration product of the hornblende is calcite and chlorite which sometimes forms reaction rims around the larger mineral grains (129 feet).

Chlorite. The chlorite content of the amphibole porphyry rocks averages about 25%. This chlorite is pleochroic toward green and occurs as fibrous aggregates associated with the groundmass and also as platy minerals surrounding or including the amphibole phenocrysts. The composition of the chlorite determined by X-ray (Schoen, 1962) is close to diabantite, which is similar to the chlorite of the spilite flow (Table 5).

Accessory and Minor Constituents. The minor constituents consist of quartz, epidote, calcite, and sericite. The accessory minerals are clinopyroxene, and magnetite granules.

## Mineralogy of the Albite-Diabase Dike

Feldspar. The average feldspar content of the albite-diabase dike is around 30% (Table 9) with an anorthite content varying between $An_4$ and $An_{10}$. No orthoclase was detected within the albite lattice. This feldspar has an average crystal size of 1 mm. in length, it is commonly

altered into sericite, and it is usually twinned according to the Albite-Carlsbad and Manebach twin laws (Table 1).

Clinopyroxene. The content of clinopyroxene is close to that of feldspar (Table 9) in the albite-diabase dike. This pyroxene is colorless and subhedral with an average diameter of about 0.5 mm. The composition of this pyroxene, calculated according to the Hess (1949) method, is similar to the clinopyroxene of the spilite ($Ca_{50}Fe_9Mg_{41}$) which falls close to the diopside corner of the Diopside-Clinoenstatite-Clinoferrosilite-Hedenbergite diagram (Fig. 5).

Chlorite. The chlorite content of the albite-diabase dike is about 20 percent and occurs usually as platy and fibrous aggregates replacing the pyroxene crystals. Using the methods of Brindley and Gillery (1956) and Schoen (1962), the composition of chlorite was found to be a diabantite.

Accessory and Minor Constituents. The accessory minerals found in the albite-diabase rocks consist of yellowish-green epidote, magnetite, fibrous actinolite and minor amounts of sphene.

The sphene mineral content may be as great as five percent in some zones. This crystal sometimes shows an acute rhombic cross section with a characteristic prominent parting. Sphene is euhedral and colorless and associated with chlorite.

## Mineralogy of the Andesine-Diabase Dike

Feldspar. With the Universal Stage Method, it was found that the plagioclase (about 35%) of the andesine-diabase dike is an oligoclase-andesine

with an anorthite content varying between $An_{29}$ and $An_{42}$. The plagioclase of this dike has an average size of 1 mm. in length, and plots on the high temperature albite curve of Slemmons (1962) (Fig. 3). The larger feldspar phenocrysts show replacement products of a more sodic plagioclase ($An_8$ - $An_{10}$). The andesine-diabase dike contains less replacing sodic plagioclase than the albite-diabase dike. Inclusions of small pyroxene granules and chlorite along cleavage planes is also common. The plagioclase is usually euhedral with respect to pyroxene. The coarsest plagioclase grains show undulatory extinction, probably due to the presence of original more calcic plagioclase relics.

The plagioclase of the andesine dike is usually twinned according to the albite and baveno twinning laws. Manebach and Carlsbad twinning laws occur only occasionally (Table 1). The main difference between the twinning of the plagioclase in the different dikes and extrusive rocks encountered here is due to the fact that the albite of the spilite has a simple twin or sometimes none, and the plagioclase of the dikes has polysynthetic twins.

Clinopyroxene. The clinopyroxene of the andesine-diabase dike is coarse grained subhedral to anhedral and ophitically associated with the plagioclase. The clinopyroxene averages around 30% (Table 9) and usually appears to be colorless, with the exception of its margin which is pinkish due to the concentration of titanium and iron. The composition of the clinopyroxene calculated according to the Hess (1949) method is close to $Ca_{36}Fe_{24}Mg_{40}$ (Fig. 5, Table 3). The clinopyroxene of this andesine-diabase dike is slightly altered into chlorite and amphibole (probably

actinolite).

Chlorite. Chlorite is a minor constituent (<10%) of the andesine-diabase dike. Chlorite occurs as pale green fibrous aggregates filling interstices between plagioclase laths and associated with actinolite as alteration products of pyroxene.

The chemical composition of this chlorite was also determined by using the X-ray method of Brindley and Gillery (1956) and Schoen (1962). This later technique showed that the chlorite of the andesine-diabase dike is an aphrosiderite (iron-rich chlorite) (Table 5).

This type of chlorite contains less $Mg^{2+}$ and more $Fe^{2+}$ than the chlorite from the spilite flow (Fig. 6). The amount of $Al^{3+}$ replacing $Si^{4+}$ is similar to that of the spilitic chlorite.

Amphibole. The amphibole occurs only as a minor constituent in the andesine-diabase dike. This mineral, usually associated with chlorite, occurs as columnar to fibrous aggregates, with higher relief than chlorite and pleochroic toward green. The elongated sections are length-slow and the maximum extinction in longitudinal sections varies from $10^{\circ}$ to $16^{\circ}$. The optic axis shows a 2V (-) varying between $80^{\circ}$ and $95^{\circ}$. It is inferred that, from the above data, the amphibole encountered in the andesine-diabase dike is an actinolite. The Universal Stage Method and a normal polarizing microscope were used to determine the composition of this amphibole.

Accessory and Opaque Minerals. These accessory minerals of the andesine-diabase dike consist of magnetite, epidote, calcite and quartz.

# PETROGRAPHY

## Spilite

### General Statement

Spilitic flows from the Water Island Formation (Virgin Islands) previously described by Donnelly (1966), show that these flows vary in thickness from about 5 to 10 feet to several hundred feet. These spilite flows may assume different forms. They may be massive and lack columnar joints and pillow structure. Other flows, located at Elk Bay in St. John, show true pillow structure (Donnelly, 1966). Donnelly (1966) found also that most thicker flows exhibit reddish or yellowish segregates, or patches. The most typical patchy flow consists of hematitic, amygdular patches, several inches in size within a chloritic, less amygdular matrix (Donnelly, 1966). Patchy structure is also found in the spilite flow of the core from St. John.

The spilites, which are extrusive and comprise two-thirds of the portion of the core studied here, are usually fine-grained rocks. The fine-grained nature of the groundmass and the rare occurence of phenocrysts, mostly pyroxene, indicates that the cooling of these rocks happened relatively quickly. The groundmass consists of microphenocrysts and microlites which are mostly plagioclase. A dark mesostasis scattered with iron dust is commonly seen in the groundmass. These spilites are further divided into two groups according to their appearance. There is a patchy spilite zone comprising the upper half (650 feet) of the flow. This zone contains dark colored patches averaging

2 cm. in diameter set into a green, chlorite-rich groundmass. This patchiness diffuses with depth and finally disappears completely, and gives rise to the second zone called a non-patchy spilite.

Another part of the spilite flow is the brecciated zone, which is also extrusive and is named according to its textural appearances; these rocks occur at the bottom of the area of the core studied here, between 1003 and 1180 feet. Obliteration of microlitic texture and consequent recrystallization gave rise to the formation of the epidote-chlorite-quartz mineral association which characterises this brecciated zone.

Patchy Spilite. The upper part of the core (above 650 feet) is formed with dark gray patches varying in diameter between 0.5 and 6 cm. which are set into a grayish green matrix. The individual dark patches may assume different forms, ellipsoidal, spherical, angular and irregular (Plate 4, Fig. 13, 14, 15 and Plate 5, Fig. 16). These dark patches are always separated from each other and often they show a thin pale green rim representing a transitional zone with the grayish green matrix. Sometimes the green matrix shows light green spots irregularly shaped and averaging about 3 mm. in diameter. The spotty appearance of the green matrix is usually due to chlorite enrichment. Megascopically it seems that the dark patches contain more vesicles than the surrounding matrix. However, microscopic analyses showed that no difference in the amount of vesicles was noticed between the two zones.

These patchy zones pass gradually (below 650 feet) to a massive non-patchy spilite (Plate 5, Fig. 17, 18). The non-patchy zone is dark

grayish green, fine-grained and sometimes abundantly veined. More detailed description about this zone will be given later.

Features of other lava flows which should be compared to the patches of the spilite are pillow structures and agglomerates. However most pillows, ranging from 10 cm. to 7 m. in diameter, have a radial jointing and a glassy crust. True pillows are commonly but not invariably separated partly or wholly from each other by detrital material (MacDonald, 1967). Agglomerates (accumulations of bombs) are usually found in or near the vent of volcanos. The form assumed by the bombs is related to the viscosity of the magma and they may be angular, spherical, fusiform, etc. These agglomerates do not show any constant pattern of occurrence and they may be tightly molded to each other. The patches encountered in the spilite flow cannot either be pillow or agglomerates because no columnar jointing was observed. They are always separated from each other by the matrix which does not appear to be an accumulation bombs but rather represents a simple eruptive event. In addition, these patches show also a certain mineralogical continuity with their respective green matrices.

The general textural feature of these spilites is variolitic to pilotaxitic and has a tendency to be trachytic. Sometimes coarse grained pyroxene and plagioclase are scattered throughout the rock, but these grains rarely attain the size of phenocrysts (Plate 2, Fig. 1). There is a general increase of chlorite, sphene and calcite as we go deeper in the core and also a gradual decrease in pumpellyite, prehnite, iron minerals, and pyroxene. The patches decrease in size with depth, and

their shape appears to be more elongated (at 700 feet) due to the parallel arrangement of plagioclase laths.

Veinlets and veins of calcite, epidote, feldspar, quartz, and chlorite seem to increase also with depth in the spilite flow when fluidal textural feature, limited in small diffuse patches, becomes more prominent than in the upper portion of the core. These veins and veinlets cross-cut the main pilotaxitic to fluidal texture of the rock (759 feet). This indicates that the mineral concentration of the veins occured after consolidation of the groundmass. Vesicularity and vesicle size in spilites of the core show neither variation with depth or between dark patches and the green matrix. The percentage of vesicles varies between 1 and 15 percent, with corresponding size increases from .05 mm. up to 4.0 mm. in diameter. These vesicles are usually filled with minerals similar to the veins and veinlets.

The patchy spilite is found at a depth between 0 and 650 feet, as mentioned before. This zone consists of three different textural units: (1) dark patches; (2) transitional zone; and (3) green matrix. The patches are distinguished from hand specimens by their darker appearance due to iron bearing minerals which enrich their groundmass.

1. Dark Patches. The dark patches consist of a variolitic to intersertal textural feature. The principal components of the patches are plagioclase (with an estimated content around 45%), minor amounts of clinopyroxene ($< 10\%$), chlorite ($< 25\%$), calcite and occasional epidote and sphene. Granules of opaque minerals occur throughout the patches but are generally less than 20%. The dark patches are usually very

PLATE 2, Figure 5 - A fresh clinopyroxene phenocryst set into a fine grained groundmass showing intersertal to subtrachytic texture in the patchy spilite zone (101 feet). Rounded vesicles filled with chlorite are also seen (45° Nicol).

PLATE 2, Figure 6 - Transitional zone with trachytic texture. This zone is located between the dark patch (DK) and the green matrix (GM) in the patchy spilite flow and shows parallel arrangement of plagioclase microlites. Small vesicles filled with chlorite are also present (503 feet, 45° Nicol).

PLATE 2, Figure 7 - Glassy textural feature in the green matrix of the patchy spilite zone (345 feet). Sharp outlined edges are crowded with magnetite granules. Chlorite is the main alteration product of the glass. The plagioclase laths are rare and quartz crystal abound (45° Nicol).

PLATE 2, Figure 8 - Glassy textural feature (dark area) with sharp edges, in the patchy spilite zone (454 feet). Chlorite, epidote, and magnetite have replaced the original glass (45° Nicol).

# PLATE 2


FIGURE 5

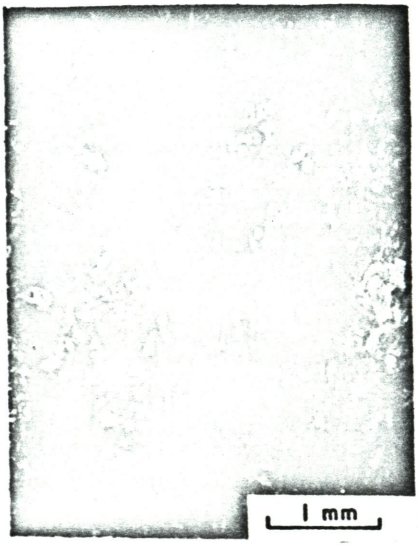


FIGURE 6


FIGURE 7

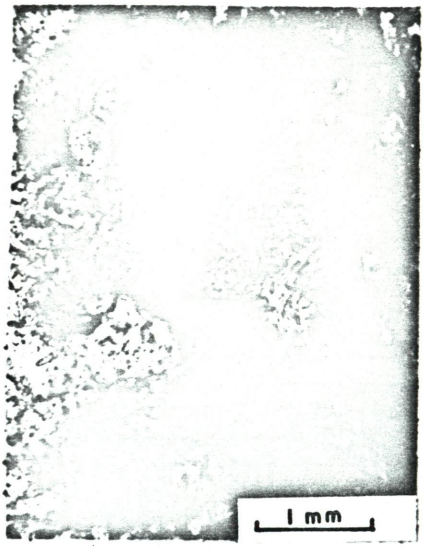


FIGURE 8

fine-grained, but occasional microphenocrysts of fresh pyroxene and altered plagioclase xenocrysts occurred. Relics of pyroxene microphenocrysts also occur and are replaced by calcite-chlorite-sphene-quartz or epidote-chlorite-quartz assemblages. Sometimes the plagioclase shows a sieve texture of chlorite and sericite towards its border and an overgrowth of a clearer and more sodic plagioclase. The groundmass which forms the main part of the rock is comprised of a dark mesostasis consisting of plagioclase laths, intersertial chlorite, iron granules, sphene, epidote, occasional granules of pyroxene, and a few calcite grains.

Rounded vesicles (0.6 mm. in diameter) abound in the dark patches. These vesicles are either filled with chlorite, quartz, and calcite, or with chlorite-epidote and chlorite-plagioclase assemblages. Sphene is frequently associated with the chlorite of these vesicles. Veinlets and veins are rare or completely absent in the patchy zone.

2. Transitional Zone. This zone is lighter green in the form of a thin band (average 3 mm. in thickness) surrounding most dark patches. This represents a transitional zone between the green matrix and the dark patches. This zone has a general trachytic texture due to parallel and sub-parallel arrangements of plagioclase laths (Plate 2, Fig. 6). The principal mineral components of this transitional zone are abundant chlorite, epidote granules and tiny plagioclase laths (0.2 mm. in length). Sphene occurs as a minor component. Calcite and quartz were also seen but not as abundantly as in the green matrix. Vesicles are rare or completely absent in this transitional zone.

3. Green Matrix. The green matrix surrounds the dark patches and the transitional zone. The general textural feature of this zone is pilotaxitic with a tendency to be trachytic. The green color of this matrix is due to the abundance of chlorite.

The green matrix contains similar mineral associations to the dark patches and the transitional zone. The plagioclase content is less than 34%, chlorite averages around 36%, and quartz is higher than 7%. The content of clinopyroxene in the green matrix is less than 5% and epidote, sphene, amphibole, and calcite are usually more abundant (18%) than the dark patches and transitional zone. The plagioclase of the green matrix is altered often into sericite, and sometimes it shows inclusions of epidote and, to a lesser extent, chlorite. The size of the plagioclase crystals of the green matrix have a tendency to be smaller than in the dark patches. Chlorite occurs in flaky aggregates, sometimes with bent texture around areas rich in quartz crystals (236 feet). But chlorite associated with granules of sphene is most commonly seen as filling irregularly shaped vesicles, sometimes elongated or having a glassy, shard-like structure (345, 425, 446, 454 feet) (Plate 2, Fig. 7, 8). These vesicles may also be filled with albite twinned feldspar having undulatory extinction and clouded with very fine semi-opaque anhedral granules of sphene. These latter vesicles are surrounded by a chlorite rim (446 feet). The clinopyroxene occurs usually as altered microphenocrysts. Chlorite and actinolite needles surround these pyroxene crystals. Pyroxene completely replaced by a core of chlorite surrounded by calcite (325 feet) and by quartz-chlorite-epidote (582 feet) was also observed.

Relationship Between Dark Patches, Transitional Zones, and Green Matrices. A broad textural difference exists, as noticed above, between the dark patches, transitional zones, and green matrices, varying generally from interstitial and trachytic to pilotaxitic, respectively. The mineralogical association does not vary between the different zones; however, the relative proportion of the components and their distribution does. The ratio of quartz/feldspar together with a microcrystalline groundmass of quartz, chlorite, and magnetite increases towards the green matrix. Calcite crystals increase also outwards from the dark patches. Calcite, quartz, and epidote veins increase in the same direction. The veins are usually discontinuous and sometimes have the appearance of elongated non-oriented patches. Another considerable difference between this zone and the dark patches is the relatively high amount of round quartz grains which occur as the distance from the dark patches increases.

The shape of the vesicles or amygdules varies between the dark patches and the green matrix. The vesicles of the dark patches are usually well rounded and the vesicles of the green matrix are irregularly shaped, usually with tendencies to be elongated. The transitional zone contains only occasional vesicles, which are usually rounded.

Non-patchy Spilite. The non-patchy spilite zone was distinguished within the spilite flow at about 650-847 feet. These rocks are fine-grained, and the general textural feature is pilotaxitic with tendencies toward trachytic (Plate 3, Fig. 10). The variolitic texture characteristic of the patchy zone has disappeared, and the fluidal texture is well distinguished, with microlites of plagioclase bent around coarse grained

PLATE 3, Figure 9 - A zone of a dark patch showing rounded vesicles filled with chlorite and a fine grained matrix crowded with plagioclase microlites. A microphenocryst of partially altered pyroxene crystal is also observed (251 feet, 45° Nicol).

PLATE 3, Figure 10 - Elongated shaped vesicles filled with "clear" albite laths and calcite, in the non-patchy spilite zone (724 feet). The groundmass shows a pilotaxitic texture (X Nicol).

PLATE 3, Figure 11 - Outline of an original amphibole phenocryst completely replaced by epidote and chlorite (1101 feet, 45° Nicol).

PLATE 3, Figure 12 - Flow texture of chlorite flakes, epidote and magnetite granules bent around coarse grained epidote minerals. Segregation of individual minerals of quartz occurs in association with the chlorite flakes. This type of texture characterizes the bottom of the brecciated zone (1131 feet, 45° Nicol).

# PLATE 3


FIGURE 9

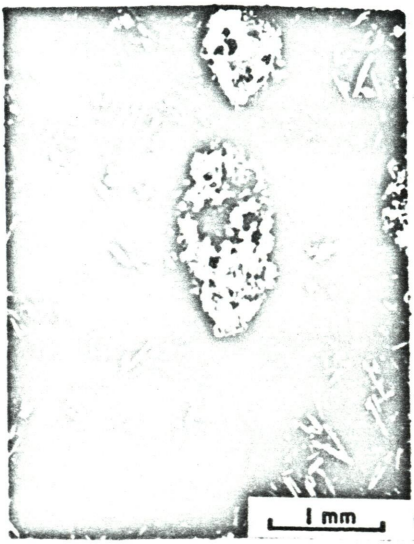


FIGURE 10


FIGURE 11


FIGURE 12

pyroxenes or their relics. Sometimes these ghosts of pyroxene are replaced by chlorite.

The plagioclase content is similar (35%) and the clinopyroxene content is lower (5%) than the above patchy spilite flow (Fig. 8). The chlorite content has slightly increased in the non-patchy zone (Fig. 8). Quartz, epidote, and amphibole content seem to be very similar to the patchy zone (Fig. 8). However, pumpellyite and prehnite are not encountered in this lower spilite flow (non-patchy spilite).

Veinlets and veins increase also with depth (Plate 5, Fig. 17). However, the green matrix of the patchy spilite zone in the upper part of the core also showed an increase of veins towards the outer margin of the dark patches. The veinlets and veins are usually irregular and discontinuous and consist of quartz, epidote, calcite, and chlorite.

The non-patchy spilite zone also contains amygdules as large as 0.6 mm. in diameter and usually less than 7% in content. These amygdules remain constant in content throughout the non-patchy spilite flow with the exception of a zone rich in amygdules (10 - 15%) at 695-710 and 761 feet in the core (Plate 5, Fig. 18). This amygduloidal zone consists of amygdules (4 mm. in diameter) composed mainly of coarse grained quartz or plagioclase at the center and fine grained plagioclase laths toward the margin. A few vesicles filled by calcite were also seen within the amygduloidal zone. These amygdules are set into a fine grained variolitic groundmass of chlorite, plagioclase

PLATE 4, Figure 13, 14, 15 - Patchy spilite zone at 83, 126 and 473 feet respectively. These zones contain dark patches with rounded vesicles of quartz, chlorite and calcite. A lighter zone (transitional) surrounds the dark patch (Fig. 15). The dark patches are set into a recrystallized green matrix. Veins of calcite, epidote cut across the core (Fig. 13).

# PLATE 4

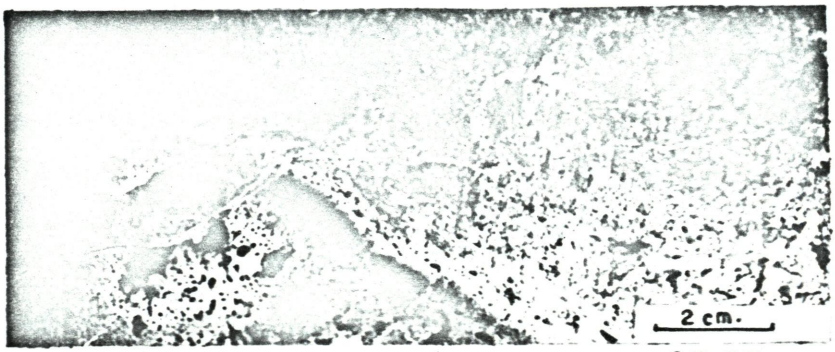


FIGURE 13 — 83 FT.

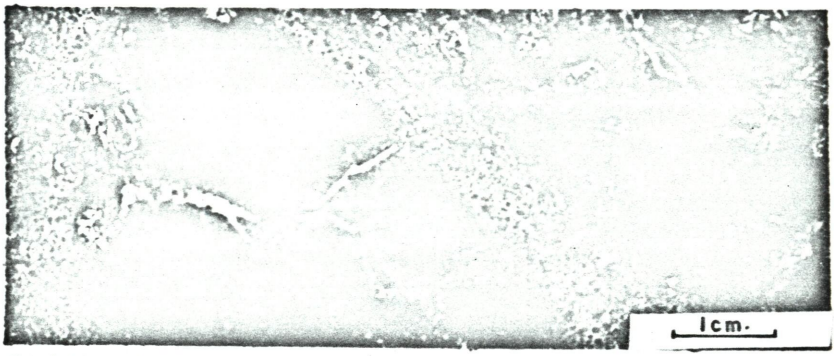


FIGURE 14 — 126 FT.

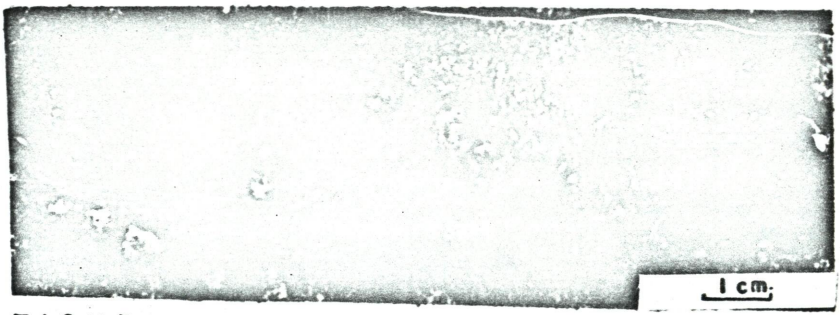


FIGURE 15 — 473 FT.

PLATE 5, Figure 16 - Patchy spilite (492 feet) with dark patches and their matrices. The green matrix shows lighter spots rich in chlorite and secondary quartz.

PLATE 5, Figure 17 - Non-patchy spilite (668 feet) vesicles and veins of plagioclase and calcite.

PLATE 5, Figure 18 - Non-patchy spilite (761 feet amygduloid zone) containing large vesicles filled with chlorite, calcite and plagioclase. The veins consist mainly of calcite.

# PLATE 5


FIGURE 16 492 FT.


FIGURE 17 668 FT.

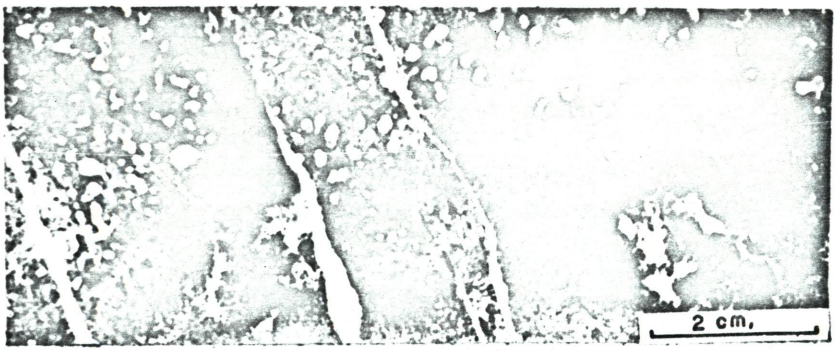


FIGURE 18 761 FT.

microlites, calcite, chlorite, and magnetite (Plate 3, Fig. 10).

This local increase in vesicularity could indicate that the non-patchy spilite zone (650-847 feet) was originally a separate flow from the above patchy spilite zone. Volume percent vesicles and the size of the vesicles in some submarine basalts was shown by Moore (1965) to be related to water depth covering the lavas. If the non-patchy spilites were originally similar in composition to the basalt of Moore (1965), then one might suggest that the non-patchy zone was extruded at a relatively shallow water depth before the above patchy spilite zone. However, this later consideration is questionable since no evidences of discontinuity or sharp contact of two different flows were noticed in the spilite. Instead, textural features and mineralogical associations indicate a certain continuity within one spilite flow. Hence, it is most likely that the vesicularity increase at 695-710 and 761 feet in the core indicates an original volatile rich magma which has concentrated most of its fluid phase within a certain zone. With the increase of volatiles, more chlorite and calcite veins or amygdules will occur. This is also what is observed near the bottom of the spilite flow.

## Brecciated Spilitic Rocks

This type of rock occurs between 1003 and 1180 feet in the core and consists mainly of calcite, chlorite, epidote and quartz. Plagioclase is much less abundant than in the spilite. The general textural feature of this zone is sheared; strained and rounded quartz grains

occur in a recrystallized matrix containing chlorite, quartz, and occasional albite and sphene.

The pilotaxitic and variolitic texture encountered on the spilite of the upper part of the core is less distinct due to the obliteration of texture with the exception of occurrences of spilitic rocks at 1060-1070 feet and around 1100 feet. These spilites consist of a fine-grained variolitic texture with zones enriched in epidote.

Pseudomorphs (up to 3 mm. in length) of replaced minerals of amphibole shape (prismatic) occur at 1096 feet (Plate 3, Fig. 11). These pseudomorphs (5%) are composed of mainly epidote and minor amounts of chlorite, and they are set into a fine-grained plagioclase-quartz-chlorite-epidote assemblage. Phenocrysts ($\simeq$ 30%) of plagioclase partially replaced by epidote abound throughout this thin section.

Veins, 0.5 to 1 cm. thick, of calcite, epidote, and quartz are scattered towards the bottom of this brecciated rock. It is often difficult to identify the groundmass of these rocks but sometimes the clear flow texture of the chlorite flakes accompanied with magnetite granules and epidote indicates that some type of cataclastic deformation has occurred (Plate 3, Fig. 12). This later textural feature is emphasized mostly towards the bottom of this brecciated zone, in the vicinities of the keratophyre flow, not included in this study, where angular fragments ($\simeq$ 1 cm. in diameter) of keratophyre breccia occur at about 1130 feet. Fluidal textural features were also observed around amygdules of epidote at 1131 feet and at the margin of some relatively thick calcite veins due to the parallel arrangement of

plagioclase laths in proximity to the vein. This later occurrence was observed close to the andesine-diabase dike, at about 1012 feet in the brecciated zone.

## Dike Rocks

Amphibole Porphyry. These are dike rocks with chilled margins. There is alteration product, as calcite and epidote replacement increase, towards the margin with a relative decrease of amphiboles. The general texture is porphyritic characterized by euhedral phenocrysts of feldspar set into a dense, fine-grained groundmass. The amphibole contains inclusions of calcite and chlorite; sometimes the green hornblende shows a concentric rim of calcite and chlorite at its edge.

The groundmass is xenomorphic and consists of plagioclase, calcite chlorite, magnetite and occasional epidote grains. Sericite occurs as the main alteration product of the feldspar phenocrysts. The tiny fibers of micas are mostly concentrated at the center of the crystal and represent the alteration product of a calcic plagioclase.

Albite-Diabase. The upper albite-diabase dike differs from the bottom andesine-diabase dike mostly by the anorthite content of the plagioclase, which varies between $An_4$ and $An_{10}$. Also, the chlorite content is slightly higher and the plagioclase content lower than the bottom, andesine-diabase dike; other major differences are the presence, in the upper dike (albite-diabase), of "clear" pyroxene with no pinkish rim, and an increase in sphene. These rocks are usually holocrystalline with a subophitic texture and there is a tendency of the plagioclase

to be porphyritic. The coarser plagioclase laths are strongly seritisized, and pyroxene granules and chlorite are included. The plagioclase shows a strong undulatory extinction which is emphasized mostly in the larger grains.

The clinopyroxene determination by index of refraction and X-ray methods indicates a more calcic member of the augitic family than the bottom dike. The main alteration product of pyroxene is chlorite. The low temperature mineral assemblages (epidote, calcite, chlorite, and also sphene) are generally more abundant in the albite-diabase dike than the andesine-diabase dike. The distribution of plagioclase in the albite-diabase dike is usually the same or slightly higher than the spilite flow (Fig. 9).

Chlorite composition was determined by X-ray methods (Brindley and Gillery, 1956; Schoen, 1962 (Table 5). This later result shows that chlorite in the albite-diabase dike is richer in magnesium and poorer in iron than the bottom andesine-diabase dike. The composition of the chlorite follows closely the composition of the pyroxene. The dike's border zone near the spilite flow is finer grained and shows an increase in the alteration product of the pyroxene, which is almost completely replaced by chlorite. This border zone also shows a general increase in chlorite, and the plagioclase has lesser undulatory features, probably because it is secondary. Veins of calcite are more abundant here, also, it is probable that the quenching effect due to a rapid cooling of the magma and the availability of volatiles from the wall rock has concentrated more low temperature

assemblages at the border zone of the dike and has also concentrated calcite minerals into late fractures (veins).

Andesine-Diabase. The andesine-diabase rock differs from the upper albite-diabase rock by the anorthite content of the plagioclase in the former ($An_{28-42}$). The andesine-diabase rocks are holocrystalline granular with ophitic to subophitic texture. In places the grain size increases generally but there is no tendency toward a bimodal size distribution (porphyritic), since the size of the matrix also increases proportionally. The plagioclase shows undulatory extinction due to the presence of secondary albite crystals which have a different orientation. Occasional sericite flakes occur as inclusions in the plagioclase. The coarser crystals of plagioclase contain a narrow rim of sericite due to magmatic alteration during the crystallization of the plagioclase. This may also indicate that the magma was enriched in volatiles even prior to the late magmatic crystallization.

The pyroxene is a clinopyroxene of augitic composition. This mineral occurs usually as rounded grains filling the interstices between idiomorphic plagioclase laths. The pyroxene has a pinkish rim probably reflecting the presence of titanium and iron. The main product of pyroxene alteration is chlorite and, in places, needles of actinolite surround the crystal. Some of the coarser pyroxene shows a complete replacement by chlorite. Granules of pyroxene were observed to be concentrated between cleavage planes of the plagioclase.

Chlorite is not abundant in these rocks and usually occurs as interstitial material associated with granules of magnetite between

plagioclase laths. The interstitial chlorite is probably due to a later alteration of pyroxene.

The accessory minerals, which consist of epidote, calcite, and quartz in thin veinlets, are concentrated toward the border zone of the dike where the chlorite content also increases. At about 950 feet, in the dike, there is a thin zone composed of contorted veins of calcite, epidote, and quartz-chlorite-sphene assemblages. The quartz shows undulatory extinction and the chlorite crowded with magnetite surrounds most of the rounded grains of quartz. The coarsest plagioclase laths contain inclusions of epidote and chlorite. These rocks have a general brecciated appearance due to their semi-fluidal texture.

# SUMMARY OF THE MINERALOGICAL AND PETROLOGICAL INVESTIGATIONS

The mineralogical and petrographical study of the core shows the following main results:

1. Plagioclase ($An_2$-$An_{11}$) occurs in the spilite, brecciated zone, and in the upper albite-diabase dike. Andesine oligoclase occurs in the lower andesine-diabase dike. The albite of the amphibole porphyry has about 5% orthoclase.

2. The clinopyroxene, phenocrysts and microphenocrysts, decrease with depth in the spilite flow. Below a certain depth, approximately 650 feet, the clinopyroxene appears to be more deeply altered and only relic crystals occur. The composition of the pyroxene in the spilite and albite-diabase dike is close to a diopsidic augite and becomes titanaugite in the andesine-diabase dike.

3. The chlorite content increases with depth in the spilite flow. The chlorite is diabantite in the spilite, in the brecciated zone, and in the albite-diabase dike and aphrosiderite in the andesine-diabase dike.

4. The minerals pumpellyite and prehnite disappear with depth in the spilite flow. Actinolite occurs throughout the core and hence cannot be considered a characteristic mineral for distinguishing the different metamorphic grades in the core.

5. The mica minerals encountered near the top of the spilite flow (patchy spilite zone) are of two kinds: a) muscovite (sericite) as a product of alteration of plagioclase and b) green biotite, which

is less common than the muscovite. This biotite is fine grained, with prismatic habit, no trace of resorbtion, and it is associated in chlorite - filled vesicles.

6. The upper 847 feet of the spilite flow is divided into a patchy and non-patchy zone. The patchiness decreases with depth in the flow.

7. The main difference between the dark patches and their green matrix consists in their degree of alteration. The dark patches contain more phenocrysts of fresh clinopyroxene and less low-temperature minerals such as epidote, chlorite, calcite and quartz. On the other hand, the green matrix is enriched in the latter minerals, and in addition it contains veins and veinlets of these low temperature assemblages. The clinopyroxene of the green matrix shows alteration into chlorite and actinolite.

8. The texture and mineral distribution of the green matrix, subparallel arrangement of plagioclase laths, chlorite flakes included in vesicles and the increase of low temperature minerals of the patchy zone indicate that this green matrix may have been originally glassy. The dark patches were solidified prior to the matrix. This is emphasized by the fluidal textural feature of the transitional zone which indicates that interstitial liquid between the two zones of the green matrix and the dark patch occurred after the partial or complete crystallization of the dark patches.

9. The non-patchy spilite zone (650-847 feet) belongs to the same flow that originated the above patchy spilite zone. The increase in

vesicularity in certain areas of the non-patchy spilite zone indicates an enrichment in volatiles within these zones or a difference in physical conditions leading to a difference in mode of segregation and, ultimately, escape of the volatiles.

10. From the dark patches towards the green matrix of the rock the vesicles and amygdules vary in shape but there is no evidence of their decrease in size or content. The vesicles of the dark patches are well rounded and the vesicles of the green matrices have tendencies to be elongated or irregular in shape. Evidence has been found that the vesicles or amygdules are formed during the last stage of magmatic crystallization. This is well illustrated at 707 feet in the non-patchy spilite zone where the amygdules show an elongated or ellipsoidal shape presumably towards the direction of flow. These amygdules consist of calcite, quartz and feldspar and are set into a groundmass of plagioclase laths associated with iron bearing mineral granules and chlorite.

11. The bottom brecciated zone contains relics of textures and mineralogical assemblages (abundant laths of plagioclase, chlorite, epidote) very similar to the above spilite flow which may indicate an extrusive origin for this zone. This brecciated zone shows also a sheared texture (breccia fragments) and fluidal arrangement of chlorite flakes concentrated mostly near the bottom of this zone.

12. The contrast in texture between the spilite and the dikes suggests that these rocks were not solidified in the same way. The fine grained spilites are extrusive and have crystallized in a shorter period of time than the dikes.

13. The dike rocks consist of amphibole porphyry, albite-diabase, and andesine-diabase, and show lesser amounts of low temperature assemblages such as epidote, chlorite, and calcite than do the spilite and brecciated zones.

# MAJOR - ELEMENT CHEMISTRY

## General Statement

The chemical analyses of the rocks sampled from the Virgin Island core are listed in Table 10, 11 and 12, and the variation of their oxides with depth is shown in figure 9. The $SiO_2$ shows generally the lowest values towards the base of the patchy spilite zone (Fig. 9). The $TiO_2$ content is less than 0.60 percent in average but it is slightly higher at the bottom of the spilite flow. The $Al_2O_3$ content (15.40 average percent) remains essentially constant throughout the spilite. The total iron as FeO and MnO follow the same trend as $TiO_2$, and are higher in the lower part of the spilite flow. The MgO content does not show any noticeable variation with depth in the spilite flow. The CaO content is higher in the bottom brecciated spilite zone than the above spilite (Fig. 9). The amount of $K_2O$ decreases markedly with depth with extensive scattering of values in the upper part but consistently low values below the patchy spilite zone (Fig. 9). $Na_2O$ is quite variable, but it seems to be higher at the base of the spilite flow (5.0 average percent) and lower in the brecciated spilite zone (0.7 average percent). In general the brecciated rocks are also depleted in $SiO_2$ and $K_2O$, except for certain zones containing relics of spilitic rocks (see petrography) comparable to the overlying spilite flow. The $TiO_2$ content of the brecciated zone is relatively high (0.90 average percent). MgO and FeO have also increased slightly in this zone (Table 10 and 11).

The chemical composition of the dike rocks shows different

Figure 9. Variation diagram of different oxides plotted against depth in the core. (●) Spilite; (O) Amphibole Porphyry Dike; (×) Albite Diabase Dike; (▽) Andesine Diabase Dike; (R) Relic of spilitic rocks and ($R_1$) Relics of amphibole pseudomorph bearing rocks.

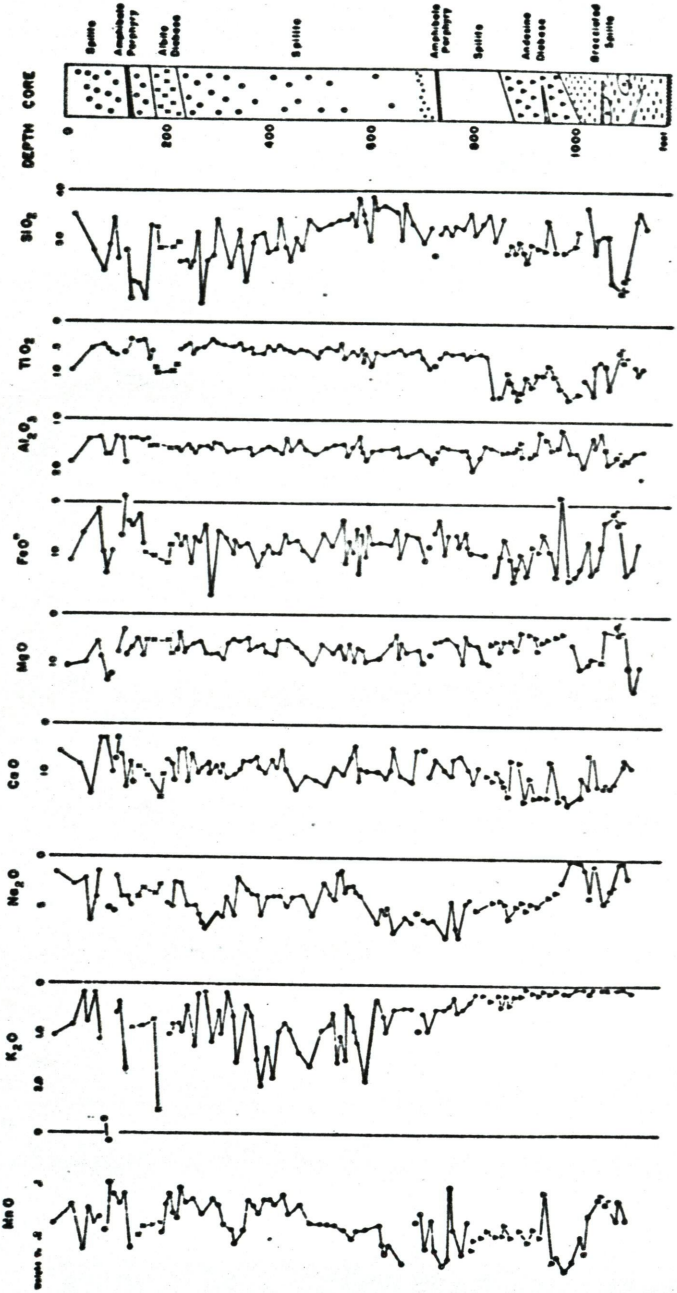
Spilite
Amphibole Porphyry
Albite Diabase
Spilite
Amphibole Porphyry
Spilite
Andesine Diabase
Brecciated Spilite
DEPTH CORE
0
200
400
600
800
1000
feet
SiO2
TiO2
Al2O3
FeO*
MgO
CaO
Na2O
K2O
H2O

patterns of variabilities between these rocks. The dike rocks differ in their chemistry from the spilite and the brecciated rocks encountered in this section of the core. The amphibole porphyries show higher $SiO_2$ (55.2 percent in average) than the albite and andesine-diabases (49.5 and 46.4 percent average respectively). The $TiO_2$ of the amphibole porphyries (0.6) is less than the albite and andesine-diabases (0.9 and 1.1 percent in average respectively). The FeO follows similar distribution to the $TiO_2$. Total iron as FeO and CaO appear to be high in content within the albite and andesine diabase dikes (FeO = 10.2, CaO = 10.6 and FeO = 10.1 and CaO = 10.6 percent average respectively). The MgO content of the amphibole porphyry is comparable to the albite and andesine-diabase dikes. The main differences between the dike rocks are in their potassium and sodium content. The $K_2O$ content of these dikes decreases from the amphibole porphyries to the albite-diabase and the andesine-diabase (2.6, 1.2 and 0.2 percent in average respectively). The $Na_2O$ content is higher in the amphibole porphyry (5.0 percent in average) than the albite and andesine-diabase (3.3 and 4.3 percent in average respectively).

## Chemistry of the Spilite

The chemical analyses of the spilites from the core are listed in Table 11 . The average of these analyses is compared to the averages of spilites which Wells (1923), Sundius (1930) and Donnelly (1966) have analyzed from other locations (Table 10). The spilite of the core shows lower $TiO_2$ (0.6 percent) and FeO (8.6)but higher MgO (7.4) and CaO (8.0) than the average spilites from previous analyses

(Table 10). The $SiO_2$, $Na_2O$ and $K_2O$ appear to be similar to the values previously reported. However, the very low $K_2O$ content (about .05) of the oceanic spilitized basalts (Melson and Van Andel, 1966 and Cann and Vine, 1967) do contrast markedly with the spilite of the core (Table 10).

The spilite of the core is subdivided into two types according to their different textural features (see petrography): The patchy spilite typical of the upper part of the flow, and the non-patchy spilite which becomes more abundant with depth. The bulk chemical analyses of the different zones are listed in Table 11. The slight increase of silica is accompanied with an increase of $K_2O$ near the top of the core (Fig. 9). The high $SiO_2$ content above about 350 feet (Fig. 9 and 10) is related to the increase of dark patches.

$Al_2O_3$ and CaO do not vary considerably with depth (Fig. 9). The average $Al_2O_3$ content of the above mentioned patchy zone and the non-patchy zone is 15.4 and 15.2 respectively. Other oxides showing minor variation with depth in the spilite flow are $TiO_2$ and FeO. The dark patches have a $TiO_2$ content around 0.5 percent and an FeO content around 10 percent (Fig. 12), which is comparable to the average $TiO_2$ (0.7 percent) and FeO (9.0 percent) of the non-patchy spilite. The MgO content of the dark patches and surrounding matrices is higher in the upper part of the patchy spilite zone than the bottom part of this zone (Fig. 12).

Figure 10. $K_2O$ and $Na_2O$ variation diagram of spilite (●) and brecciated spilite rocks (○).

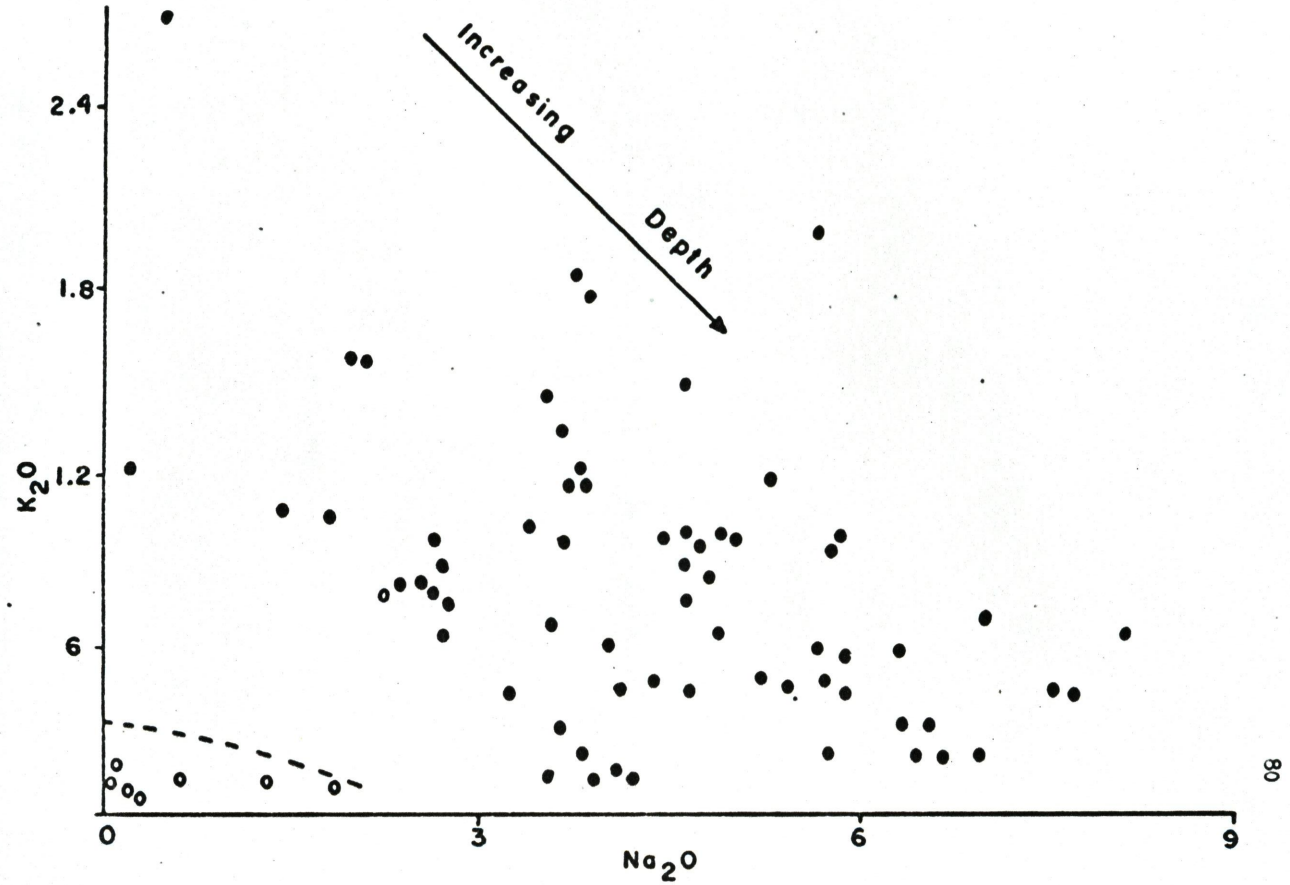
Increasing
Depth
2.4
1.8
1.2
6
$K_2O$
0
3
6
9
$Na_2O$
80

## Alkali Variation in the Spilite Flow

The differences between the patchy spilite and the non-patchy spilite zone is emphasized mainly by their respective variation in alkalis. The patchy spilite is depleted in sodium near the top of the flow and enriched in potash. The $K_2O$ content is lower than 0.60 percent between 200 and 300 feet, and higher than 0.70 percent between 300 and 650 feet (Fig. 9). Below 650 feet, there is another continuous decrease of $K_2O$ down to the bottom of the section studied. Separate analyses of the patches and their respective matrices of the upper part of the flow show that the $K_2O$ content is concentrated in the green matrices and that the dark patches are generally depleted of this oxide (Fig. 12).

The $Na_2O$ content of the spilite flow is quite variable but a general trend is one of increasing with depth down to about 850 feet (Fig. 9, and 10). The $K_2O$ content seems to follow an opposite trend to $Na_2O$. This is illustrated in figure 10. The lower left corner of the diagram (Fig. 10) shows the field of the bottom brecciated zone of the core to be depleted in both potassium and sodium.

Figure 11 shows a decrease of $K_2O/K_2O+Na_2O$ ratio with depth from the patchy to the non-patchy spilite zone. The atomic percent calculation of Kx100/Na+K ratio gave a value of 11.1 and 5.0 in the patchy and non-patchy zone respectively. The brecciated spilite zone shows a $K_2O/Na_2O+K_2O$ ratio higher than the above non-patchy spilite zone and similar to the patchy spilite (Fig. 11).

Figure 11. Variation diagram $K_2O/Na_2O+K_2O$ versus depth in the core. (Am.P) Amphibole-porphyry dike, (Al.D) Albite-diabase dike, (Sp.) Spilite, (An.D) Andesine-diabase dike, (B.) Brecciated spilite rocks.

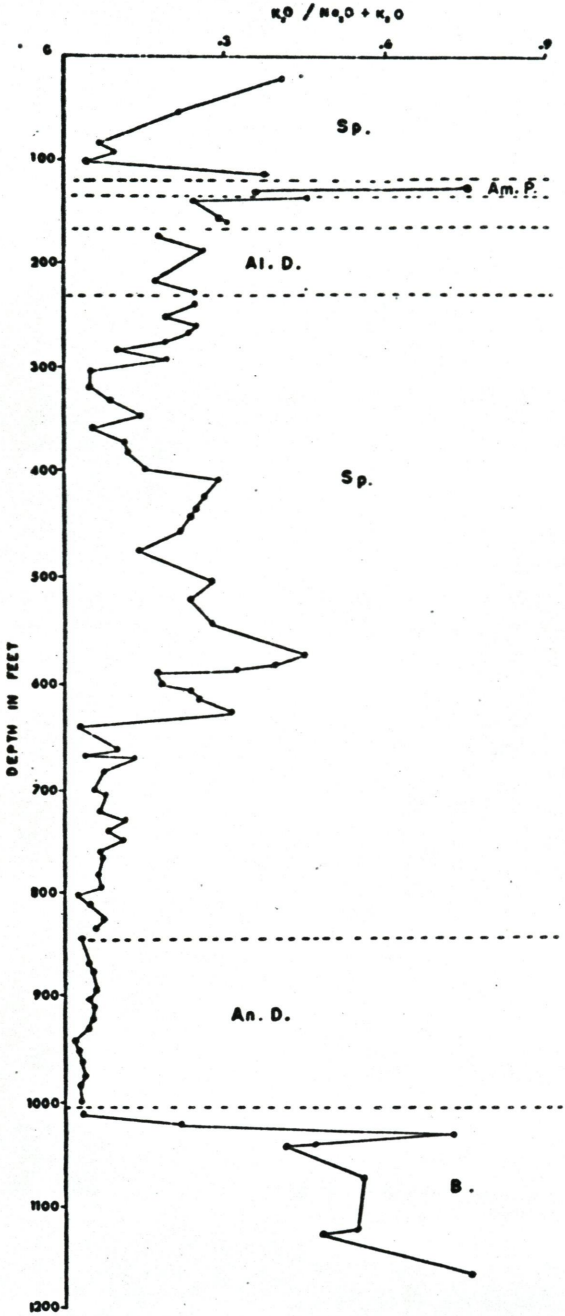
$K_2O / Na_2O + K_2O$
.3
.6
.9
0
100
200
300
400
500
600
700
800
900
1000
1100
1200
DEPTH IN FEET
Sp.
Am. P.
Al. D.
Sp.
An. D.
B.

## Chemistry of Dark Patches and Green Matrix of the Spilite Flow

The patches are dark colored zones of various, but generally rounded, shapes, having diameters as large as 6 cm. and set into a green colored matrix (see petrography). Thirty-four chemical analyses of the patchy spilite were made. Each pair of analyses represents a dark patch and its surrounding green matrix. The boundary between the dark patches and green matrix is the transitional light green zone (see petrography) which divides the two. Chemical analyses are listed in Table 12 and the variation diagram of the different oxides are plotted against depth in Figure 12. There is not a continuous trend of variation with depth within each zone, with the exception of MgO and $TiO_2$. The total iron (as FeO) does not seem to be included only into the chlorite or the clinopyroxene phenocrysts but also occurs as magnetite granules scattered throughout the groundmass of the dark patches. This also explains the irregular behavior of the iron trend between the dark patches and the green matrix of the spilite flow.

Figure 13 shows a generally negative trend between the $K_2O$ (molecular percentages) and $Na_2O$ content between the dark patches and their corresponding green matrix. The zones at 119-163 and 379-446 feet show a positive trend of $K_2O$ and $Na_2O$ variation between each pair of samples with a $K_2O$ content usually higher than 1 percent (weight percent). These latter zones usually contain biotite (see mineralogy). The same diagram (Fig. 13) shows also a field of a relatively low $Na_2O$ content of the green matrix ($<3$ percent by weight). This zone of low sodium

Figure 12. Chemical analyses of the dark patches (●) and their corresponding green matrices (○) varying with depth in the upper part of the core.

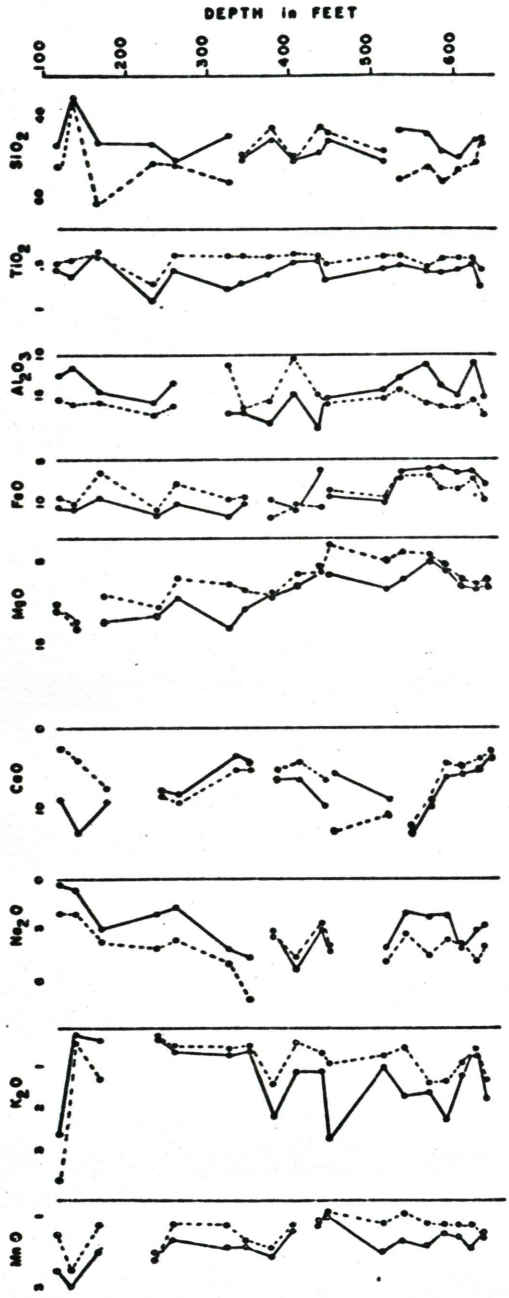
DEPTH in FEET
100
200
300
400
500
600
SiO2
TiO2
Al2O3
FeO
MgO
CaO
Na2O
K2O
MnO

Figure 13. $K_2O$ - $Na_2O$ Molecular Percentage variation diagram of dark patches (●) and their corresponding green matrices (O) related with a solid tie-line.

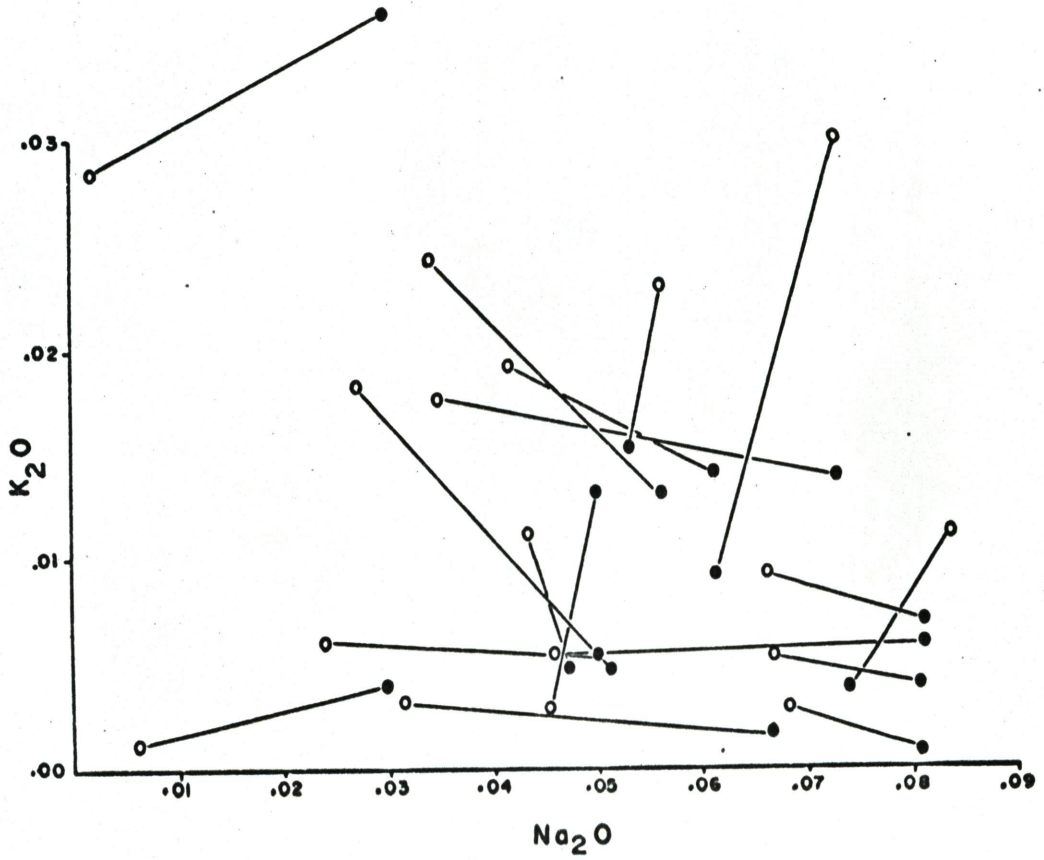
.03
.02
.01
.00
$K_2O$
.01
.02
.03
.04
.05
.06
.07
.08
.09
$Na_2O$

Figure 14. $TiO_2$ - FeO variation diagram for dark patches (●) and green matrices (○) of the spilite.

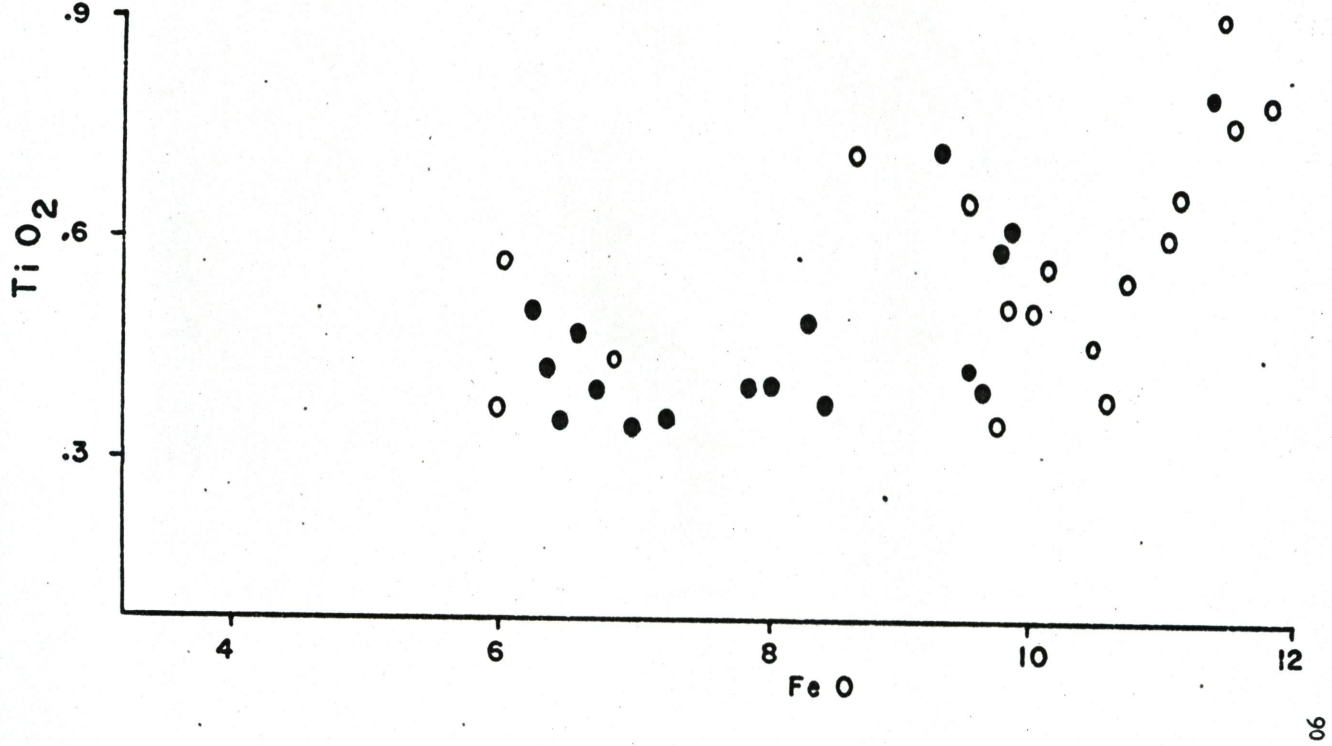
.9
.6
.3
Ti O2
4
6
8
10
12
Fe O

content also occurs at 119-163 feet and it is accompanied by a relative increase in CaO content.

The $Al_2O$ and CaO do not show any consistent trends of variabilities with depth or between dark patches and surrounding green matrices (Fig. 12). The $Al_2O_3$ is lower in the dark patches than in the green matrices above 300 feet and below 450 feet. Between 300 and 450 feet the $Al_2O_3$ content is higher in the dark patches than the green matrices (Fig. 12). The CaO variation of the dark patches and corresponding green matrices is irregular and less consistent than $Al_2O_3$ (Fig. 12).

The MgO content of the green matrices is generally higher than the corresponding dark patches, with the exception of sample 134, (Fig. 12). The magnesium trend for both patches and matrices decreases slightly below about 400 feet (Fig. 12). The titanium and iron follow similar trends; the green matrix tends to be usually higher in both $TiO_2$ and FeO (Fig. 14). In summary, the green matrix surrounding the dark patches is enriched in $K_2O$, $TiO_2$, MgO and variable in FeO; however, $Na_2O$ and to a lesser extent $SiO_2$ are depleted in the matrix.

## Chemistry of Brecciated Spilitic Rocks

The brecciated rocks occur at the bottom of the section studied here. This zone is limited in its upper part by the andesine-diabase dike and its lower part is at contact with a keratophyre flow not included in this study. Chemical analyses of nine brecciated rocks are listed in Table II. The brecciated rocks are abundantly veined and

sheared, sometimes including small fragments of keratophyres (see petrography).

The chemistry of this brecciated zone indicates an enrichment of MgO, FeO, and $TiO_2$ (8.8, 10.8, and 0.90 average percent respectively), and lower $Na_2O$, $K_2O$ and $SiO_2$ (0.7 and 0.1 and 46.5 average percent respectively (Table 10 and Fig. 9). The average $Al_2O_3$ content is around 17.0 percent.

## Chemistry of Later Dikes

Three types of dikes, one andesine-diabase dike, one albite-diabase dike, and two amphibole porphyry dikes, were encountered at 847-1003 feet, 177-266 feet, 129-134 feet and 732 feet respectively.

Chemical analyses of andesine-diabase (15 samples), albite-diabase (4 samples), and amphibole porphyry (3 samples) are listed in Table 13. All the dikes encountered in the core have a comparable average MgO content (5.6, 5.8, and 6.0 percent respectively). However, the average FeO content of the albite and andesine-diabase (10.1 and 10.2 percent respectively) is higher than the amphibole porphyry (7.5 percent). The type of dikes encountered in the core differs in their alkalis and silica content. Figure 15 shows the variation diagram of $SiO_2$ and total alkalis for these dikes. The major difference is emphasized by the higher alkalis and $SiO_2$ content of the amphibole porphyry with respect to the andesine and albite-diabase dikes (Fig. 15). The main differences between the alkali content of these dikes is the potash variation with depth, as noticed in the spilite flow. The $K_2O$ content of the amphibole

Figure 15. $SiO_2$ - $(Na_2O+K_2O)$ weight percent variation diagram for dike rocks.

● Amphibole Porphyry

X Albite-Diabase

▽ Andesine-Diabase

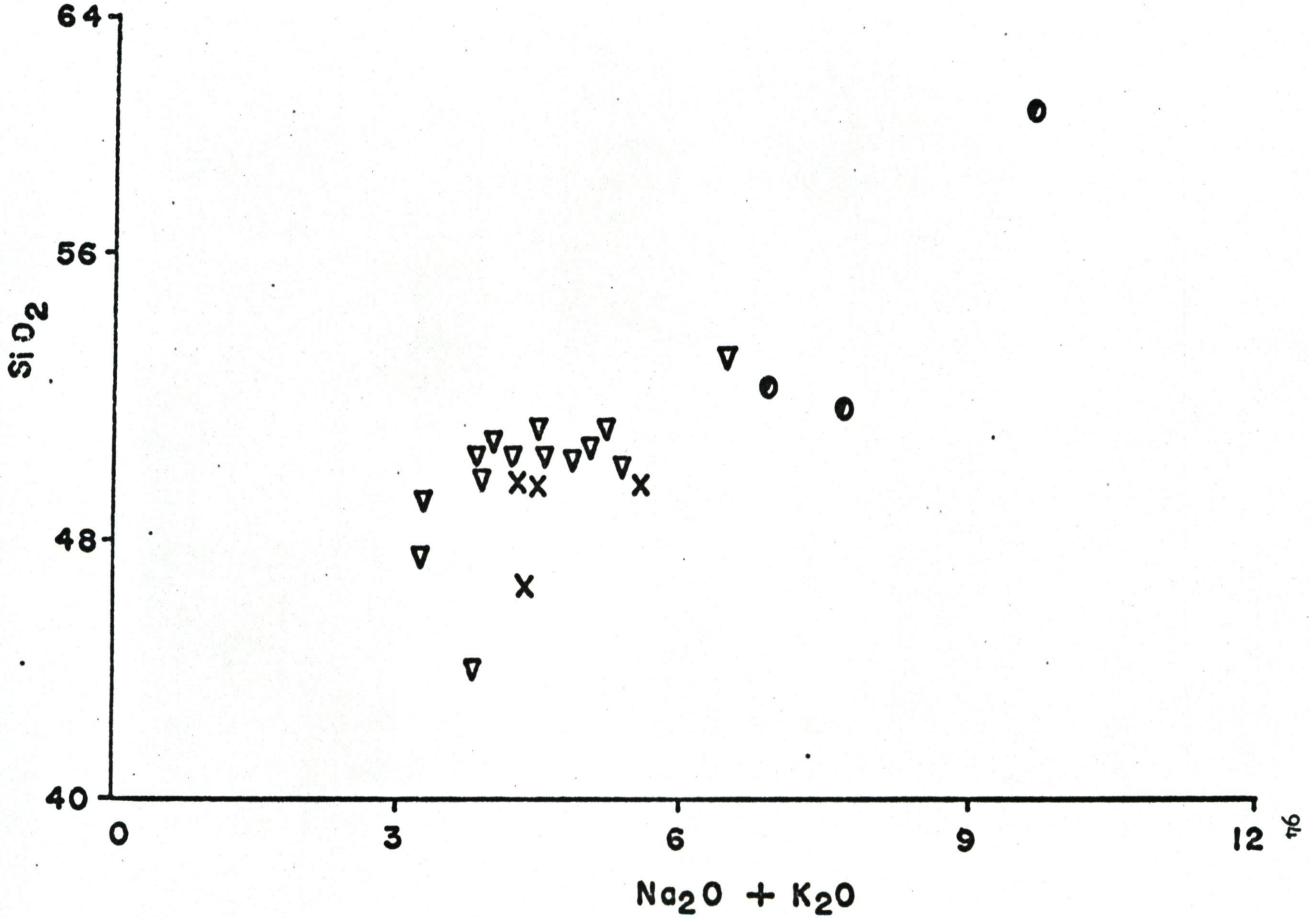
64
56
48
40
SiO2
0
3
6
9
12
%
Na2O + K2O

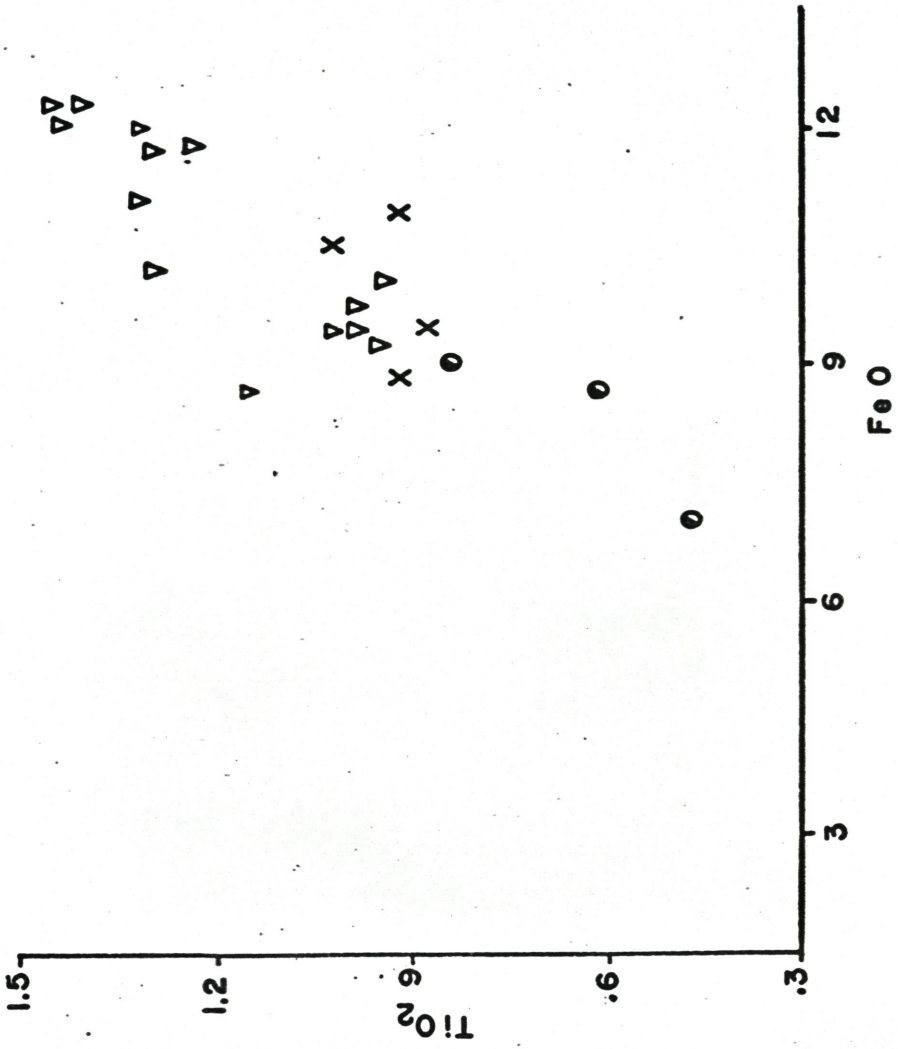


Figure 16. $TiO_2$ - FeO variation diagram for dike rocks. (●) Amphibole porphyry, (×) Albite diabase and (▽) Andesine diabase.

porphyry dike at 732 feet depth in the core is lower (0.96) than the upper amphibole porphyry dike at 129-134 feet (3.45 average). Similar variation applies between the bottom (847-1003 feet) andesine-diabase dike and the upper (177-226 feet) albite-diabase dike. Figure 9 shows a high $K_2O$ and a low $Na_2O$ content of the upper dike while the reverse trend is true for the bottom dike.

The distribution of $Al_2O_3$ and CaO is less variable between the andesine and albite-diabase dike (average $Al_2O_3$ = 13.8%, CaO = 10.6%, and $Al_2O_3$ = 14.4%, CaO = 10.6% respectively) and the amphibole porphyry, which has an average $Al_2O_3$ up to 16.8 percent and CaO is lower (4.8 average percent) with respect to the other dikes. The relative low $Al_2O_3$ content in the andesine-diabase and albite-diabase with the relative high CaO content indicates that these zones are poor in plagioclase or alkalis with respect to the amphibole porphyry.

The $TiO_2$ content varies between the dikes: the andesine-diabase and the albite-diabase have an average of 1.14 and 0.87 percent respectively while the amphibole dikes average around 0.63 percent. Figure 16 shows a continuous decrease of FeO towards the amphibole porphyry. The andesine-diabase has the highest $TiO_2$ and FeO and the lowest total alkalis content within the dike rocks.

## Summary of the Chemical Investigation

The chemical study of the core shows the following main results:

1. The $Na_2O$ content increases with depth in the spilite flow below about 700 feet (non-patchy spilite zone).

2. The $K_2O$ content decreases sharply below about 700 feet. This decrease of potassium characterises both the spilite flow and the later dikes.

3. The brecciated rocks at the bottom of the spilite flow are enriched in titanium, magnesium and to a lesser extent in iron. This brecciated zone is also considerably depleted in sodium and to a lesser degree in potassium.

4. The dark patches are enriched in silica and sodium. The green matrix has more magnesium, titanium and potash than the immediate dark patches.

5. The dike rocks are enriched in $TiO_2$ with respect to the spilite flow.

6. The FeO/MgO ratio of the albite-diabase and the andesine-diabase are comparable. The FeO/MgO ratio of the amphibole porphyry dikes is much lower than the albite and andesine-diabase dikes.

# PETROGENESIS

## General Statement

The problem of the origin of spilitic rocks is related to the genesis of their low temperature mineral assemblages, consisting of albite, chlorite, epidote, quartz, actinolite, pumpellyite and prehnite. In addition to these minerals, biotite and relics of calcic plagioclase were encountered in the spilite flow of the core (see petrography). Although the presence of intersertal and pilotaxitic texture is typical of many extrusive igneous rocks, the mineralogical assemblages (prehnite-biotite-pumpellyite) of the spilitic rocks are not those of normal mafic igneous rocks.

A certain heterogeneity exists within the spilite flow. The concentration of dark patches surrounded by the green matrices probably reflects a mode of submarine eruption where the patch and matrix material were intimately erupted together. The chemistry of the flow shows a certain pattern of mobility of the alkalis. This variation is not uniform throughout the core and the decrease of one oxide does not seem to necessitate an equivalent increase of another (example, $Na_2O$ - $K_2O$ variation).

Additional facts which appear to be relevant for the evaluation of significant processes that could have given rise to the present heterogeneous texture and chemistry of the spilite and associated rocks are listed below and will be discussed later.

1. The potash and sodium relationship with depth in the core.
2. Variation of mafic compounds with depth in the core.

3. The potash and sodium relationship between dark patches and their immediate green matrix.

4. Systematic potassium variation with depth and the significance of locally high potassium concentration in certain zones of the upper spilite flow and dike rocks.

5. Distribution and occurrence of biotite within the upper part of the spilite flow.

The complicated aspect represented by the mineralogical occurrences and the chemical variations of the different lithologic units of the core together with the geological setting of the core suggest the consideration of several independent processes (autometasomatism, metamorphism). The possibility of the effect of the combined processes and criteria for their separation will be discussed. Finally the most probable explanation for the present appearance of the spilite will be considered and diagnostic criteria evaluated.

## Petrogenesis of Spilite

The spilite represents the extrusive phase of a mafic magma which has undergone some redistribution of the major components. The origin of the emplacement of the spilite is believed to be related to the explanation of the occurrence of the dark patchy zones and their relationship with the massive non-patchy spilitic rocks.

Origin of Patches. In order to explain the concentration of the different cations within the patches and their groundmass, two possible explanations may be given.

(1) The green matrices were originally centers of crystallization of early formed pyroxene and plagioclase altered by hydrothermal solutions. The patches formed later from residual fluid trapped between these crystalline centers of the green matrix. Potash migrated from the lower part of the spilite flow and was concentrated around the dark patches.

(2) The green matrix may represent a chilled margin, probably once glassy, and enriched in $K_2O$ and $H_2O$ while $SiO_2$ and $Na_2O$ were less abundant because they were fixed in a feldspar rich zone of the dark patches. The transitional zone, between the dark patches and the green matrix, shows a fluidal texture due to alignment of plagioclase laths parallel to the margin of the dark patches (see petrography). Hence the dark patches were crystallized shortly before their surrounding green matrix. Chlorite may be an alteration product from an original glassy groundmass. The relatively high $H_2O$ content of the basic lavas suggests mineral adjustments took place in aqueous environments. These could have occurred during cooling or after consolidation (Vallance, 1965). Once the bulk rock was crystallized, the glassy selvedge (green matrix) was transformed into chlorite while migration of $TiO_2$ and MgO from the dark patches was occurring simultaneously.

The second alternative seems to best explain the concentration of different cations in the patches and matrices of the spilite. The upper part of the core (patchy spilite) solidified faster than the rest of the flow. This relatively quick chilling contributed to the formation of an original glassy green matrix.

Relationship between Patchy and Non-Patchy Spilite. Potassium and sodium seem to have been the most migratory elements in the core. The vertical distribution of these elements showed that the dark patches and the bottom non-patchy zone are interrelated.

Alternative processes are considered to explain the textural mineralogical and the chemical differences between the upper patchy and the lower non-patchy zone of the spilite: (1) differentiation by crystal settling; (2) two different flows which changed composition during extrusion; (3) a single homogeneous flow and altered with later migration of certain ions.

(1) Evidence of a crystal settling process may be given by the increase in titanium, and a slight decrease in silica with depth. The lower part of the spilite flow, the non-patchy zone, is enriched in some compounds ($Na_2O$ = 5.8, $TiO_2$ = 0.6, and poor in others ($SiO_2$ = 47.3, $K_2O$ ≐ 0.5 average percent; Table 10). The same Table (10) shows a $Na_2O$ = 4.0, and $TiO_2$ = 0.6 in average values for the upper patchy spilite zone. Hence it is likely that a mild differentiation by crystal settling after the extrusion of the magma played a role in the formation of this portion of the core.

(2) If the patchy and non-patchy zone of the spilite flow are considered to represent separate flows, the two flows were extruded during a relatively short interval of time since no appreciable trace of sedimentary debris was noticed. The concentration of large vesicles (about 5 mm. in diameter) near the top of the bottom flow (at about 700 feet) may indicate a shallow depth of extrusion, or some type of isostatic

movement had decreased the water depth. The increase of $Na_2O$ and the decrease of $K_2O$ in the non-patchy zone could be due to the reaction with sea water. Potassium may have escaped into the sea water with a subsequent introduction of $Na_2O$. However, no contact was noticed between the upper patchy spilite and the lower non-patchy spilite. Both zones are envisioned as part of a single flow, thus invalidating the second alternative.

(3) Migration of ions throughout the spilite might have been an important process for the redistribution of certain major oxides. Silica, sodium and potash might be most affected by such a process. Since seritization of the plagioclase increases relatively near the top of the flow, it is likely that the $K_2O$ dissolved in the fluid solution had migrated upward in the core. The schematic diagram of Figure 17 summarizes the alkalis variation within the spilite flow. The same diagram shows the non-patchy spilite zone enriched in Na migrating from either the top or from the bottom of the core. The vertical migration of these alkalis in the core is also accompanied by a local exchange between the dark patches and the immediate green matrix (Fig. 17). The increase of veins within the spilite indicates that local redistribution of $Al_2O_3$, CaO, MgO and $TiO_2$ was more effective near the bottom. The veins, veinlets, and amygdules of calcite resulted from the decomposition of calcic plagioclase and Ca-rich clinopyroxene, since the composition of the clinopyroxene of the spilite is close to the composition of a pure diopside (Fig. 5). Wilshire (1959) also noticed the redistribution of calcium from decomposition of an original clinopyro-

Figure 17. Sketch of patchy spilite (left) showing the dark patches (D.P.) with fresh clinopyroxene and abundant rounded vesicles and the green matrices (G.M.) with calcite, quartz, epidote and occasional glassy "shard—like" texture of chlorite. Diagramatic variation (right) of alkalis in the spilite flow.

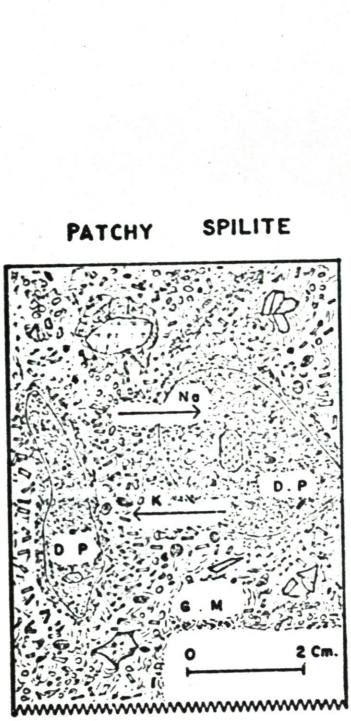
PATCHY SPILITE
Na
K
D. P
D P
G M
0
2 Cm.

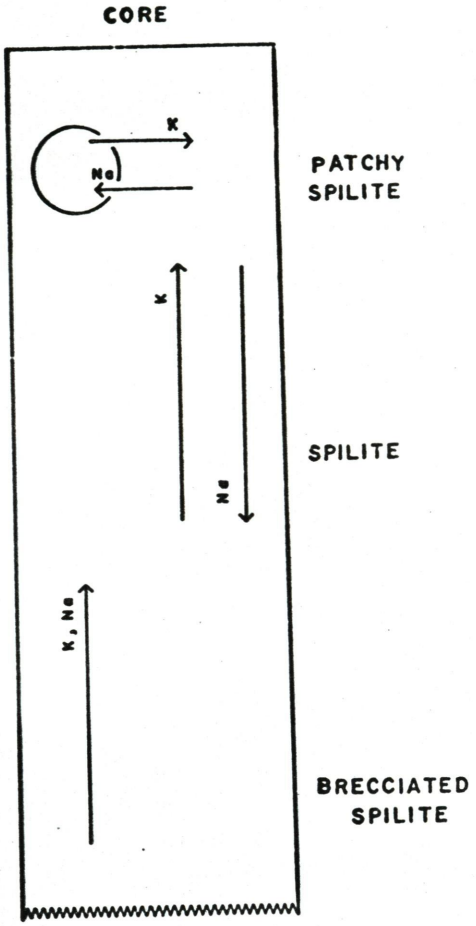
CORE
K
Na
PATCHY SPILITE
K
Na
SPILITE
K, Na
BRECCIATED SPILITE

xene in volcanic rocks. The formation of chlorite and calcite is attributed to the decomposition of an original pyroxene and calcium rich plagioclase.

Figure (9, 18, 19) shows the respective variation of mafic oxides with the combination of $SiO_2$ and alkalis. The MgO and $TiO_2$ do not show any strong pattern of variation with depth. It is unlikely that magnesium and titanium have migrated as effectively as sodium and potassium with the fluid solution. These mafic compounds were instead redistributed locally and the depth factor plays no part in their migrations.

In summary, the mild differentiation effected by crystal settling together with the later migration of elements seems to be the most plausible solution for the chemical variation in the spilite flow. The migration of elements may have been initiated during the last stage of cooling but it is equally probable that the migration may have arisen during burial metamorphism.

## Petrogenesis of the Brecciated Spilite Rocks

This zone, originally similar to the upper spilite flow, is an extrusive phase of a mafic magma. Veins and veinlets with lesser amounts of amygdules characterize the bottom part of the core studied here.

Relationship to the Spilites. The sheared texture and the veinations of these rocks seem to have masked the original fabric of this zone which makes any correlation with other rock types difficult. Heterogeneity in their texture is reflected by the different mineral associ-

Figure 18. $SiO_2$ - MgO variation diagram of spilite (●) and brecciated spilite rocks (o).

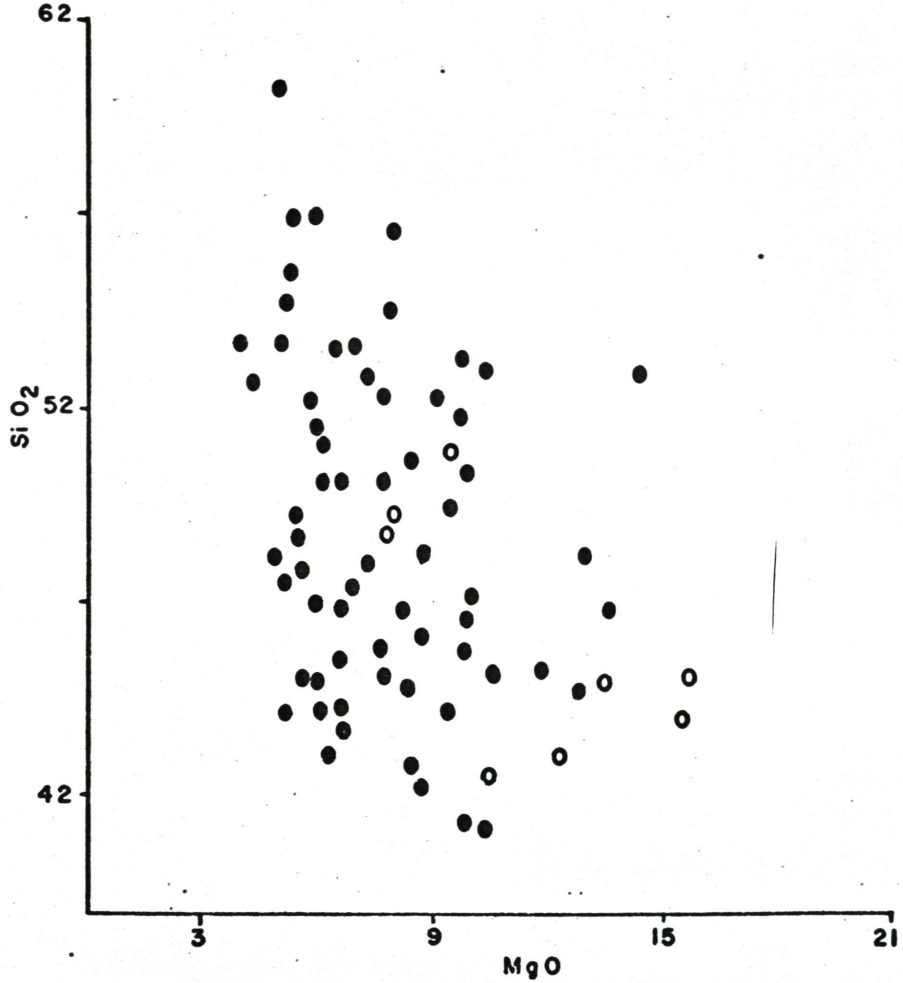
62
52
42
Si O2
3
9
15
21
MgO

Figure 19. Above. $TiO_2$ - ($Na_2O$ + $K_2O$) variation diagram for dike rocks.

Below. $TiO_2$ - ($Na_2O$ + $K_2O$) variation diagram for spilites (●) and brecciated spilite rocks (O).

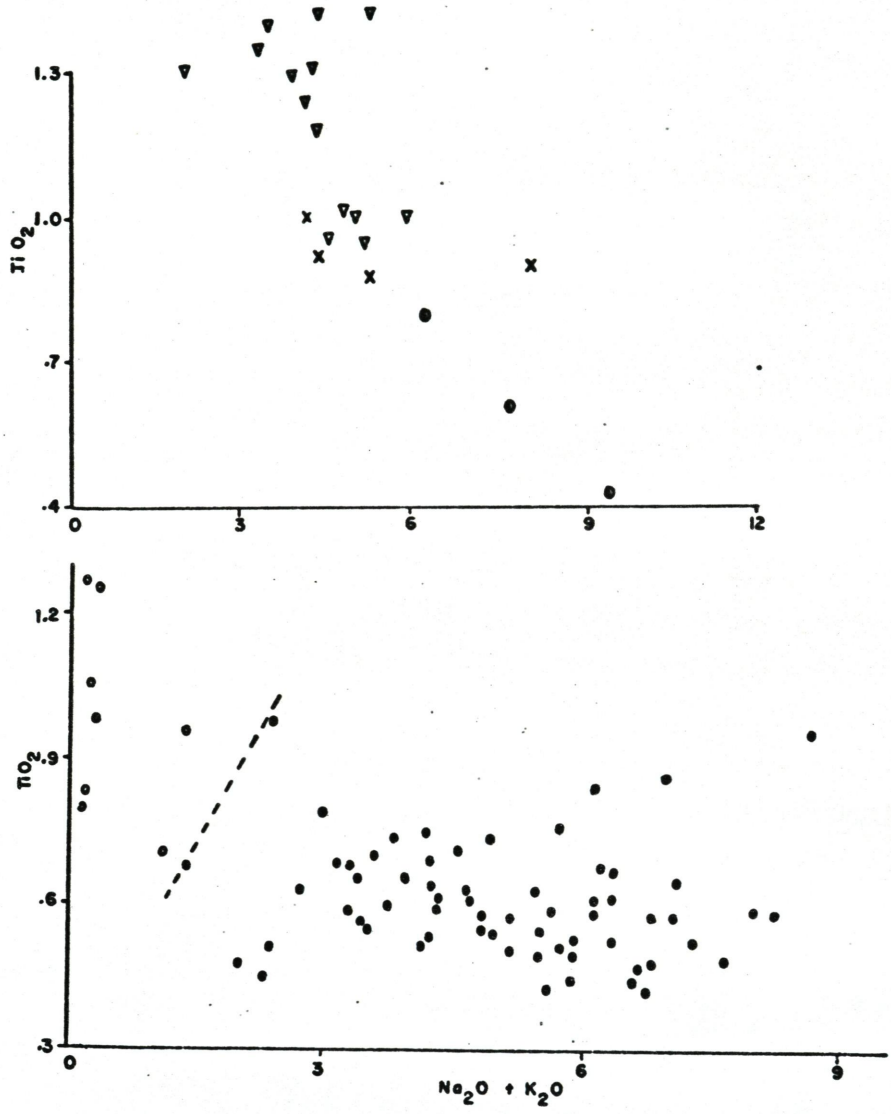
1.3
1.0
.7
.4
$TiO_2$
0
3
6
9
12
1.2
.9
.6
.3
$TiO_2$
0
3
6
9
$Na_2O + K_2O$

ations (see petrography). Large veins and veinlets (1051 feet) of quartz, epidote, calcite and preserved relics of spilitic rocks (1066, 1096, and 1145 feet) are the probable cause of dissimilarity in the chemistry. The decrease of one mineral type is accompanied by an increase of other mineral associations through veins and veinlets. It is believed that interstitial fluid solutions may have played an important role. This fluid solution was rich in volatiles and reacted with the early formed minerals, resulting in total destruction of the original texture and mineral association. Consequently, chlorite, secondary quartz, and epidote would be the new major mineral assemblage distributed throughout this brecciated zone.

The ratio of FeO/MgO in the spilite and in the brecciated zone is comparable (1.1 and 1.07 respectively) and this may represent the original ratio in the parental rock. In the ternary diagram (Fig. 20) AFM, the field of the brecciated rock lies close to the FeO/MgO join. If these rocks were formed independently from an originally differentiated mafic rock, we might expect a lower $SiO_2$ and a much lower $Al_2O_3$ content than observed in the brecciated zone. However the $Al_2O_3$ content of this zone is comparable to the above spilite (15.4 and 17.0 percent average respectively). Hence some type of differentiation could have occurred only within an original spilitic type of flow. During crystal settling pyroxene and lesser amounts of Ca-plagioclase separated. These minerals were later altered by fluid solution.

The increase in mafics and the relative decrease in felsics may also indicate an early differentiation process by crystal settling. The

Figure 20. MgO - FeO - Alkalis variation diagram of spilites (●) and brecciated spilite rocks (O).

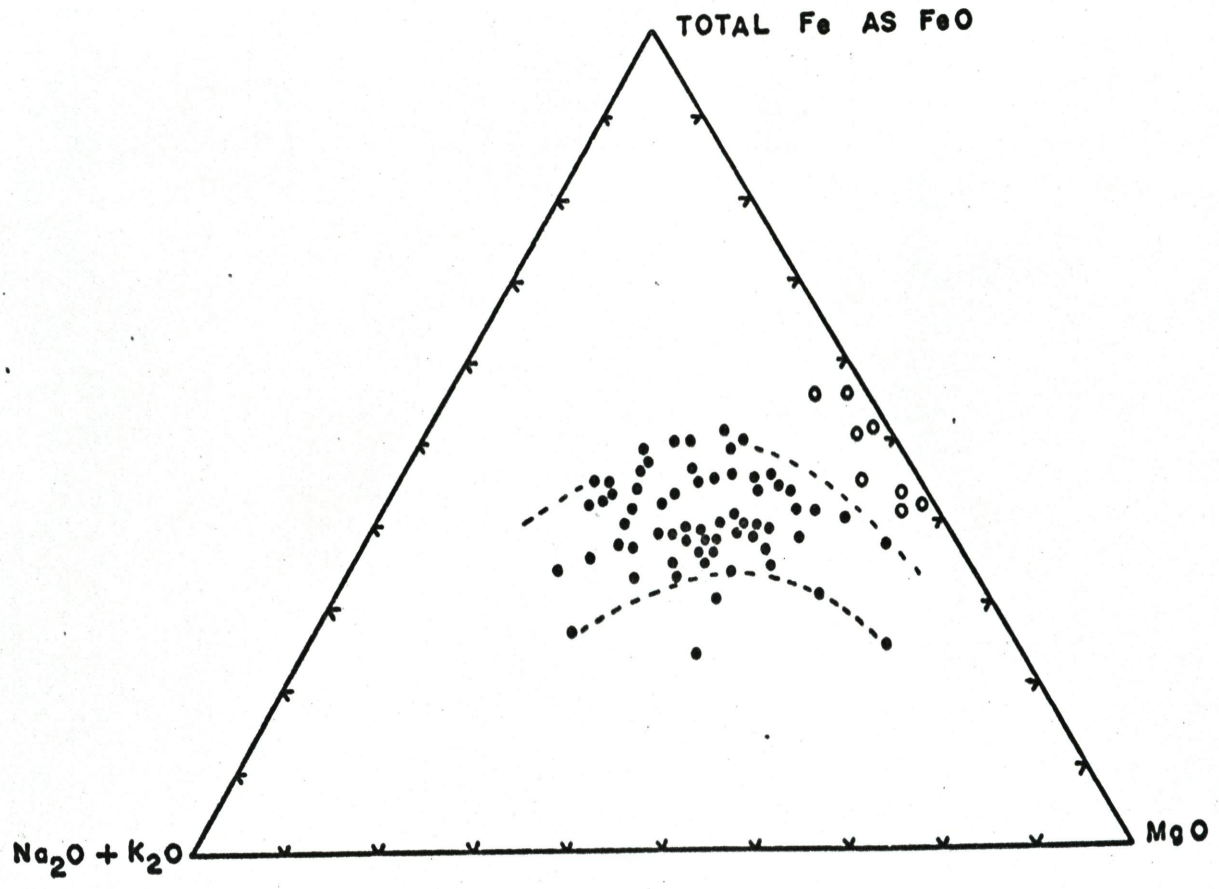
TOTAL Fe AS FeO
$Na_2O + K_2O$
MgO

relics of spilitic rocks encountered in the brecciated zone are slightly richer in total mafic compounds than the above spilite flow. Differentiation is also emphasized by the relative decrease of $SiO_2$ content of the brecciated zone with respect to MgO as illustrated in Figure 18. The same diagram shows also a few samples from the brecciated zone richer in $SiO_2$ and falling in the field of the spilite; such samples were found to contain quartz veins. Figure 21 shows the increase of MgO and FeO from the spilite flow to the brecciated zone. Some of the brecciated rock samples are richer in MgO than others, and have deviated towards the magnesium rich area of the diagram (Fig. 21). Chlorite minerals abound in these later rocks. One brecciated rock (1044 feet) falls also in the field of the spilite. This later is due to an increase of CaO with a decrease of MgO and FeO content. Figure 22 shows also a general increase of $TiO_2$ and FeO with a slight discontinuous trend between the spilite, and brecciated rocks. There is less $TiO_2$ and FeO in the spilite than in the brecciated rock. The increase of $TiO_2$ in this brecciated zone may be due to the high concentration of pyroxene which was consequently altered. The ratio of $FeO/TiO_2$ for the spilite is about 16.0 and for the brecciated zone 12.9 and this may indicate that iron bearing minerals have continued to crystallize in the matrix of the spilite flow. The increase of mafics in the brecciated zone might have decreased some of the alkalis content during differentiation.

Discussion on the Present Appearance of the Brecciated Zone. Two alternative processes may be suggested for the occurrence of brecciation in this portion of the core studied: (1) by hydrothermal fluid solution

Figure 21. FeO - MgO variation diagram of spilite (●) and brecciated spilite rocks (o).

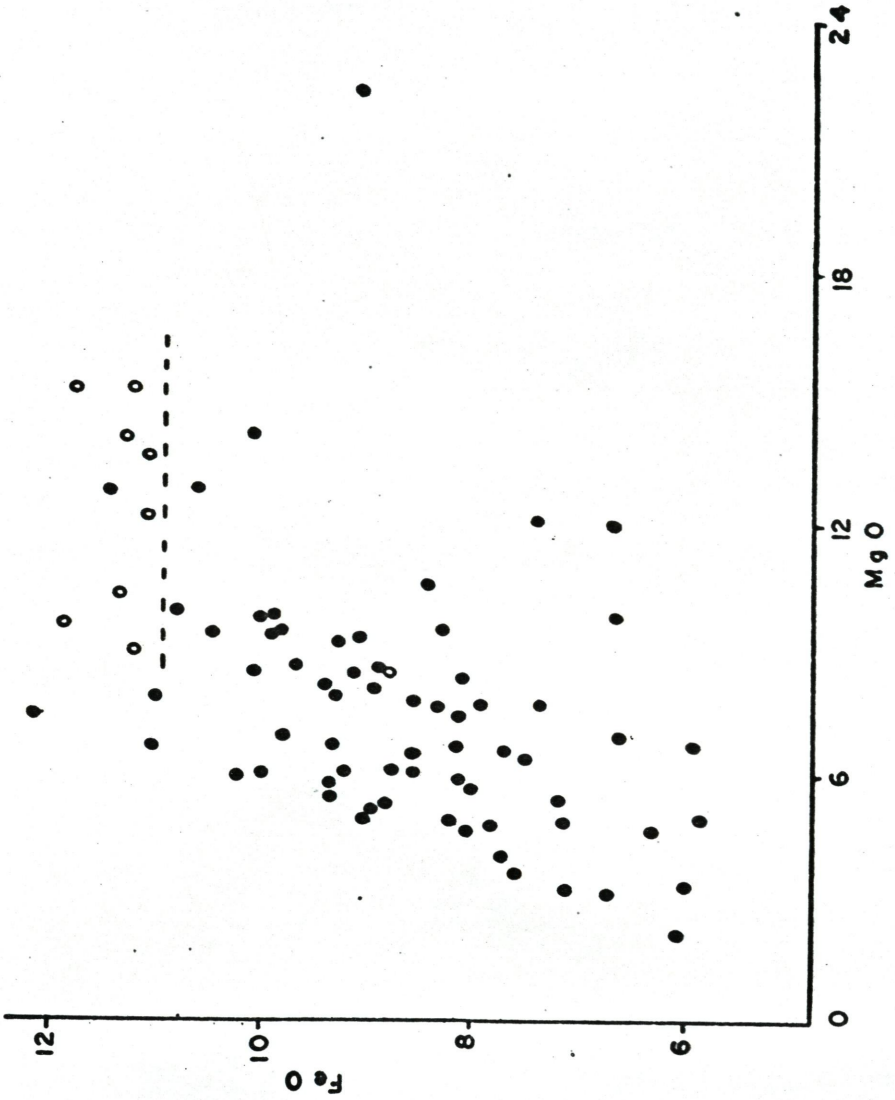
12
10
8
6
FeO
0
6
12
18
24
MgO

Figure 22. $TiO_2$ - FeO variation diagram of spilite ( ● ) and brecciated spilite rocks ( ⊙ ).

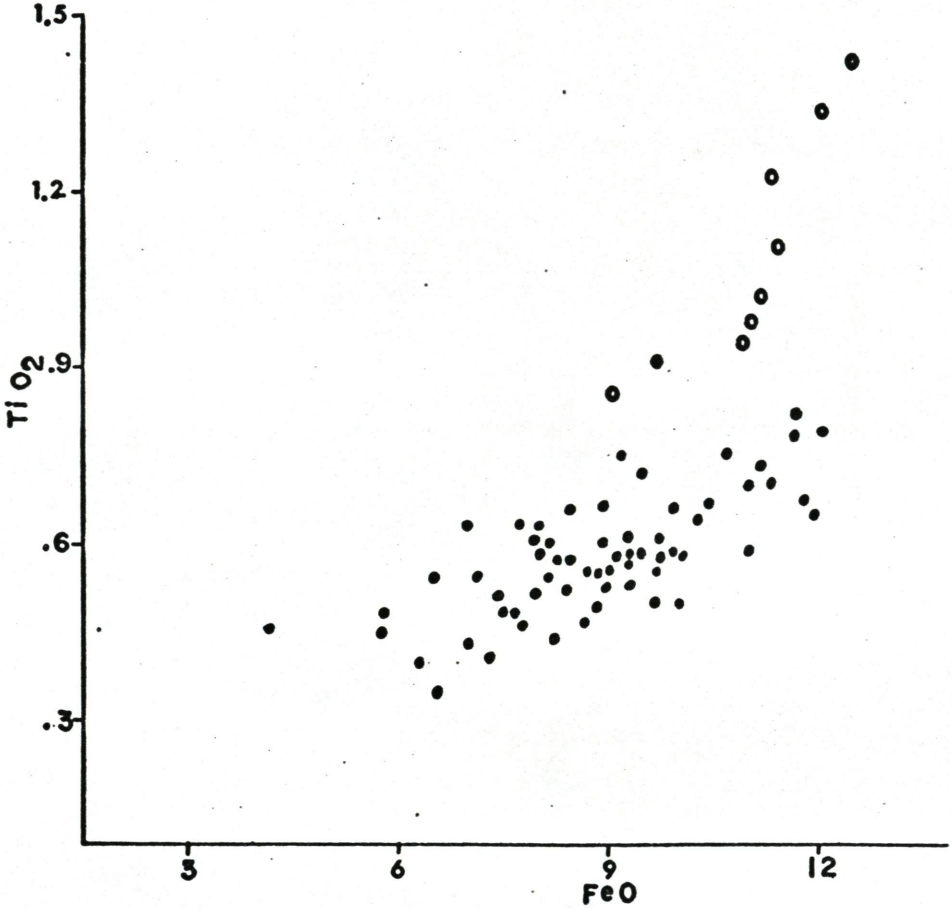
1.5
1.2
.9
.6
.3
TiO2
3
6
9
12
FeO

inherent in the magma itself and (2) by tectonic fracture of an original spilitic rock.

1) It was previously mentioned that this brecciated spilite zone is depleted in both $Na_2O$ and $K_2O$ (0.7 and 0.1 average percent respectively) with respect to the above spilite flow. Late fluid solutions carrying felsic and mafic compounds have been responsible for some type of "autometasomatic differentiation." Fluid solutions enriched in volatiles and alkalis during magmatic crystallization may have altered the original mineralogical assemblages. Figure 19 shows the variation of $TiO_2$ with $Na_2O + K_2O$ of the spilite and brecciated zone. The trend between this brecciated zone and the spilite flow is continuous. There is a strong depletion of alkalis with an increase in titanium. The unusual decrease of potassium and sodium in the brecciated zone is due to a more effective migration of these elements (Fig. 17) than the migration of other elements. Titanium stays in place or migrates for only a short distance (on the order of millimeters). During the later alteration Ti, Fe, and Mg-bearing compounds almost immediately precipitated from the fluid solution and redistributed as low temperature minerals (Table 9) in this brecciated zone.

Brecciation (sheared texture) increases near the bottom of this brecciated zone (see petrography). This could imply that some type of differential movement occurred near the contact with the previous flow (not studied here). It is likely that a combined effect of a relatively quick chilling near the bottom of the flow and the continued movement of the magma has contributed to such increase in brecciation with depth.

2) The textural features reported above may also be attributed to a late tectonic movement of the area. This tectonic movement could have been the cause of an intensive fracturing of the spilite flow. Evidence for late postconsolidation movement is given by the occurrence of sheared textural features and by the presence of intensively altered coarse grained rocks showing relic outlines of replaced amphibole phenocrysts (1060 feet) (see petrography). It is believed that these coarse grained rocks, containing plagioclase phenocrysts, quartz and ghosts of amphiboles, represent an original amphibole prophyry dike altered during faulting.

From the above considerations it seems that the major processes which caused the present brecciated zone are due to a late tectonic movement accompanied by faulting. Hydrothermal alterations during magmatic crystallization might have been important, but they were masked by postconsolidation processes.

## Petrogenesis of the Dikes

The chemical differences between the three types of dikes encountered in the core are emphasized mostly in the amphibole porphyry dikes, and, to a lesser extent, between the upper albite-diabase and the lower andesine-diabase dikes. Silica, aluminum, and total alkalis are higher, and iron, calcium, and titanium are lower in the amphibole porphyry than in the albite and andesine-diabase dikes. MgO is comparable in all these dikes (6.0, 5.8, and 5.9 percent average respectively). This indicates some type of differentiation towards iron enrichment for the

andesine and albite-diabase dikes. This relationship is also illustrated on the AFM ternary diagram (Fig. 23).

Chemical differences between the upper albite diabase and the lower andesine-diabase are insignificant (Table 13). The average FeO/MgO ratio is 1.8 for both the andesine-diabase and the albite-diabase. The $TiO_2$ is slightly less in the upper albite-diabase dike (0.9 percent average). However, differences in the mineral assemblages exist between these two dikes (see petrography). Their plagioclase and pyroxene compositions are different and the upper dike contains more low temperature mineral associations such as epidote, chlorite, and sphene. Sphene was seen occasionally in the bottom andesine dike.

## Relationship of the Spilite with the Later Dikes

The igneous bodies present in the core show contrasting chemistry and mineralogical similarities, with the exception of the amphibole porphyry dike. This is due to the different distribution of the same mineral assemblages.

The difference between the extrusive rocks, spilites, and the dike rocks, amphibole porphyry, albite-diabase and andesine-diabase, may be characterized by their content of alkalis. Figure 19 shows a plot of $TiO_2$ versus total alkalis. The $TiO_2$ content of the dike rocks decreases sharply with the increase of the total alkalis (Fig. 19). However, the variation of $TiO_2$ and alkalis is less pronounced in the spilite rocks (Fig. 19). No clear distinction can be made between the spilites and the amphibole porphyry as far as titanium is concerned, since both con-

Figure 23. MgO - FeO - Alkalis variation diagram of dike rocks

● Amphibole porphyry.

X Albite diabase.

▼ Andesine diabase.

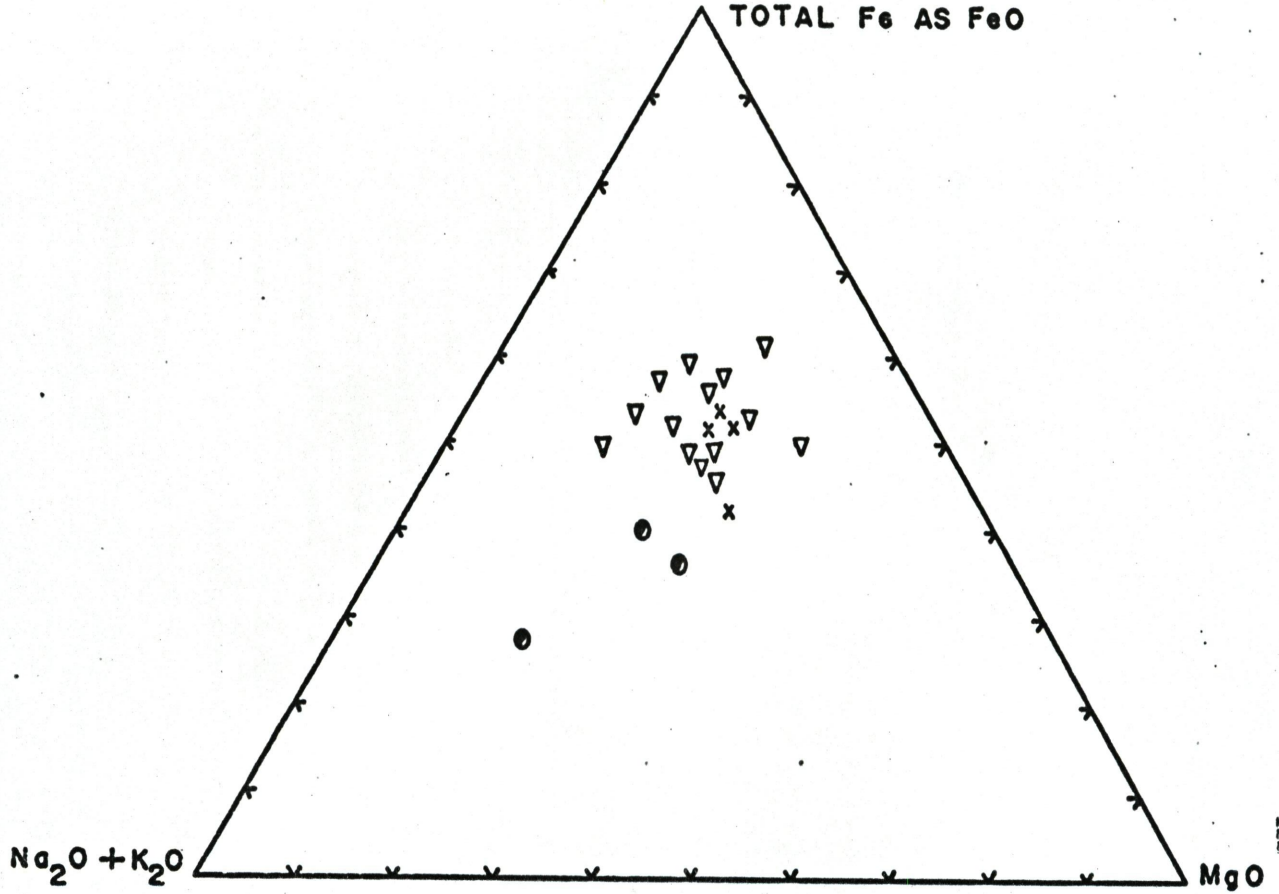
TOTAL Fe AS FeO
$Na_2O + K_2O$
MgO

tain small amounts of this element (0.59 and 0.63 respectively). The titanium content of the andesine-diabase is mostly concentrated into the pyroxene crystals and may be some opaque minerals; sphene occurs, but not as much as in the spilite or the upper albite-diabase.

In summary, the main chemical differences between the intrusive dikes, the spilite and the brecciated zone, consist in their alkalis, iron, titanium and calcium content (Table 10). The amphibole porphyry differs from both spilites and the dikes by its relatively high silica and potash content ($SiO_2$ = 55.18 and $K_2O$ = 2.62 percent in average). The bottom brecciated zone is comparable to the andesine and albite-diabase dikes as far as $TiO_2$, and FeO are concerned (Table 10) and differs by its high MgO and very low total alkalis content (Table 10). The mineralogy of the spilite flow and the dike rocks is comparable. However, the amphibole porphyry dikes contain hornblende phenocrysts and the andesine-diabase dike contains more calcic plagioclase than the rest of the units (see petrography).

The spilite and dike rocks represent probable intrusions of different magmas originated under different conditions. There are two processes which are interrelated with each other and which could have caused the present compositional variations between the spilite and the dike rocks: the physical condition under which these rocks were originated, and the late concentration of volatiles which altered different minerals and caused either a complete disappearance (brecciated zone) or the preservation of original textural features (spilite and dike).

## Theories on the Origin of Spilite

Several hypotheses have been offered for the origin of spilites: alteration of basaltic magma by sea water during extrusion (or by impregnated sediment): during solidification of a melt (autometasomatism); and by burial metamorphism of mafic rocks.

Magmatic Origin. One view for the origin of spilitic rock is the purely magmatic derivation of these rocks. Such spilites are envisioned as acquiring their present character because of features inherent in the magma or special conditions of crystallization. Evidence has been given to suggest that spilite mineralogy represents adjustments to conditions of low temperature and abundant water. The adjustment might conceivably occur at an early stage while the lava is a liquid mush (Wilshire, 1959 and Hentschel, 1961). The dominant constituents of fluids causing alteration are probably $H_2O$ and $CO_2$. These fluids could carry dissolved material released by alteration of the original high temperature minerals (Wilshire, 1959).

Several authors (Burri and Niggli, 1945; Vuagnat, 1946; Amstutz, 1958) postulated that spilites are derived from a basaltic magma rich in volatiles, mainly water, and these volatiles are retained during magmatic cooling. The high volatile content was postulated to lower the temperature of crystallization so that albite and chlorite could crystallize directly from the magma. The pyroxene association with albite and chlorite in the spilites could be due to the preservation of early formed pyroxene which remained stable at low temperatures due to a reduction of fluid solution activity.

By most definitions, albite is the essential feldspar of spilites. Dewey and Flett (1911) showed that in their British spilites the albite is filled with chlorite and epidote. These authors (Dewey and Flett, 1911) suggested that the calcium of the epidote was supplied through the replacement of a more calcic plagioclase by the present albite host. There are, however, examples in which the feldspar are free from inclusions and occur in environments at least locally deficient in calcium (Vallance, 1960; Smith, 1968). Such albites which are free of inclusions have been interpreted as primary in origin by Van Overreem (1948) and Amstutz (1954). Battey (1955) found that clear albite intergrows with fresh pyroxene, and considered the albite as primary. This author (Battey, 1955) suggested that albite and pyroxene formed an eutectic which shifted towards albite under high water pressure. The low temperature optics found in albite of spilitic lavas indicate adjustment to the ordered state. Donnelly (1963) in his study of albite minerals from the spilite-keratophyre sequence of the Water Island Formation in the Virgin Islands postulated a primary origin of the albite. Evidence of this is given by the fact that the quartz-keratophyre and spilites association of the Water Island Formation contains bent crystals of low, intermediate, and high temperature albite with no sign of recrystallization subsequent to bending. The matrix shows no signs of deformation and the bending could only have occurred during the final stages of consolidation of a viscous magma (Donnelly, 1963).

Sea Water Alteration. Some authors noticed the occurrence of spilites associated with sedimentary sequences in geosynclinal environments and

attribute an important role in the formation of spilitic rocks to sea water or to wet sediments. The study of spilites from the Olympic Peninsula in Washington brought Park (1946) to consider the possibility of connate water in sediment as a primary source for the alteration of an original basaltic magma. Gjelsvik (1958) in his study of soda rich rocks in the Karelian zone of Norway postulated potash and sodium exchange between basaltic magma and adjacent wet sediment in a geosynclinal environment. The reaction of sea water with molten magma was also postulated by Rittman (1958) as the main source of sodium for the spilitic rocks. Most recently, however, many doubt that spilites do in fact have a high Na content (Amstutz, 1967; Smith, 1968; Vallance, 1960). Rittman (1958) and Szaseczky-Kardoss (1958) claimed that under high water pressure in deep sea environments low temperature mineral assemblages, such as chlorite, albite and epidote, appear instead of augite and calcic feldspar. Rittman's theory involves the formation of pneumatolitic and hydrothermal solutions due to retention of water and other volcanic gases ($CO_2$, HCl, $H_2S$, $H_2$, etc.) by the lava and gas transfer substances ($FeCl_3$, $MnCl_2$, $SiCl_4$, etc.) which escaped from the roof of the outflowing lava. However this sea water exchange theory cannot be generally applied because not all the spilites are formed beneath oceans, and if spilites were formed by a reaction of basic lava with sea water, it is surprising that most of the known ocean floor is made up of unaltered basaltic rocks.

Oceanic spilitized rocks (albitized basalts) were found in the Mid-Oceanic Ridge in the North Atlantic (Melson et al., 1968) and in the

Carlsberg Ridge, Indian Ocean (Cann and Vine, 1967; Hekinian, 1968). These authors attributed the origin of spilites to the alteration of basaltic rocks by regional and cataclastic metamorphism due to faulting and uplift of the area. These later conclusions are mainly based upon the fact that the areas of recovery of these oceanic altered rocks are connected with fracture zones.

Burial Metamorphism. Spilites are often associated with tuffs and greywackes (Tyrrell, 1933). Burial metamorphism as the main agent for the transformation of basic lava into spilitic rocks was demonstrated by Coombs et al. (1959) in his study of rocks from New Zealand. These sedimentary units show the growth of minerals such as albite, chlorite, epidote, prehnite, pumpellyite and zeolite after deposition. Coombs et al. (1959) shows a systematic change in mineralogy with depth. Recently, Smith (1968) in his study of geanticlinal marine sequences of Ordovician basic volcanics showed that the chemical and mineralogical rearrangement within basic lavas post-dated their solidification and resulted in a spilitic mineralogy. A similar rearrangement of chemistry and mineralogy is developed with the associated sedimentary and pyroclastic rocks. Consequently, the spilitization in this case must be due to burial metamorphism.

## Magmatic Origin of the Spilite from the Virgin Island Core

Discussion of the Magmatic Origin. The probabilities of a crystallization from a hydrated parental magma with retention of volatiles, and of

a burial metamorphism of basic rocks seem to be the most compatible with our present observations. There can be little question that the spilite once represented an original magmatic eruption. (1) The textural relations are similar to those from extrusive mafic rocks; (2) subtrachytic texture of the plagioclase laths indicate crystallization from a liquid; (3) the bulk chemistry of spilitic rocks does not differ greatly from the average extrusive mafic rock composition with the exception of alkalis relations in spilites. However it is the low temperature, hydrous mineralogy (albite-chlorite-epidote etc.) that requires explanation.

Observations by Donnelly (1966) led to a proposal of autometasomatic origin of the spilites from the Virgin Island. These observations are the following: (1) the occurrence of the spilite-keratophyre suite as thick and monotonous flows with little brecciation and little development of pyroclastic facies. (2) the occurrence of abundant bent spilitic albite laths and phenocrysts in an undeformed matrix shows that the albite was bent prior to the cessation of flow. (3) the texture of intersertal chlorite is not that of low grade metamorphic rocks. (4) deformed calcite aggregates occur in amygdules but the surrounding rock shows no sign of deformation. The variability of mineral content from amygdules to amygdule and the deformation of many amygdules suggest that they might have been semi-solid bodies before the rock itself was completely solid.

The spilites from the core show heterogeneous textural features. The occurrence of dark patches and green matrices is a primary (igneous)

feature. While some arguments favor the strict magmatic origin for some of the features, such as flow texture around amygdules and the presence of patchiness, other features undercut this theory. These other structures are mainly the thickness of the flow which could have helped to retain both heat and volatiles. It was shown that the disappearance of certain minerals with depth is due to burial metamorphism. Burial metamorphism is indicated by the presence of pumpellyite also reported in the overlying Louisenhoj Formation by Donnelly (1966). Still other textural features that are also found in the core, such as curved phenocrysts and microlites of albite, have been proposed as indicative of preconsolidational albitization (Donnelly, 1966). However, Smith (1967) found similar features in spilitic basalt from the low-grade metamorphosed sequence of Australia, and concluded that, while the curving of microlites is a feature of lava consolidation, albitization was due to burial metamorphism. Hence, the significance of curved albite crystals in the genesis of spilites is inconclusive. The calcite crystals, encountered in the vesicles, are usually coarse grained. The presence of deformed calcite in amygdules could also be attributed to postconsolidation processes and the preferential deformation of certain minerals rather than the bulk rock may be due to differences in grain sizes. It is possible that finer grained minerals could adjust much easier to the new equilibrium exercised by postconsolidation processes than the coarser grains of calcite.

These later considerations do not disprove the theory of autometasomatism but they do show that burial metamorphism may account for

the observed mineral and chemical features encountered in spilitic rocks. The only mineral which may prove the exception to the above explanations of origin is the biotite in the upper part of the spilite flow.

Autometasomatism. Evidence for autometasomatism in the spilite flow of the core has been discussed above. The main general features that are encountered in the spilite, and which indicate an autometasomatic process are: (1) the textural and mineralogical heterogeneity existing between the dark patches and the green matrices of the spilite, and (2) the difference in alkalis between most dark patches and the green matrices. This process of autometasomatism is directly related to the crystallization of the magma, and the agent of autometasomatism is a fluid solution of the last aqueous residues of the magma. This fluid solution was probably enriched in $H_2O$, $CO_2$, $Na_2O$, $K_2O$ and lesser amounts of $SiO_2$. The presence of $H_2O$ and $CO_2$ is inferred from the content of hydrated silicates and calcite. These alkalis and silica are the most mobile components; the migration of these compounds was facilitated by the occurrence of veinlets and veins which are up to 5-10 cm. thick in places (1050 feet) and the green matrix may also be acting as a comparatively permeable channel. The heavy compounds, MgO, FeO and $TiO_2$ are also mobile, but to a lesser extent.

The plot (Fig. 24) of K x 100/Na + K average ratio versus the FeO/FeO + MgO ratio for the patchy zone (dark patches and green matrix), the non-patchy zone and the brecciated zone, shows a lack of relationship of these ratios with depth. It is probably that the K x 100/ Na + K ratio fixation is not due to a simple process of magmatic dif-

Figure 24. K + 100/Na + K vs. FeO/MgO + FeO variation diagram of spilite.

G.M. - Green matrix.

D.P. - Dark patch.

B. - Brecciated spilite rocks.

N.P. - Non-patchy spilite.

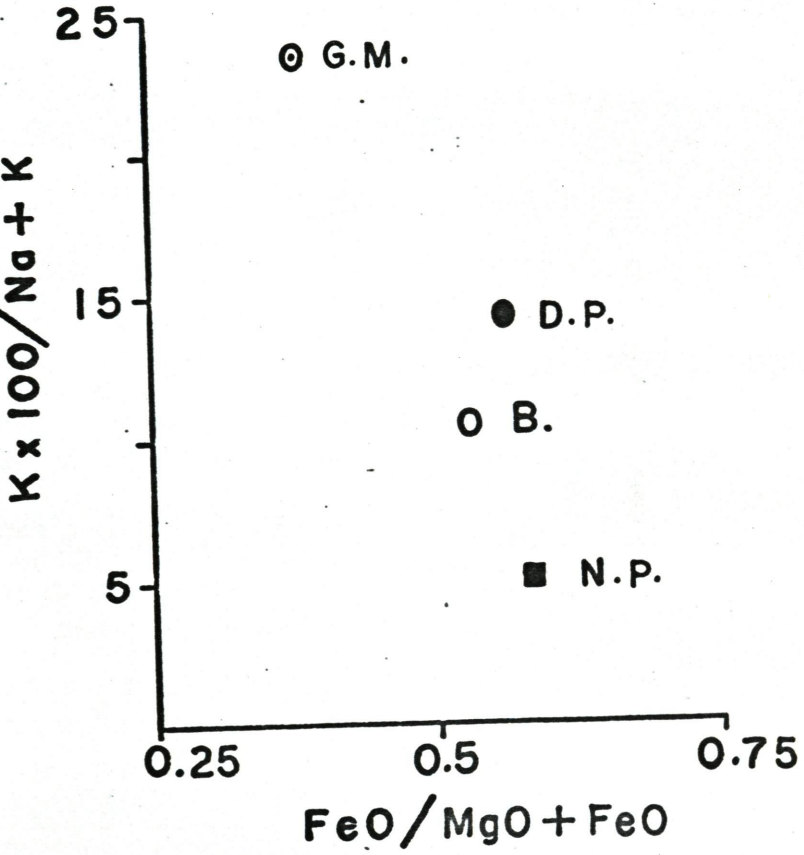
25
15
5
K x 100/Na + K
G.M.
D.P.
B.
N.P.
0.25
0.5
0.75
FeO/MgO + FeO

ferentiation. This diagram shows also that the brecciated rock with K x 100/Na + K = 10.4 had a fluid solution enriched in sodium, silica and lesser amounts of potash with respect to the above non-patchy zone (K x 100/Na + K = 5.0). The fluid solution in the region of the non-patchy zone was probably enriched in potash which had migrated upward. Finally the patchy zone (dark patches K x 100/Na + K = 14.8 and green matrix K x 100/Na + K = 24.0), above 650 feet, was the site of potash enrichment migrated from the non-patchy zone. With the increase of potash, the sodium content of the patchy zone migrated towards the dark patches or downward into the spilite flow.

In summary it is believed that a process of autometasomatic differentiation has facilitated the concentration of some mafic components close to their source in the brecciated zone and concentrated some of the alkalis plus some silica further away, possibly at a higher level in the core. However, autometasomatism does not fully explain the presence of certain minerals and the discontinuous chemical variation of potash in the upper part of the core.

## Role of Metamorphism (Burial Metamorphism)

The rock types encountered in the core from the Virgin Island have undergone some type of metamorphism. These changes were produced primarily by temperature variations and burial metamorphism. Previous studies in the Virgin Island (St. John) show a progressive decrease in contact metamorphism from the North to the South (Fig. 1). This decrease in metamorphism goes from Hornblende-Hornfels Facies to Albite-

Epidote-Hornfels Facies (Longshore, 1965). The Hornblende-Hornfels Facies is well defined but the Albite-Epidote-Hornfels Facies may merge into burial metamorphism. The Virgin Island core studied here was drilled within a visual radius of about 7 km. from the intrusive batholith of the Virgin Island. The lack of foliation and the preserved original textures in most of the rocks brought Longshore (1965) to conclude that dynamic processes played a minor role in the metamorphism of the Virgin Island rocks.

Systematic Chemical Variation. To explain the systematic chemical distribution, an ACF plot was prepared to show first the bulk rock analyses (Fig. 25), and second the patch-matrix pairs joined by tie-lines (Fig. 26). These diagrams are used to show chemical variation in terms of the minerals stable under the temperature-pressure-fluid conditions at the time of formation of these "alteration minerals". The diagram is equally useful for showing trends regardless of whether the alteration took place during the late stage of lava cooling or during burial metamorphism. It is of further use as other workers on spilitic rocks have used similar plots (Vallance, 1967); (Smith, 1968).

To calculate the percentages of the components and plot them in the ACF diagram, the following rules were observed (Turner and Verhoogen, 1960, p. 410). The percentages of the various components were calculated as molecular percentages, $Al_2O_3$, $Na_2O$, $K_2O$, CaO, total iron as FeO, and $TiO_2$. $TiO_2$ was added to the mafic components because of the presence of sphene in the spilite and in the brecciated rocks.

The ACF diagram (Fig. 25) used also by Vallance (1967) to con-

Figure 25. Plot of molecular proportions $Al_2O_3 - (Na_2O + K_2O)$: $CaO:FeO + MgO + TiO_2$ in altered mafic rocks (spilite and brecciated rocks). Small size circles (•) represent spilite above 700 feet. Medium size circles (o) represent non-patchy spilite below 700 feet. Larger circles (O) represent brecciated rock samples.

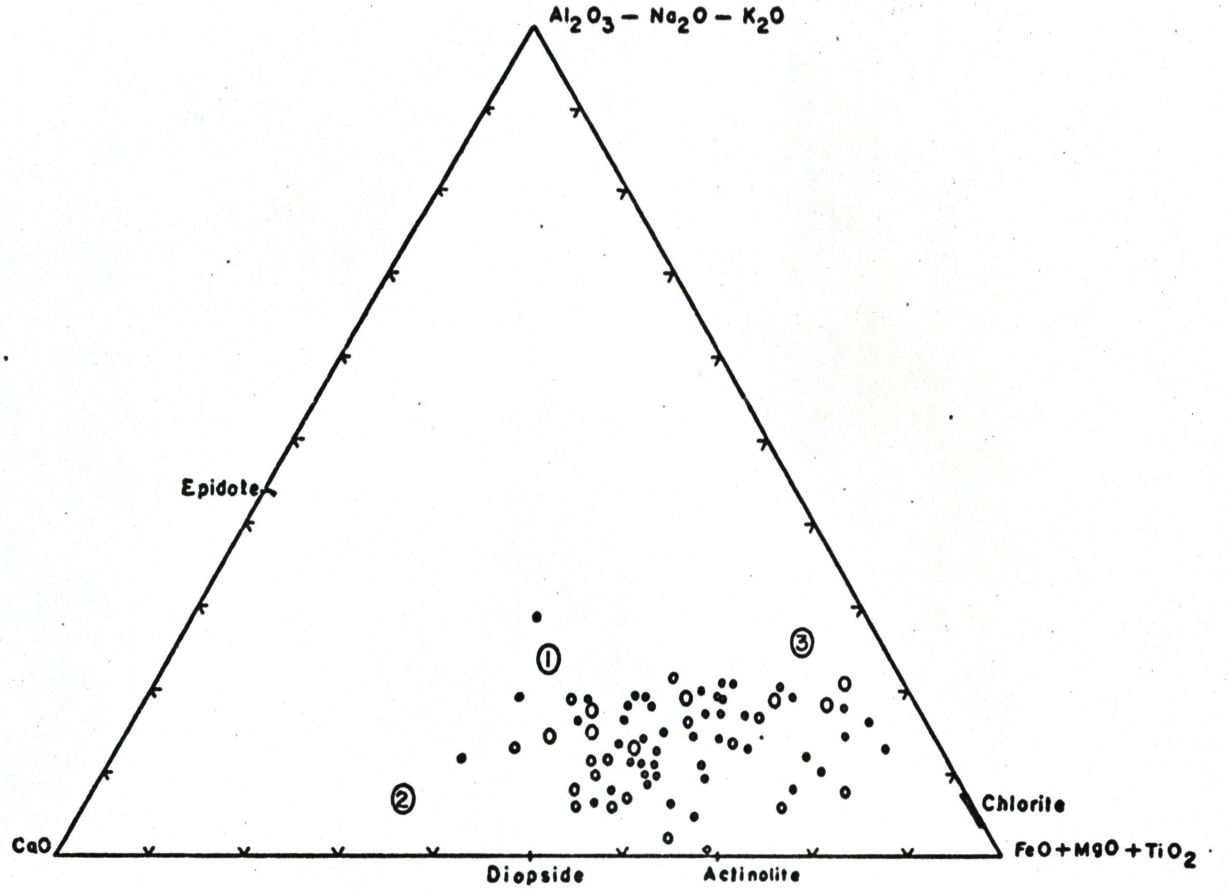
$Al_2O_3 - Na_2O - K_2O$
Epidote
CaO
Diopside
Actinolite
Chlorite
$FeO + MgO + TiO_2$
①
②
③

trast mafic altered lavas from North South Wales (Australia), gives some idea about the "intensity of alteration" among altered rocks. Such intensity of alteration could be proportional to the amount of spreading that an average composition of the parental rock of the spilite would have endured during alteration. The chemical analyses of some of the altered rocks, patchy spilite, non-patchy spilite and the ACF diagram (Fig. 25) show at least three hypothetical broad pattern of variability spreading from the chlorite to the CaO (calcite) corner (Fig. 25). These patterns of variability are: (1) a field containing moderate amounts of CaO and FeO. This field shows the occurrence of microphenocyst of calcic plagioclase and common epidote. The brecciated rocks falling in this same field contain veins and vesicles of calcite and epidote. (2) a field enriched in CaO ($> 8\%$) and FeO. In addition the rocks falling into this field contain calcic pyroxene, lesser amount of epidote and abundant plagioclase microlites. (3) a field depleted in CaO ($< 6\text{-}7\%$) and enriched in MgO with vesicles, veins and groundmass rich in chlorite and quartz. The samples of patchy spilites and brecciated rocks of this latter field show extensive development of chlorite. The calcium lost from these rocks is accumulated in veins and amygdules a few feet away or closer.

Figure (26) shows the ACF diagram of the patchy spilite. The dark patches and their surrounding green matrices are related together with a tie-line. This also shows three hypothetical broad patterns of variability: (1) a field of predominently plagioclase-epidote; (2) a field of epidote-actinolite and lesser amount of plagioclase microlites; (3)

Figure 26. Plot of molecular proportion $Al_2O_3$-($Na_2O$ + $K_2O$): CaO: FeO + MgO + $TiO_2$ in the altered patchy spilite. The dark patches (●) are related with their respective green matrix (o) with tie-lines.

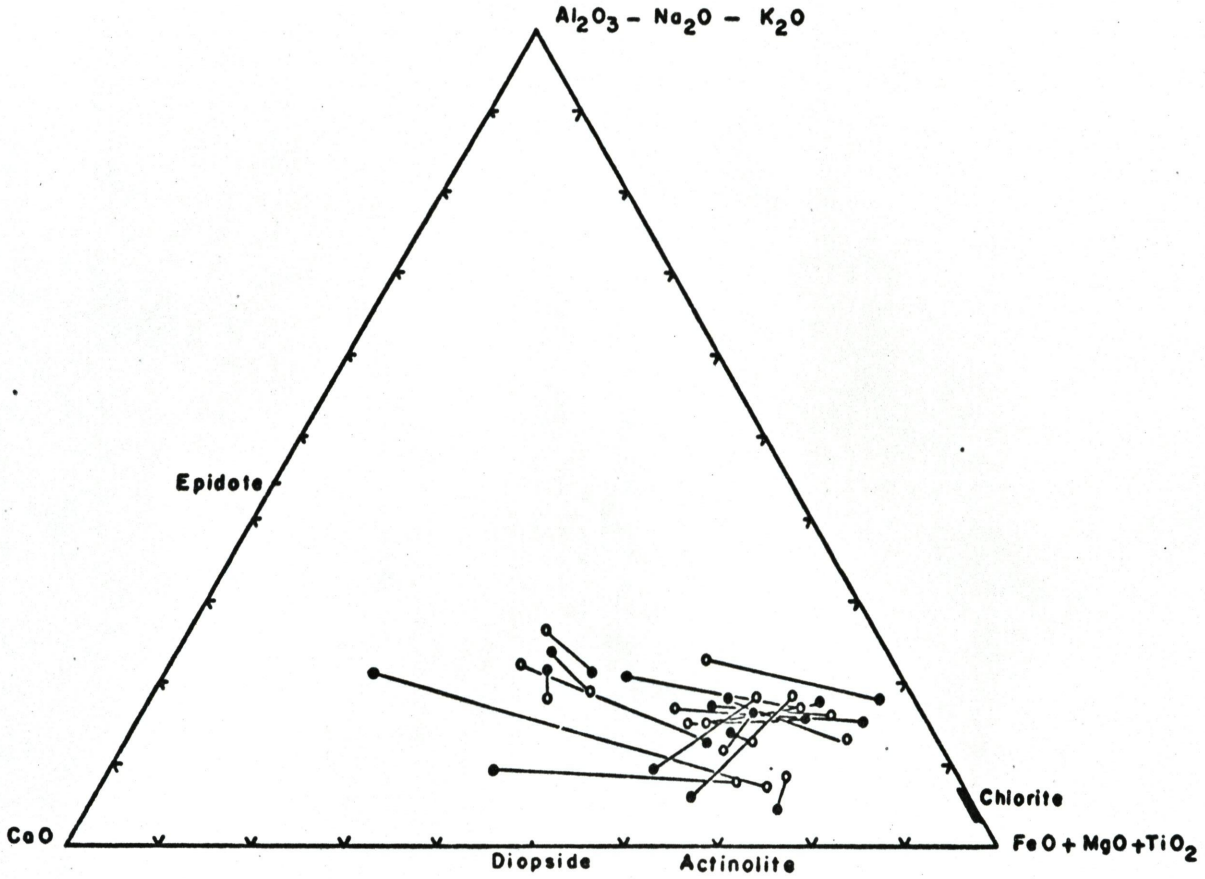
$Al_2O_3 - Na_2O - K_2O$
Epidote
CaO
Diopside
Actinolite
Chlorite
$FeO + MgO + TiO_2$

a field enriched in MgO and in chlorite. These last two fields enclose rocks containing quartz and plagioclase filling vesicles, veins, and veinlets. The tie lines relating each dark patch with its matrix may cross the different fields. This might be due to local loss of various elements during alteration. In the field of epidote actinolite and chlorite three different mineral associations may be recognized according to their relative abundance. Samples analysed and falling closer to the F (mafic) corner (Fig. 26) are richer in sphene and chlorite, probably after alteration of pyroxene or original glass. Rock samples falling near the actinolite corner contain fair amounts of this mineral, which often surround a pyroxene phenocryst (560 feet). These rocks are usually characterized by depletion in potash ($<1\%$) but are relatively enriched in calcium with respect to the samples falling close to the chlorite corner (Fig. 26). When increasing the calcium content the variation trend will either shift towards the epidote composition or fall close to the calcite field (CaO). Some of the dark patches plot nearer to the Ca-poor field (chlorite corner) than their respective green matrix (Fig. 26). The Ca- lost from these dark patches may have accumulated in the green matrix as calcite filling vesicles and veins. In this particular case the redistribution process of calcium occurred locally within a close distance (order of millimeter). The variability of CaO distribution between the dark patches and the matrices could be due to the fact that calcium migrated more slowly than the alkalis. Some of the green matrices falling close to the chlorite corner (Fig. 26) are enriched in veins and amygdules. Unlike the pre-

viously mentioned dark patches of the same field, these green matrices contain more recrystallized minerals, quartz, plagioclase and chlorite.

The wide spread of these analysed samples, patchy spilite, non-patchy spilite and brecciated rocks, reflects their mineralogical and chemical composition. This compositional variation, existing in a single flow and even in a single restricted zone (patch-matrix), suggests an intense process of alteration.

Burial Metamorphism. A process which is believed to have influenced the original rock is burial metamorphism. The presence of pumpellyite and prehnite noticed above the first 700 feet of the core indicates that some alteration due to load pressure has been effective. Coombs et al. (1959) suggest a zone of transition between the zeolite and greenschist facies called the prehnite-pumpellyite facies. The pumpellyite and prehnite minerals are interpreted in the "Alpine facies" of New Zealand as having been derived mainly from the breakdown of detrital calciferous plagioclase (Coombs et al., 1959). The relationship of alteration to depth is one of decreasing hydration with depth causing the release of silica. Epidote may be produced by dehydration of pumpellyite and prehnite (Coombs et al., 1959). However, this latter process probably had a minor effect in the core since prehnite and pumpellyite are apparent only in traces or as accessory components. Epidote occurs everywhere in the core and its concentration cannot be related to depth.

The occurrence of epidote, chlorite, prehnite, and pumpellyite may be due to the overlapping of two processes such as load pressure and

autometasomatism related uniquely to a temperature gradient. The production of albitized plagioclase could very well be due to a late deuteric and hydrothermal alteration. Most of the sericite replacing some calcic cores of plagioclase could also be the product of late magmatic reactions.

The prehnite-pumpellyite facies transitional between the zeolite and greenschist facies occurs at less than 300°C and at about 3000 bars of water pressure (Coombs, 1960). Low temperature of this order, therefore, excludes the possibility that the pyroxene grains are metamorphic. The clinopyroxene is generally fresh, being metastable, and was no doubt an early product of magmatic crystallization.

### K-Distribution and the Occurrence of Biotite

Evidence of postconsolidation potash introduction is suggested by the decrease in potash content in dike rocks with depth, especially of the amphibole porphyry dikes (129-134 and 732 feet; $K_2O$ = 3.45 and $K_2O$ = 0.96 percent respectively). Also, the sharp increase of potash (up to about 2 percent) in certain zones of the spilite flow (110, 163-234, 417-446, 503-542, 573-590 and 632 feet) may indicate an overlapping process of alteration which might have followed the late magmatic alteration.

The distribution of $K_2O$ is illustrated in Figure 27 showing the average alkalis distribution of the upper part of the core. This diagram shows also two arbitrary fields of potash distribution: one is the field with a $K_2O$ content less than 1 percent and decreasing constantly with depth below about 650 feet. This more or less

Figure 27. Alkali variation at the upper part of the spilite flow. Shaded area represents zones of potash enrichment. (B) Zones with biotite.

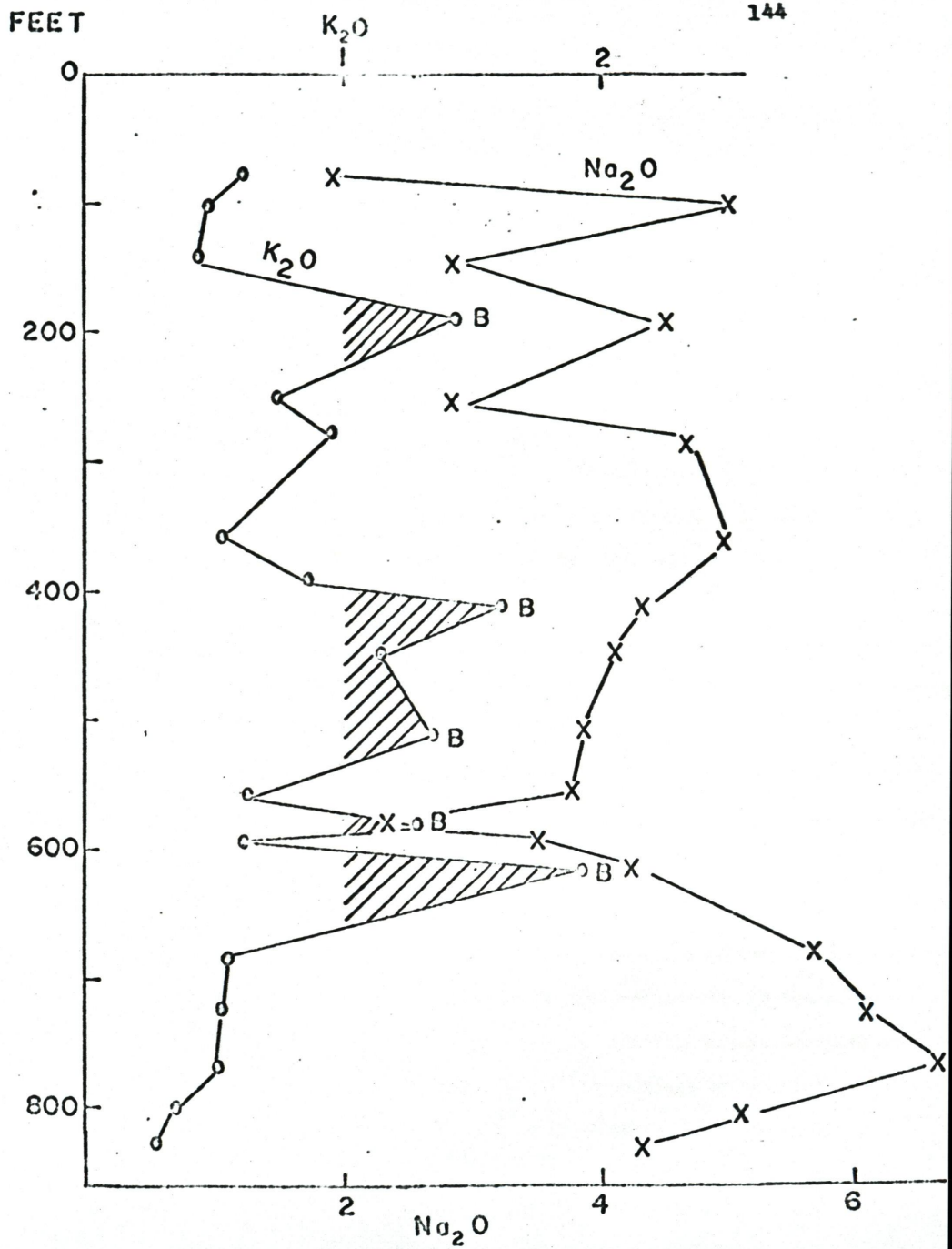
FEET
$K_2O$
0
2
$Na_2O$
$K_2O$
B
200
400
600
800
2
4
6
$Na_2O$

uniform decrease in potash, may be due to autometasomatism. The second half of the diagram (Fig. 27) is characterised by a sharp $K_2O$ increase in potash usually higher than 1 percent occurring only above 650 feet. It is believed that this irregular increase in potash of the upper part of the core is due primarily to postconsolidation of potash distribution. This distribution of potash was not necessarily accompanied by a decrease of soda content in the bulk rock (Fig. 27), probably because the redistribution of soda occurred locally in adjacent vesicles and veins. The high potassic zone (>1 percent) contains sericite. The process of seritization involved the displacement of soda elsewhere and the appearance of clear albite in vesicles. The petrography shows also that the order of change in the above zones has been first towards soda enrichment and then towards the enrichment of potash. In addition to sericite, biotite also occurs in the above restricted zones of potash enrichment (110, 163-234, 417-446, 503-542, 573-590 and 632 feet). The kind of process that increased the potash content of the restricted zone in the upper spilite flow is not well known. However some speculation on the occurrence of biotite and its disappearance with depth may be made. The presence of biotite could be attributed to two different processes: 1) autometasomatism (primary biotite), or 2) burial metamorphism.

1) The primary origin of biotite could be explained by a process of differential cooling between the top and the bottom of the spilite flow. The relatively rapid cooling of the upper part of the flow (patchy spilite) did not allow all the biotite to alter into chlorite.

It is true, as shown before (see petrography), that the top part of the spilite cooled more rapidly than the rest of the flow. This biotite (primary) could have been hydrated during magmatic crystallization and altered into chlorite. However, if this was the situation causing primary biotite, we would expect the presence of resorbed crystals of biotite. This latter expectation was not observed and hence it is unlikely that the biotite found in the upper part of the core is primary.

2) Another alternative for the occurrence of biotite in the upper part of the core could be due to a postconsolidation process. It is likely that burial metamorphism might have been the cause of some potash migration near the top of the spilite flow. This K increase enhanced the formation of biotite in certain zones of the core (Fig. 27). Turner (1968, p. 118) in his survey of experimental data on the stability field of pure biotite concludes that the first development of this mineral, under water pressure of a few kilobars, occurs at temperatures between 300 and 400°C. However mixed-layer biotite might be stable at temperatures lower than 300°C. This latter temperature range is compatible with the stability of other mineral association (prehnite-pumpellyite) observed in the upper part of the spilite flow.

## Inferred Origin of the Parental Magma of the Spilite

Most authors consider spilites as derivative of basaltic lavas, and some textural features seem to substantiate this theory of basaltic

origin. However the chemistry of the spilites may also indicate an origin from amphibolite. These two possibilities will be discussed.

The AFM diagram (Fig. 28) shows the analyses of the spilites plotted together with the brecciated rocks. The fact that the bulk analyses of the spilitic rocks do not fall on a continuous liquid line trend of descent is worth consideration. The scattering (Fig. 28) of these analyses is probably due to a heterogeneous distribution of the alkalis in the spilite flow of the core.

Wager and Deer (1939) and later Wager (1960) in their study of the Skaergaard intrusion of eastern Greenland and subsequently Walker and Poldervaart (1949) and Tilley (1950) demonstrated that basaltic magma under volcanic or plutonic conditions produces a more effective crystallization in the femic than in the felsic mineral group of Bowen's reaction series. As a result the residual liquids become progressively enriched in iron while enrichment of alkalis is less pronounced. The variation of the Skaergaard liquid line trend of descent may be due to the composition of the initial magma type (Wager, 1960).

Figure 28 shows the AFM diagram for the Skaergaard intrusive magma trend (1), the spilite and associated rock of the Caribbean Island Arc (2 and 3), and the trend of some of the quartz, and hornblende-andesine porphyry rocks from St. John (4). It is known that many mafic trends start off in the direction of the basaltic trend and then switch their direction. The usual broadening of the spilitic and associated rocks of the Caribbean Islands Arc samples

Figure 28. AFM diagram of various rock types.

Skeargaard liquid trend (Wager, 1960).

B Average of 41 basalts from the Mid-Atlantic Ridge (Muir and Tilley, 196 ).

G One gabbro from the Indian Ocean (Hekinian, in press).

P One pyroxenite from the Indian Ocean (Hekinian, in press).

Sp Average of two serpentinites from the Puerto Rico Trench (Hess, 1964).

M Average of 4 greenstones from the Mid-Atlantic Ridge (Melson and VanAndel, 1966).

* One metamorphosed basalt from the Carlsberg Ridge, Indian Ocean (Cann and Vine, 1967).

V Average of 92 spilites from various localities Vallance, 1960).

W Average spilites of Wells, (1923).

S Average spilites of Sundius, (1930).

R Average metamorphosed basalts from Australia (Smith, 1968).

D Average of 25 Andesites from the Virgin Island (Donnelly, 1966).

$D_1$ Average of 4 Hornblende-Andesine-Porphyry dike from St. Thomas, Virgin Island (Donnelly, 1966).

$D_2$ Average of 2 Hornblende-Andesine Porphyry dike from

St. Thomas, Virgin Island (Donnelly, 1966).

$D_3$ Average of 43 spilites from the Virgin Island (Donnelly, 1966).

■ Average 46 analyses of the Diorite-Tonalite Batholith from the Virgin Island (Longshore, 1965).

⊗ Average of 20 spilites from the Virgin Island, (Longshore, 1965).

● Average of 19 Hornblende-Andesine dike rocks from the Virgin Island (Longshore, 1965).

▼ Average of 18 Quartz - Andesine dike rocks from the Virgin Island (Longshore, 1965).

L Average of 5 spilites from Puerto Rico (Lidiak, 1963).

O Average of 63 spilites from the core (St. John) (Present work).

X Average of 4 albite-diabase dike rocks from the core (present work).

◐ Average of 3 amphibole-porphyry dike rocks from the core (present work).

▽ Average of andesine-diabase dike rocks from the core (present work).

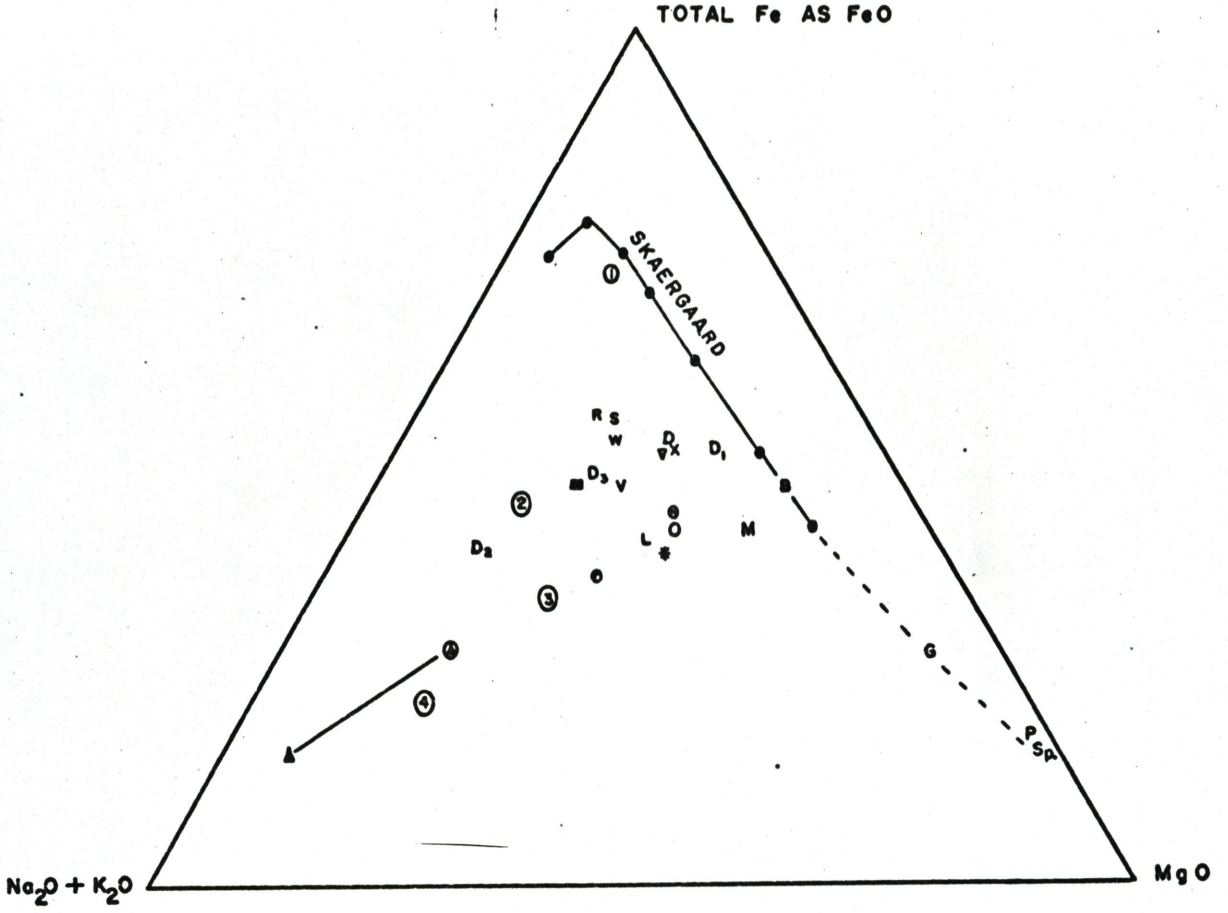
TOTAL Fe AS FeO
SKAERGAARD
R
S
W
$D_x$
$D_1$
$D_3$
V
M
$D_2$
L
G
$P_{SG}$
$Na_2O + K_2O$
MgO

may be attributed to the original fractional crystallization of a mafic hydrated parental magma.

A hypothetical model for the origin of hydrated magma from the Virgin Island was suggested by Donnelly (1966) and Longshore (1965). These authors suggested that 1) gradual partial melting of a hydrous mafic material with the lowest melting fraction extruded as sialic rocks, and 2) temperature increases, produced the basic rocks. This later assumption was based upon the fact that the FeO/MgO ratio in the melt is controlled by the same ratio as in the parental material, and that the high value of magnesium in the spilites must be explained by the subtraction of sialic material which left the unmelted material enriched in magnesium. From this later consideration it is likely that the spilite and the felsic associated material (diorite-tonalite batholith, spilite, hornblende-andesite porphyry) will fall on a same hypothetical differentiated liquid trend (2) (Fig. 28). The iron enrichment of this latter type of rock assemblages (2) indicated that they were derived from the melting of a more differentiated mafic magma than the spilite and amphibole porphyry rocks (3) (Fig. 28). It is possible that the spilites and their various rock type associations are derived from the melting of mafic rocks at different depths in the crust or in the upper mantle. However, this cannot be always accepted and there are the following facts against such rocks being related genetically: (1) there is a time and location difference between members of the trends; (2) other spilitic rocks do not fall on either trend of

the intermediate type of rocks (Fig. 28).

Yoder and Tilley (1962, p. 463) showed in their water pressure-temperature diagram that a variety of basalts, olivine tholeiite, high alumina basalt, and the alkali basalt, melt between 870°C and 1150°C at 2000 bars water pressure. From the same curve (Yoder and Tilley, 1962) it is also shown that these basalts melt between 650°C and 1050°C at 10,000 bars water pressure. Donnelly (1966) advanced the possibility that the mafic igneous rocks encountered in the Virgin Islands have an over-all similarity with the high-alumina basalts from the other regions of the world, and that these rocks might have a common origin. Donnelly (1966) has presented evidence suggesting that the extrusive rocks of the Virgin Islands were derived from an hydrated portion of the sub-crust or the upper mantle.

The chemistry and the fabric of the spilitic rocks from the core are comparable to basaltic rocks. Some average analyses of oceanic basalts dredged from the Mid-Atlantic Ridge of the Atlantic and Indian Oceans are shown in Table 14. This Table (14) shows that the soda content of the average analyses of the upper spilite flow plus the bottom brecciated rocks are close to the soda content of the average oceanic basalt. The average soda content of the upper spilite flow (patchy and non-patchy spilite, Table 10) is 5.0 percent which is much higher than the average soda content in the basaltic rocks (Table 14). However the control of alkalis in the brecciated part of the core is ambiguous since later tectonic

movement might have affected the distribution of K and Na of this zone. Most fresh basalts have a total water content of less than 2 percent; however the spilitic zones of the core have a much higher water content ($\simeq$ 5 percent calculated water). Some of the hypothesis advanced for the occurrence of water in spilites favor the retention of volatiles, chiefly water, from a basaltic magma during the cooling period (Burri and Niggli, 1945; Vuagnat, 1946; Van Overeem, 1948; Amstutz, 1954, 1958). Nevertheless, this author does not believe it is a necessary condition for the basaltic rocks to have retained their volatiles during magmatic solidification. This idea will be developed in the forthcoming discussion.

Previous authors have considered the possibilities of basaltic rocks being metamorphosed to the amphibolite facies. Evans and Leake (1960) in their study of amphibolites from Connemara, Ireland, showed that these rocks have an $Na_2O$ content of up to 4 percent and a water content of about 2-5 percent, and that prior to metamorphism these amphibolites were of basaltic composition (Evans and Leake, 1960). These authors have based their conclusions upon the fact that the major compounds ($SiO_2$, $Al_2O_3$, MgO, CaO) and the minor compounds ($TiO_2$, $Na_2O$, $K_2O$, MnO, $P_2O_3$) of these amphibolites together with their variation trends in the AFM diagram (Evans and Leake, 1960, p. 353) are comparable to tholeiitic and alkali basaltic rocks.

Amphibolite was also reported associated with spilites in Puerto Rico (Tobish, 1968). Among the different interpretations for the origin of these amphibolites the one on regional metamorphism

of an original mafic rock or older mafic rocks regionally metamorphosed seems to be favored by the author (Tobish, 1968). The mafic origin for these amphibolites was tentatively based on the lower strontium content of the amphibolite (para-amphibolite) compared to other amphibolites (ortho-amphibolite). The average chemical analyses (Tobish, 1968, p. 568) seems also to be similar to the average normal basalts. These amphibolites from Puerto Rico may represent part of a lower layer of oceanic crust brought to the surface as tectonic inclusions with other mafic rocks (Tobish, 1968).

Thus another possible alternative for the origin of the spilite from the Virgin Island core could be the melting of an amphibole bearing rock beneath the Virgin Island. The type of magma generated from these rocks with the proper amount of alkalis close to the observed alkalis content in the spilite may switch the normal liquid differentiation trend (1) of the AFM diagram (Fig. 24) toward the $Na_2O + K_2O$ corner.

The above two hypotheses, origin from partial melting of basaltic rocks and the origin from partial melting of amphibolites are complementary to each other since they both involve derivation of this spilite suite from a mafic parental magma. The basaltic lava, during their accumulation in the Island Arc regions, may have been metamorphosed to the amphibolite type of rocks. The water was probably retained by the parental rock during metamorphism. After metamorphism a high temperature gradient is needed in the amphibolite to allow partial melting. Tectonic movements with thicken-

ing of the crust under the Island Arc and subsequent lowering of the crust-Mantle boundary may account for the partial melting of these mafic rocks. This recycling process involving the change of basalt to amphibolite and finally, after an appropriate readjustment to a new equilibrium environment, gives rise to a spilitic type of rock. However, this later theory is weakened because: (1) no amphibolites have been found associated with spilites in the area of sampling and (2) there is a lack of knowledge about the composition of the crust or the upper mantle beneath the Virgin Islands.

## Possible Depth of Origin of the Spilite Parental Magma

It is assumed that the most important component of the volatile part of the parental magma of the spilite is water. The presence of water in the parental magma could be proved by the crystallization of chlorite as a late deuteric mineral. Since no analyses for $H_2O$ were made during this study, an estimate of this water may be extrapolated from the chlorite content of the spilite. This estimate was made by calculating the molecular weight percent of chlorite. This method shows that the chlorite of the spilite from the core contains about 11 weight percent of $H_2O$ which corresponds to about 5 weight percent of $H_2O$ in the bulk rock. The role of the volatile components, especially water, in the crystallization of the magma consists in the lowering of the melting point.

Burnham and Jahns (1962) studied the albite glass in the Harding pegmatite (New Mexico). This study determined the solubility of water in silicate melts by the excess-water method as a function

of pressure up to 10,000 bars and at temperatures of the $H_2O$ saturated liquids for each melt. Burnham and Jahns curves (1962) enabled an extrapolation of the solubility value for the albite melt at temperatures of 900°C and pressure of around 2000 bars to be 5 weight percent of water.

On the basis of present data the melting of the parental magma for these spilites could not have taken place at a pressure much lower than 2000 bars and not higher than 10,000 bars. However, this lower limit of pressure is purely speculative since such value was based upon the present content (5 percent) of water in the spilite. The initial water content in the magma is not known and much of this water could have been lost during the ascent of this magma.

Experimental data on the system $MgO$-$SiO_2$-$TiO_2$ (MacGregor, 1965) indicates that the minimum melting composition changes with pressure. This ternary diagram for a model peridotite composition shows that with increasing pressure, the $TiO_2$ content increases and the $MgO/SiO_2$ ratio decreases from 1 atm to 10,000 bars (MacGregor, 1965). Since the titanium in the spilite and the brecciated zone did not migrate more than relatively small distances (millimeters), it is safe to conclude that the amount of $TiO_2$ in these rocks is original. The $MgO/SiO_2$ ratio of the spilite, the upper albite-diabase and the andesine-diabase dikes is 0.16, 0.11, and 0.12 respectively. This ratio ($MgO/SiO_2$) decrease is followed by a $TiO_2$ increase (0.60, 0.90 and 1.14, see Table 10). It has been suggested (Chayes, 1964) that the $TiO_2$ content of basalts is related to the depth from which these

rocks have been tapped. The average $TiO_2$ and $MgO/SiO_2$ ratio is compared to the average ($TiO_2$ = 1.28 and $MgO/SiO_2$ = 0.17) of 37 oceanic basalts from the Mid-Atlantic Ridge (Engel and Engel, 1964; Muir and Tilley, 1964, 1966; Nicholls et al., 1964).

Extrapolating from the above experimental data, and assuming an original composition close to a basaltic melt, we may conclude that the different types of rocks encountered in the core were tapped at different levels in the Earth with a lower limit of 40 km. (10 kbs), (extrapolated from the curve of Yoder and Tilley, 1962, p. 498).

# CONCLUSIONS

The complexity of the mineralogical assemblages, the variability of their chemistry and the general geological setting of the area suggest that the spilite and the associated dikes encountered in the Virgin Island core have undergone several processes of both magmatic and postconsolidation in origin. In order to retrace these different processes, various criteria dealing with composition, texture and comparison with similar types of rocks from other localities are considered.

Generally the magmatic origin of the spilite is recognized by their preserved texture similar to normal extrusive mafic rocks. Other facts validating the magmatic origin of the spilite were observed during this study and will be recalled. For this purpose the spilite flow is separated into three zones as follows:

1. The patchy spilite zone consists of dark colored patches (about 2 cm. in diameter) set into a green matrix. From petrological investigations it was noticed that the green matrix contains outlines of glassy textural features replaced by chlorite. This green matrix was probably solidified directly from the magma after the crystallization of the dark patches.

2. The non-patchy spilite, below 650 feet, is part of the same flow forming the above patchy spilite. This is well illustrated by the textural features, by mineralogical similarities, and by the lack of a contact zone between the patchy and the non-patchy spilite. The disappearance of patchiness with depth in the core is probably due

to a differential cooling effect between the patchy and the non-patchy spilite. The non-patchy zone has solidified relatively slower than the above patchy zone. The remnants of glassy texture are less conspicuous in this non-patchy zone and the phenocrysts of the clinopyroxene are partially or completely replaced.

3. The bottom brecciated zone is part of the above spilite flow. This brecciated zone is enriched in chlorite, epidote and quartz with respect to the above spilite flow but relic microlitic textures are largely oblitered. This zone also contains some relic fragments of spilite rocks and a considerable amount of veining. The general texture of these rocks has a tendency to show minerals and rock fragments (keratophyre breccia) strained and fractured. Phenocrysts of pseudomorphed amphibole indicate the occurrence of a dike rock which has been recrystallized completely. From the above facts it is believed that a tectonic movement of faulting affected this part of the spilite flow.

Previous theories on the origin of spilites from the Virgin Island have mentioned that autometasomatism was the main process contributing to the formation of these rocks. However, the author recognizes that autometasomatism might have been only a partial possibility in the explanation for the present occurrence of the spilite rocks of the core. During the crystallization of the parental magma late hydrothermal solutions played a certain role in the process of altering the parental magma of the spilite. The redistribution of some of the main cations, such a sodium, potas-

sium and silicon was facilitated by the passage of late magmatic fluid enriched in volatiles at the close of crystallization. A few lines of evidence suggest that this later type of autometasomatism is due to migration of fluid solutions: 1) there is a certain heterogeneity between the dark patches and their respective green matrices, in that the former is usually higher in potassium and the latter is higher in sodium; 2) low temperature mineral assemblages are more abundant in the green matrices than their corresponding dark patches.

Postconsolidation process of burial metamorphism could explain the occurrences of features which might seem inexplicable if only autometasomatism were considered. Burial metamorphism of the prehnite-pumpellyite facies and of the lower greenschist facies is characterized by the disappearance of prehnite and pumpellyite and the appearance of actinolite (Coombs, 1960, and Smith, 1969, in press). In the drill core prehnite and pumpellyite have disappeared below about 650 feet with a concomitant increase in actinolite. This change is in agreement with observed increases in burial metamorphic grade from other areas (Coombs, 1960; Otalora, 1964; and Smith, 1969).

The parental magma giving rise to the spilite and the dikes from the Virgin Island core is most likely the result of the melting of mafic rocks. Extrapolating from previous experimental works it was found that the spilite's parental magma originated close to or within the lower Crust beneath the Virgin Islands, at depths of about 40 km. The parental magma of these spilites could have had either the composition of a basalt or the composition of an amphibolite. Rocks of

intermediate composition such as spilites, amphibole porphyries, albite-diabase and andesine-diabase do not fall on the same liquid line of descent of progressive magmatic crystallization. This discrepancy has to be solved in terms of different parental compositions. The increase of total iron and titanium content in the albite and andesine-diabase rocks of the core indicates that they are derived from a more differentiated original magma than the spilite flow.

# BIBLIOGRAPHY

Amstutz, G. C., 1954. Geologie und Petrographie der Ergussgesteine im Verrucano des Glarner Freiberges. Vulkaninstitut Imm. Friedlaender. Pul. No. 5 (Zurich).

_____, 1958. Spilitic Rocks and Mineral Deposits Bull. Missouri School of Mines and Metallurgy, Tech. Serl., No. 96, p. 11.

_____, 1968. Spilites and Spilitic Rocks in Basalts, the Poldervaart Treatise on Rocks of Basaltic Composition, V. 2, Hess and Poldervaart edit. pp. 737-753.

Battey, M. H., 1955. Alkali Metasomatism and the Petrology of Some Keratophyres from New Zealand. Geol. Mag., V. 92, pp. 104-126.

Berryhill, H. L., Briggs, R., and Glover, L., III, 1969. Sedimentation and Structure of Late Cretaceous Rocks in Eastern Puerto Rico. Preliminary Report: Bull. A.A.P.G., V. 44, p. 137.

Bowin, C. O., 1966. Geology of Central Dominican Republic in Caribbean Geological Investigation, Memoir 98, Hess edit., pp. 12-68.

Brindley, G. W., and Gillery, F. H., 1956. X-ray Identification of Chlorite Species. Am. Miner. V. 41, pp. 169-186.

Brongniart, A., 1827. Articles "Roches". Dictionnaire des Sciences. Strasbourg and Paris. V. 46, pp. 98-100.

Burnham, W. C., and Jahns, H. R., 1962. A Method for Determining the Solubility of Water in Silicate Melts. Am. Jour. Sci., V. 260, pp. 721-745.

Burri, C., and Niggli, P., 1945. Die Jungen Eruptivgesteine des Mediterranen Orogens. I. Vulkaninst. Imm. Friedlander, Publ., No. 3 (Zurich).

Cann, J. R., and Vine, F. J., 1967. An Area on the Crest of the Carlsberg Ridge; Petrology and Magnetic Survey. Phil. Trans Roy. Soc. (A), V. 259, pp. 198-298.

Chayes, F., 1964. Titania and Alumina Content of Oceanic and Circumoceanic Basalt. Jour. Geophys. Res., V. 69, pp. 1593-1588.

Cleve, Per Teodore, 1881. Outline of the Geology of the Northeastern West India Islands: N.Y. Acad. Sci. Annals V. 21, p. 185-192.

Coombs, D. S., Ellis, A. J., Fyfe, W. S., and Taylor, A. M., 1959. The Zeolite Facies with Comments on the Interpretation of Hydrothermal Synthesis. Geochim. Cosmochim. ACTA, V. 17, pp. 53-107.

_____, 1960. Lower grade mineral facies in New Zealand. Rep. 21st. Int. Geol. Congr. pt. 13, pp. 339-351.

Deer, W. A., Howie, R. A., and Zussman, J., 1966. An Introduction to the Rock-Forming Minerals. John Wiley and Sons, Inc., New York, p. 528.

Dewey, H., and Flett, I. S., 1911. British Pillow-lavas and the Rocks Associated with Them. Geol. Mag., V. 8, pp. 202-248.

Donnelly, T. W., 1959. The Geology of St. Thomas and St. John, Virgin Islands. Trans. 2nd Caribbean Geol. Conference, Puerto Rico, pp. 153-155.

_____, 1962. Wairikite in West Indian Spilitic Rocks. Am.

Mineralogist, V. 47, pp. 794-802.

_____, 1963. Genesis of Albite in Early Orogenic Volcanic Rocks. Am. Jour. Sci., V. 261, pp. 957-972.

_____, 1964. Evolution of Eastern Greater Antillean Island Arc. Bull. Am. Assoc. of Petroleum Geologists, V. 48, No. 5, pp. 680696.

_____, 1966. Geology of St. Thomas and St. John, U. S. Virgin Islands: In Caribbean Geological Investigation, Geol. Soc. Am. Memoir 98, Hess edit., pp. 85-176.

Engel, A. E. J., and Engel, C. G., 1964. Composition of Basalt from the Mid-Atlantic Ridge. Science, V. 144, p. 1330-1333.

Evans, B. W., and Leake, B. E., 1960. The Composition and Origin of the Striped Amphibolites of Connemara, Ireland. Jour. Petrology, V. 1, Part 3, pp. 337-363.

Gjelsvik, T., 1958. Extremely Soda Rich Rocks in the Karelian Zone, Finnmarksvidda, Northern Norway. A Contribution to the Discussion of the Spilite Problem. Geol. Foren. Stockholm Farh., V. 80, pp. 381-406.

Green, T. H., and Ringwood, A. E., 1968. Genesis of the Calk Alkaline Igneous Rock Suite. Contr. Mineral and Petrol. V. 18, pp. 105-162.

Hekinian, R., 1968. Rocks from the Mid-Oceanic Ridge in the Indian Ocean. Deep Sea Res., V. 15, pp. 195-213.

_____, (to be published). Gabbros and pyroxenite from the Indian Ocean. Deep Sea Res.

Hentschel, H., 1961. Basischer Magmatismus in der Geosynklinale.

Sonderdruck ansder Geologishen Rundschau Band 50, pp. 33-45.

Hess, H. H., 1949. Chemical Composition and Optical Properties of Common Clinopyroxenes, Part I. Amer. Mineralogist, V. 34, pp. 621-666.

_____, 1964. The Oceanic Crust, the Upper Mantle and the Mayaguez Serpentinized Peridotite, in a study of Serpentinite. Nat. Academy of Sci., Nat. Res. Council, Washington, Publ. 1188, pp. 169-175.

_____, 1966. Caribbean Geological Investigation. Geol. Soc. Am. Memoir. 98, pp. 1-10.

Hey, M. H., 1954. Nomenclature of chlorite and oxidized chlorite. Min. Mag., V. 30, p. 277.

Kuno, L., and Hess, H. H., 1953. Unit cell dimensions of dinoenstatite and pigeonite in relation to other common dinopyroxenes. Amer. Jour. Sci., V. 251, p. 741.

Lehmann, E., 1965. Non-metasomatic Chlorite in Igneous Rocks. Geol. Mag., V. 102, No. 1, pp. 24-35.

Lidiak, E. G., 1963. Petrology of the Andesitic, Spilitic and Keratophyric Lavas, North-Central Puerto Rico. Ph.D. Thesis, Rice University, p. 118.

Longshore, D. J., 1965. Chemical and Mineralogical Variations in the Virgin Islands Batholith and its Associated Wall Rock. Ph.D. Thesis, Rice University, Houston, Texas, p. 94.

MacGregor, I. D., 1965. The Effect of Pressure on the Minimum Melting Composition in the System $MgO$-$SiO_2$-$TiO_2$. Washington Carnegie

Inst. Ann. Report of Dir. of Geophysical Laboratory. pp. 135-139.

Melson, C. W., and Andel Van, T. H., 1966. Metamorphism in the Mid-Atlantic Ridge 22°N. Latitude. Marine Geol., V. 4, pp. 165-86.

_____, Thompson, G., and Van Andel, T. H., 1968. Volcanism and Metamorphism in the Mid-Atlantic Ridge, 22°N. Latitude. Jour. Geophys. Res., Vol. 73, No. 15, pp. 5925-5941.

Moore, J. G., 1965. Petrology of deep-sea basalts near Hawaii. Amer. Jour. Sci., V. 263, pp. 40-52.

Muir, J. D., and Tilley, C. E., 1966. Basalts from the Northern part of the Mid-Atlantic Ridge. Jour. Petrology, V. 7 (2), pp. 193-201.

Nicholls, G. D., 1959. Autometasomatism in the Lower Spilites of the Builth Volcanic Series. Q. Jour. Geol. Soc. Lond. 114, pp. 137-162.

_____, Nawalck, J. J., and Hays, E. E., 1964. The Nature and Composition of Rock Samples dredged from the Mid-Atlantic Ridge between 22°N. and 52°N. Mar. Geol., V. 1, pp. 33-343.

Nockolds, S. R., 1966. The Behavior of Some Elements During Fractional Crystallization of Magma. Geochimica and Cosmochimica ACTA, V. 30, pp. 267-278.

Orville, P. M., 1963. Alkali Ion Exchange Between Vapor and Feldspar Phase. Am. Jour. Sci., V. 261, pp. 201-237.

Otalora, G., 1964. Zeolites and related Minerals in Creataceous Rocks of East Central Puerto Rico. Am. Jour. Sci., V. 262, pp. 726-734.

Park, C. F., Jr., 1946. The Spilite and Manganese Problems of the Olympic Peninsula, Washington. Amer. Jour. Sci., V. 244, pp. 305-323.

Poldervaart, A., 1949. Three methods of graphic representation of chemical analyses of igneous rocks. Trans. Roy. Soc. S. Africa, V. 32, pp. 177-188.

Rittman, A., 1958. Geosynclinal volcanism, ophiolites and barramiya rocks. Egyptian Jour. Geol., V. 2, pp. 61-65.

Routhier, P., 1963. Les gisements Metalliferes. Mason Paris. pp. 643, 651, 654.

Roy, D. M., and Roy, R., 1957. System $CaO-Al_2O_3-SiO_2-H_2O$ VI: The Grossularite-$3CaO.Al_2O_36H_2O$ Join. Bull. Geol. Soc. Am. V. 68, p. 1788.

Shapiro, L., and Branock, W. W., 1962. Rapid Analyses of Silicates, Carbonates, and Phosphate Rocks. eol. Survey Bull. 1144-A, p. 56.

Shoen, R., 1962. Semi-quantitative analysis of chlorites by X-ray diffraction. Am. Min., V. 47, pp. 1384-1392.

Slemmons, D. B., 1962. Determination of volcanic and plutonic plagioclases using a three-or-four-axis universal stage: Geol. Soc. Amer., special paper 69, p. 64.

Smith, R. E., 1967. Curved albite microlites in spilitic lavas from a Low-grade metamorphosed sequence. Geol. Soc. Am. abstract. p. 208.

_____, 1968. Redistribution of major elements in the alteration of some basic lavas during burial metamorphism. Jour. Petrology,

V. 9, Part 2, pp. 191-219.

_____, 1969. Zones of Progressive Regional Burial Metamorphism in Part of the Tasman Geosyncline, Eastern Australia. Jour. Petrology, V. Part I, pp.

Sundius, N., 1930. On the Spilitic Rocks. Geol. Mag., V. 67, pp. 1-17.

Szadeczky-Kardoss, E., 1958. On the Petrology of Volcanic Rocks and the Interaction of Magma and Water. ACTA Geologica (Budapest), V. 5, pp. 197-233.

Tilley, C. E., 1950. Some aspects of Magmatic Evolution. Q. Jour. Geol. Soc. Lond., V. 106, pp. 37-61.

Tobish, T. O., 1968. Gneissic Amphibolite at Los Palmas, Puerto Rico, and its significance in early history of the Greater Antilles Island Arc. Geol. Soc. Am. Bull., V. 79, pp. 557-574.

Tomblin, J. F., (in press). Chemical Analyses of Volcanic Rocks from the Lesser Antilles. Univ. West Indies Seismic Research Unit Spec. Publ. 15.

Turner, F. J., 1968. Metamorphic Petrology. Intern. Science in the Earth and Planet. Sci. Publ., McGraw-Hill, p. 403.

Tyrrell, G. W., 1933. Greenstone and Greywackes. Bull. Comm. Geol. Finlande. No. 102, pp. 24-26.

Vallance, T. G., 1960. Concerning Spilites. Proc. Linn. Soc., N.S.W. V. 85, p. 8-52.

_____, 1965. On the Chemistry of Pillow Lavas and the Origin of Spilites. Mineralog. Mag., V. 34, pp. 471-481.

VanOverreem, A. J. A., 1948. A section through the Dalformation.

A contribution to the Geology of Dalsland, S.W. Sweden. Diss. Univ., Leiden, p. 131.

Vuagnat, M., 1946. Sur quelques diabases suisses. Contribution a l' etude du probleme des spilites et des pillow lavas. Schweiz Min. petr. Mitt., V. 26, pp. 116-228.

Wager, L. R., and Deer, W. A., 1930. Geological Investigation in East Greenland Pt. III; the petrology of the Skaergaard Intrusion, Kangerdlugssuag, East Greenland, Medd. om Greenland, V. 105, No. 4, pp. 1-352.

_____, 1960. The major element variation of the layered series of the Skaergaard Intrusion and a re-estimation of the average composition of the hidden layered series and of the successive residual magmas. Jour. petrology, V. 1, pp 364-398.

Wells, A. K., 1923. The nomenclature of the spilitic suite. Part II. The Problem of the Spilites. Geol. Mag., V. 60, pp. 62-74.

Wilshire, H. G., 1959. Deuteric Alteration of Volcanic Rocks. Jour. Proc. Roy. Soc. N.S.W., V. 93, pp. 105-120.

Winchell, A. N., and Winchell, H., 1961. Elements of optical mineralogy: An introduction to microscopic petrography. John Wiley and Sons, Inc., Publis. Part II, p. 551.

Yoder, H. S., and Tilley, C. E., 1962. Origin of Basalt Magma: An experimental Study of Natural and Synthetic Rock Systems. Jour. Petrology, V. 3, pp. 342-532.

TABLE 1 -- OPTICAL PROPERTIES OF REPRESENTATIVE PLAGIOCLASE FROM THE CORE. (ST. JOHN, VIRGIN ISLAND).

| SAMPLE DEPTHS IN THE CORE | ROCK TYPE | ANORTHITE PER CENT | | | | | |
|---|---|---|---|---|---|---|---|
| | | ALBITE TWIN | CARLSBAD TWIN | ALBITE CARLSBAD TWIN | MANEBACH TWIN | ALA "A" TWIN | BAVENO TWIN |
| 129 | AMPHIBOLE PORPHYRY DIKE | | $An_{15}$ | | | | $An_{3}$ |
| 189 | ALBITE DIABASE DIKE | | | | $An_{9-11}$ | $An_{6}$ | $An_{4}$ |
| 220 | ALBITE DIABASE DIKE | | | $An_{6-10}$ | | | |
| 236 | SPILITE | | | $An_{7}$ | $An_{7}$ | | |
| 373.5 | SPILITE | | | $A_{1-2}$ | | | |
| 503 | SPILITE | | | $An_{1-5}$ | $An_{1-2}$ | | |
| 592 | SPILITE | | | | $An_{5}$ | | |
| 624 | SPILITE | | | $An_{9}$ | | | |
| 732 | AMPHIBOLE PORPHYRY DIKE | | | | | | $n_{11}$ |
| 802 | SPILITE | | | $An_{1-2}$ | | | |
| 872 | ANDESINE DIABASE DIKE | $An_{42-43}$ | $An_{34-75}$ | | $An_{42}$ | | $An_{41}$ |

TABLE 1 -- OPTICAL PROPERTIES OF REPRESENTATIVE PLAGIOCLASE FROM THE CORE. (ST. JOHN, VIRGIN ISLAND). (CONT'D)

| SAMPLE DEPTHS IN THE CORE | ROCK TYPE | ANORTHITE PER CENT | | | | | |
|---|---|---|---|---|---|---|---|
| | | ALBITE TWIN | CARLSBAD TWIN | ALBITE CARLSBAD TWIN | MANEBACH TWIN | ALA "A" TWIN | BAVENO TWIN |
| 909 | ANDESINE DIABASE DIKE | $An_{29-30}$ $An_{42}$ | | | $An_{11-28}$ | | |
| 921 | ANDESINE DIABASE DIKE | $An_{62}$ | | | | | $An_{29}$ |

TABLE 2 -- X-RAY DETERMINATION OF FELDSPAR FROM THE CORE.

(ST. JOHN, VIRGIN ISLAND).

| SAMPLE DEPTHS IN THE CORE | ROCK TYPE | 2θ | FELDSPAR COMPOSITION |
|---|---|---|---|
| 129 | AMPHIBOLE PORPHYRY DIKE | 1.75 | $Or_5Ab_{95}$ |
| 425 | SPILITE | 1.83 | $Ab_{100}$ |
| 573 | SPILITE | 1.86 | $Ab_{100}$ |
| 732 | AMPHIBOLE PORPHYRY DIKE | 1.75 | $Or_5Ab_{95}$ |

$\Delta 2\theta = \overline{201}_{felds} - 101_{KBrO_3}$ . These values were plotted on Orville (1963) curve in order to find the Orthodose content of feldspar.

TABLE 3 -- OPTICAL DEFERMINATION OF PYROXENE FROM THE CORE. (ST. JOHN, VIRGIN ISLAND).

| SAMPLE DEPTHS IN THE CORE | ROCK TYPE | 2V | INDEX OF REFRACTION | COMPOSITION |
|---|---|---|---|---|
| 177 | ALBITE DIABASE | 57° | 1.683 | $Mg_{43}Ca_{49}Fe_8$ |
| 185 | ALBITE DIABASE | 58°, 60° | 1.681 | $Mg_{44}Ca_{49}Fe_7$ |
| 189 | ALBITE DIABASE | 61°, 58°, 58° | 1.680 | $Mg_{45}Ca_{49}Fe_6$ |
| 242.5 | SPILITE | 59° | 1.677 | $Mg_{44}Ca_{51}Fe_5$ |
| 349 | SPILITE | 58° | N.D. | N.D. |
| 417 | SPILITE | 61° | 1.675 | $Mg_{43}Ca_{50}Fe_7$ |
| 425 | SPILITE | 60°, 59°, 60°, 60° | 1.685 | $Mg_{42}Ca_{49}Fe_9$ |
| 481 | SPILITE | 62° | N.D. | N.D. |
| 492 | SPILITE | 58° | 1.674 | $Mg_{48}Ca_{49}Fe_3$ |
| 891 | ANDESINE DIABASE DIKE | 50° | 1.697 | $Mg_{37}Ca_{41}Fe_{22}$ |
| 909 | ANDESINE DIABASE DIKE | 53°, 42° | 1.691 | $Mg_{43}Ca_{38}Fe_{19}$ |
| 921 | ANDESINE DIABASE DIKE | 42°, 44° | 1.695 | $Mg_{40}Ca_{36}Fe_{23}$ |

N.D. - Not Determined.

TABLE 3 -- OPTICAL DEFERMINATION OF PYROXENE

FROM THE CORE. (ST. JOHN, VIRGIN ISLAND). (CONT'D)

| SAMPLE DEPTHS IN THE CORE | ROCK TYPE | 2V | INDEX OF REFRACTION | COMPOSITION |
|---|---|---|---|---|
| 965 | ANDESINE DIABASE DIKE | $53^{\circ}$, $47^{\circ}$, $50^{\circ}$ | 1.694 | $Mg_{39}Ca_{41}Fe_{20}$ |
| 980 | ANDESINE DIABASE DIKE | $53^{\circ}$, $48^{\circ}$, $41^{\circ}$ | 1.6925 | $Mg_{42}Ca_{39}Fe_{19}$ |

TABLE 4 -- X- RAY DETERMINATION OF THE PYROXENE FROM THE CORE. (ST. JOHN, VIRGIN ISLAND).

| SAMPLE DEPTHS IN THE CORE | ROCK TYPE | $d_{(220)}$ | $d_{(22\bar{1})}$ | $(220 - 22\bar{1})$ | COMPOSITION |
|---|---|---|---|---|---|
| 177 | ALBITE DIABASE DIKE | 3.2422 | 3.0119 | .2303 | $Di_{95}Pi_5$ - $Di_{88}Hd_{12}$ |
| 192 | ALBITE DIABASE DIKE | 3.2303 | 2.9990 | .2313 | $Di_{98}Pi_2$ - $Di_{82}Hd_{18}$ |
| 446 | SPILITE | 3.2433 | 2.9980 | .2453 | $Di_{97}Pi_3$ - $Di_{93}Hd_7$ |
| 521 | SPILITE | 3.2203 | 2.9756 | .2447 | $Di_{96}Pi_4$ - $Di_{95}Hd_5$ |
| 573 | SPILITE | 3.2200 | 2.9756 | .2444 | $Di_{96}Pi_4$ - $Di_{88}Hd_{12}$ |
| 895.5 | ANDESINE DIABASE DIKE | 3.2318 | 2.9990 | .2328 | $Di_{90}Pi_{10}$ - $Di_{72}Hd_{28}$ |
| 905 | ANDESINE DIABASE DIKE | 3.2433 | 3.0079 | .2354 | $Di_{75}Pi_{25}$ - $Di_{60}Hd_{40}$ |
| 965.5 | ANDESINE DIABASE DIKE | 3.2245 | 2.9980 | .2265 | $Di_{18}Pi_{82}$ - $Di_{70}Hd_{30}$ |

TABLE 5 -- COMPOSITION OF CHLORITE FROM X-RAY DATA.

| SAMPLE DEPTHS IN THE CORE | ROCK TYPE | $Fe^{+2}$ | $Mg^{+2}$ | $Al^{+4}$ | $Mg_{12-x-y}Fe^{+2}_{x}Al_{y}(Si_{8-y}Al_{y})O_{20}(OH)_{16}$ |
|---|---|---|---|---|---|
| 110 | SPILITE | 3.90 | 8.03 | 1.00 | $Mg_{8.03}Fe_{3.90}Al_{1.00}(Si_{7.00}Al_{1.00})O_{20}(OH)_{16}$ |
| 134 | AMPHYBOLE PORPHYRY DIKE | 2.70 | 9.20 | 1.35 | $Mg_{9.20}Fe_{2.70}Al_{1.35}(Si_{6.45}Al_{1.35})O_{20}(OH)_{16}$ |
| 140 | AMPHYBOLE PORPHYRY DIKE | 3.03 | 8.20 | .74 | $Mg_{8.20}Fe_{3.03}Al_{.74}(Si_{7.26}Al_{.74})O_{20}(OH)_{16}$ |
| 189 | ALBITE | 4.75 | 7.20 | 1.25 | $Mg_{7.20}Fe_{4.75}Al_{1.25}(Si_{6.75}Al_{1.25})O_{20}(OH)_{16}$ |
| 226 | DIABASE DIKE | 3.60 | 8.32 | .80 | $Mg_{8.32}Fe_{3.60}Al_{.80}(Si_{7.20}Al_{.80})O_{20}(OH)_{16}$ |
| 234 | SPILITE | 4.20 | 7.70 | .96 | $Mg_{7.70}Fe_{4.20}Al_{.96}(Si_{7.04}Al_{.96})O_{20}(OH)_{16}$ |
| 264 | SPILITE | 3.70 | 8.30 | .93 | $Mg_{8.30}Fe_{3.70}Al_{.93}(Si_{7.07}Al_{.93})O_{20}(OH)_{16}$ |
| 330 | SPILITE | 2.55 | 9.30 | 1.49 | $Mg_{9.30}Fe_{2.55}Al_{1.49}(Si_{6.51}Al_{1.49})O_{20}(OH)_{16}$ |
| 379 | SPILITE | 4.65 | 7.25 | 1.03 | $Mg_{7.25}Fe_{4.65}Al_{1.03}(Si_{6.97}Al_{1.03})O_{20}(OH)_{16}$ |
| 417 | SPILITE | 3.95 | 7.96 | .93 | $Mg_{7.96}Fe_{3.95}Al_{.93}(Si_{7.07}Al_{.93})O_{20}(OH)_{16}$ |
| 437 | SPILITE | 4.35 | 7.55 | .97 | $Mg_{7.55}Fe_{4.35}Al_{.97}(Si_{7.03}Al_{.97})O_{20}(OH)_{16}$ |
| 481 | SPILITE | 4.70 | 7.19 | 1.03 | $Mg_{7.19}Fe_{4.70}Al_{1.03}(Si_{6.97}Al_{1.03})O_{20}(OH)_{16}$ |
| 503 | SPILITE | 4.10 | 7.79 | 1.03 | $Mg_{7.79}Fe_{4.10}Al_{1.03}(Si_{6.97}Al_{1.03})O_{20}(OH)_{16}$ |

TABLE 5 -- COMPOSITION OF CHLORITE FROM X-RAY DATA. (CONT'D)

| SAMPLE DEPTHS IN THE CORE | ROCK TYPE | $Fe^{+2}$ | $Mg^{+2}$ | $Al^{+4}$ | $Mg_{12-x-y}Fe^{+2}_{x}Al_{y}(Si_{8-y}Al_{y})O_{20}(OH)_{16}$ |
|---|---|---|---|---|---|
| 540 | SPILITE | 3.75 | 8.16 | .96 | $Mg_{8.16}Fe_{3.75}Al_{.96}(Si_{7.04}Al_{.96})O_{20}(OH)_{16}$ |
| 581 | SPILITE | 3.55 | 8.35 | 1.02 | $Mg_{8.35}Fe_{3.55}Al_{1.02}(Si_{7.08}Al_{1.02})O_{20}(OH)_{16}$ |
| 618 | SPILITE | 3.48 | 8.42 | .96 | $Mg_{8.42}Fe_{3.48}Al_{.96}(Si_{7.04}Al_{.96})O_{20}(OH)_{16}$ |
| 668 | SPILITE | 3.95 | 7.95 | 1.03 | $Mg_{7.95}Fe_{3.95}Al_{1.03}(Si_{6.97}Al_{1.03})O_{20}(OH)_{16}$ |
| 732 | AMPHYBOLE PORPHYRY DIKE | 3.03 | 8.88 | .93 | $Mg_{8.88}Fe_{3.03}Al_{.93}(Si_{7.07}Al_{.93})O_{20}(OH)_{16}$ |
| 742 | SPILITE | 3.45 | 8.50 | .80 | $Mg_{8.50}Fe_{3.45}Al_{.80}(Si_{7.20}Al_{.80})O_{20}(OH)_{16}$ |
| 833 | SPILITE | 3.82 | 8.09 | .97 | $Mg_{8.09}Fe_{3.82}Al_{.97}(Si_{7.03}Al_{.97})O_{20}(OH)_{16}$ |
| 872 | ANDESINE DIABASE DIKE | 6.25 | 5.65 | 1.03 | $Mg_{5.65}Fe_{6.25}Al_{1.03}(Si_{6.97}Al_{1.03})O_{20}(OH)_{16}$ |
| 895 | ANDESINE DIABASE DIKE | 8.00 | 3.90 | .96 | $Mg_{3.90}Fe_{8.00}Al_{.96}(Si_{7.04}Al_{.96})O_{20}(OH)_{16}$ |
| 905 | ANDESINE DIABASE DIKE | 6.30 | 5.59 | 1.07 | $Mg_{5.59}Fe_{6.30}Al_{1.07}(Si_{6.93}Al_{1.07})O_{20}(OH)_{16}$ |

TABLE 5 -- COMPOSITION OF CHLORITE FROM X-RAY DATA. (CONT'D)

| SAMPLE DEPTHS IN THE CORE | ROCK TYPE | $Fe^{+2}$ | $Mg^{+2}$ | $Al^{+4}$ | $Mg_{12-x-y}Fe^{+2}_{x}Al_{y}(Si_{8-y}Al_{y})O_{20}(OH)_{16}$ |
|---|---|---|---|---|---|
| 1003 | ANDESINE DIABASE DIKE | 7.23 | 4.67 | 1.03 | $Mg_{4.67}Fe_{7.23}Al_{1.03}(Si_{6.97}Al_{1.03})O_{20}(OH)_{16}$ |
| 1028 | BRECCIATED ZONE | 3.20 | 8.71 | .93 | $Mg_{8.71}Fe_{3.20}Al_{.93}(Si_{7.07}Al_{.93})O_{20}(OH)_{16}$ |
| 1060 | BRECCIATED ZONE | 3.10 | 8.81 | .90 | $Mg_{8.81}Fe_{3.10}Al_{.90}(Si_{7.10}Al_{.90})O_{20}(OH)_{16}$ |

TABLE 6 -- X-RAY DIFFRACTION DATA FOR HYDROGARNET FROM THE SPILITE OF THE CORE. (ST. JOHN, VIRGIN ISLAND).

| DA | INT. | MINERALS |
|---|---|---|
| 14.85 | 50 | CHL. |
| 7.08 | 100 | CHL. |
| 4.75 | 80 B | CHL. |
| 4.28 | 35 | QTZ. |
| 4.05 | 15 | AB. |
| 3.69 | 20 M, B | AB. |
| 3.58 | 90 | CHL. |
| 3.35 | 100 | QTZ. |
| 3.22 | 100, 100 | SPH., AB. |
| 3.00 | 80 S | HYDRO. |
| 2.85 | 40 | CHL. |
| 2.68 | 100 S | HYDRO. |
| 2.59 | 90 | SPH. |
| 2.46 | 50 M | HYDRO. |
| 2.27 | 30, 12 | SPH., QTZ. |
| 2.02 | 40, 20 | SPH., CHL. |

TABLE 6 -- X-RAY DIFFRACTION DATA FOR HYDROGARNET FROM THE SPILITE OF THE CORE. (ST. JOHN, VIRGIN ISLAND). (CONT'D)

| D$\bar{A}$ | INT. | MINERALS |
|---|---|---|
| 1.82 | 17 | QTZ. |
| 1.66 | 60 B | HYDRO., QTZ. |
| 1.60 | 80 B | HYDRO. |
| 1.54 | 50 | QTZ., CHL. |

B = BROAD, S = SHARP, M = MEDIUM, M B = MEDIUM BROAD

CHL. - CHLORITE

QTZ. - QUARTZ

AB. - ALBITE

SPH. - SPHENE

HYDRO. - HYDROGARNET

TABLE 7 -- X-RAY DIFFRACTION DATA FOR MUSCOVITE (SERICITE) FROM THE SPILITE OF THE CORE. (ST. JOHN, VIRGIN ISLAND).

| D Å | INT. | MINERALS |
|---|---|---|
| 10.31 | 95 B | MUSC. |
| 7.04 | 100 | CHL. |
| 6.34 | 20 | AB. |
| 4.04 | 15 B | AB. |
| 3.85 | 15 B | MUSC. |
| 3.34 | 25 | MUSC. |
| 3.30 | 100 M S | MUSC. |
| 2.93 | 34, 15 | MUSC., AB. |
| 2.82 | 25 M S | CHL., MUSC. |
| 2.52 | 54 M S | CHL., MUSC. |
| 2.12 | 21 B | CHL., MUSC. |
| 2.00 | 46 M S | MUSC. |
| 1.83 | 3 V W | MUSC. |
| 1.77 | 3 V W | MUSC. |

B = BROAD, M S = MEDIUM SHARP, V W = VERY WEAK

MUSC. - MUSCOVITE

CHL. - CHLORITE

AB. - ALBITE

TABLE 8 -- X-RAY DIFFRACTION DATA FOR BIOTITE FROM THE SPILITE OF THE CORE. (ST. JOHN, VIRGIN ISLAND).

| DÅ | INT. | MINERALS |
|---|---|---|
| 10.50 | 100 B | BIOT. |
| 7.10 | 100 | CHL. |
| 4.65 | 50 | CHL. |
| 3.52 | 90 | CHL. |
| 3.33 | 100 M S | BIOT. OR STLP. |
| 2.56 | 40 B | BIOT., CHL. |
| 2.43 | 80 M B | BIOT., CHL. |
| 2.00 | 80 M B | BIOT., CHL. |
| 1.53 | 80 S | BIOT., CHL. |

B = BROAD, M S = MEDIUM SHARP, M B = MEDIUM BROAD, S = SHARP

BIOT. - BIOTITE

CHL. - CHLORITE

STLP. - STIPNOMELANE

TABLE 9 -- MODEL COMPOSITION OF REPRESENTATIVE ROCKS OF THE CORE. (ST. JOHN, VIRGIN ISLAND).

| SAMPLE DEPTHS IN THE CORE | PHENOG. & MICROPH. | | S P I L I T E[1] | | | | |
|---|---|---|---|---|---|---|---|
| | PRX. | PLAG. | QTZ. | CHL. | EPID. | MATRIX | OTHERS[2] |
| 26 | 0.50 | 40.30 | 10.22 | 31.50 | 3.25 | 2.05 | 12.55 |
| 92 | 0.60 | 39.15 | 3.01 | 27.10 | 3.01 | 24.09 | 3.01 |
| 140 | 6.63 | 36.73 | 4.08 | 37.34 | 2.04 | 4.08 | 4.08 |
| -50 | 6.31 | 35.63 | 7.42 | 10.36 | TRACE | 34.26 | 6.00 |
| 163 | 2.22 | 34.77 | 10.22 | 13.33 | TRACE | 38.24 | 1.20 |
| 236 | 0.41 | 37.60 | 5.85 | 38.14 | 3.71 | 13.85 | 0.41 |
| 242 | 2.78 | 35.54 | 7.31 | 31.70 | 3.20 | 8.71 | 12.54 |
| 258 | 0.36 | 37.00 | 5.41 | 29.96 | 1.08 | 25.27 | 1.0 |
| 281 | 4.26 | 26.21 | 4.92 | 24.95 | 1.21 | 36.58 | 1.82 |
| 297 | 2.32 | 25.58 | TRACE | 25.02 | 1.16 | 44.90 | TRACE |
| 302 | 1.67 | 41.89 | 1.11 | 3.35 | 10.05 | 41.89 | TRACE |
| 325 | 3.42 | 33.14 | 1.71 | 17.14 | TRACE | 38.85 | 5.71 |
| 352 | 3.60 | 40.20 | 2.60 | 9.25 | 11.15 | 25.40 | 8.01 |
| 373 | 3.04 | 49.74 | 1.12 | 16.15 | 3.55 | 16.73 | 9.64 |
| 406 | 1.96 | 30.06 | 3.92 | 24.37 | 13.72 | 25.29 | 0.65 |
| 446 | 1.86 | 30.81 | 4.96 | 24.84 | 2.48 | 30.05 | 4.96 |

TABLE 9 -- MODAL COMPOSITION OF REPRESENTATIVE ROCKS OF THE CORE. (ST. JOHN, VIRGIN ISLAND). (CONT'D)

| SAMPLE DEPTHS IN THE CORE | PHENOG. & MICROPH. | | S P I L I T E[1] | | | | |
|---|---|---|---|---|---|---|---|
| | PRX. | PLAG. | QTZ. | CHL. | EPID. | MATRIX | OTHERS[2] |
| 503 | 3.24 | 30.12 | 1.19 | 10.51 | 3.24 | 27.53 | 10.12 |
| 515 | 3.20 | 33.33 | 2.56 | 36.53 | 5.12 | 16.02 | 3.20 |
| 542 | 3.10 | 33.33 | 0.42 | 17.05 | 3.10 | 34.45 | 8.52 |
| 561 | 2.10 | 40.03 | 0.25 | 24.01 | 4.32 | 23.45 | 6.00 |
| 564 | 4.90 | 39.26 | 0.22 | 30.06 | 1.84 | 21.24 | 2.45 |
| 592 | 6.21 | 56.20 | 0.37 | 27.51 | 2.18 | 22.02 | 5.45 |
| 604 | 1.34 | 34.16 | 3.36 | 22.28 | 3.35 | 26.09 | 9.39 |
| 632 | 2.27 | 37.87 | 7.48 | 25.75 | 3.03 | 11.78 | 10.78 |
| 652 | 0.59 | 39.05 | TRACE | 18.34 | 2.36 | 24.85 | 14.78 |
| 673 | TRACE | 32.03 | 1.56 | 20.46 | 5.41 | 18.12 | 12.34 |
| 695 | 1.40 | 30.20 | 9.15 | 15.01 | 8.15 | 19.02 | 7.01 |
| 701 | TRACE | 28.27 | 13.24 | 3.44 | 2.75 | 38.62 | 13.65 |
| 717 | 0.54 | 32.96 | 2.74 | 19.78 | 1.64 | 19.78 | 22.52 |
| 724 | 2.36 | 37.91 | 0.31 | 30.80 | 2.84 | 22.43 | 3.31 |
| 778 | 3.96 | 46.03 | 2.38 | 21.42 | TRACE | 10.00 | 16.19 |

TABLE 9-- MODAL COMPOSITION OF REPRESENTATIVE

ROCKS OF THE CORE. (ST. JOHN, VIRGIN ISLAND). (CONT'D)

| SAMPLE DEPTHS IN THE CORE | PHENOG. & MICROPH. | | B R E C C I A T E D Z O N E | | | | |
|---|---|---|---|---|---|---|---|
| | PRX. | PLAG. | QTZ. | CHL. | EPID. | MATRIX | OTHERS[2] |
| 1028 | N.S. | 2.60 | 15.50 | 30.01 | 15.30 | 20.70 | 18.30 |
| 1060 | N.S. | 10.10 | 17.01 | 48.15 | 14.25 | 3.15 | 2.00 |
| 1074 | N.S. | 5.60 | 25.02 | 8.45 | 30.70 | 21.20 | 8.00 |
| 1096 | N.S. | 25.20 | 8.15 | 7.20 | 27.01 | 21.10 | 9.00 |
| 1101 | N.S. | 24.10 | 22.30 | 8.05 | 13.00 | 26.50 | 6.00 |

[1]Spilite-contains actinolite throughout.

[2]Others-include calcite magnetite, hematite, sphene, hydrogarnet, pumpellyite, prehnite and microcrystalline aggregates.

N.S. - Not Seen.

TABLE 9 -- MODAL COMPOSITION OF REPRESENTATIVE ROCKS.

| SAMPLE DEPTHS IN THE CORE | DIKE ROCKS | | | | | |
|---|---|---|---|---|---|---|
| | AMPHIB. | COARSE GRAINS PRX. | COARSE GRAINS PLAG. | QTZ. | CHL. | MATRIX AND OTHERS |
| | | | AMPHIBOLE PORPHYRY | | | |
| 129 | 10.31 | 0.17 | 39.68 | 11.11 | 7.77 | 30.93 |
| 732 | 28.68 | 0.81 | 43.09 | 4.09 | 22.13 | 27.04 |
| | | | ALBITE DIABASE | | | |
| 177 | TRACE | 35.34 | 24.82 | TRACE | 27.93 | 11.89 |
| 184 | TRACE | 39.04 | 28.57 | 5.71 | 21.90 | 4.76 |
| 189 | 0.60 | 29.26 | 40.24 | 3.04 | 23.78 | 3.04 |
| 192 | 0.62 | 36.64 | 32.91 | 3.72 | 18.63 | 7.47 |
| 220 | 0.72 | 37.22 | 29.92 | 3.64 | 18.97 | 9.48 |
| 226 | 0.30 | 32.19 | 41.20 | TRACE | 16.43 | 10.95 |
| | | | ANDESINE DIABASE | | | |
| 847 | TRACE | 36.04 | 47.09 | 2.90 | 9.30 | 4.65 |
| 872 | TRACE | 40.59 | 43.85 | 1.16 | 8.52 | 5.84 |
| 879 | TRACE | 24.85 | 29.71 | 1.00 | 12.57 | 30.85 |
| 895 | TRACE | 38.37 | 51.16 | 1.16 | 3.48 | 5.81 |
| 909 | 0.10 | 24.00 | 55.00 | 1.00 | 11.50 | 8.5 |

TABLE 9 -- MODAL COMPOSITION OF REPRESENTATIVE ROCKS. (CONT'D)

| SAMPLE DEPTHS IN THE CORE | AMPHIB. | DIKE ROCKS COARSE GRAINS PRX. | PLAG. | QTZ. | CHL. | MATRIX AND OTHERS |
|---|---|---|---|---|---|---|
| | | | ANDESINE DIABASE | | | |
| 921 | TRACE | 30.31 | 48.53 | 2.33 | 12.28 | 6.52 |
| 936 | 0.12 | 36.80 | 39.88 | 4.04 | 10.18 | 9.07 |
| 955* | 0.10 | 6.06 | 15.75 | 4.24 | 19.39 | 54.54 |
| 965 | 0.50 | 42.60 | 48.06 | 1.08 | 3.30 | 6.03 |
| 980 | 0.10 | 42.97 | 47.10 | 0.82 | 2.47 | 6.61 |

*No Dike Rock.

TABLE 10 -- AVERAGE OF PARTIAL CHEMICAL ANALYSIS OF SPILITE AND DIKE ROCKS FROM VARIOUS LOCALITIES.

| OXIDES | P.S. | N.S. | T.S. | B. | A.D. | Al.D. | A.P. | D. | W. | S. | M.V. | C.V. | V1. |
|---|---|---|---|---|---|---|---|---|---|---|---|---|---|
| $SiO_2$ | 49.36 | 47.30 | 48.33 | 46.53 | 46.35 | 49.52 | 55.18 | 49.3 | 46.01 | 51.22 | 50.11 | 50.52 | 49.65 |
| $TiO_2$ | .55 | .63 | .59 | .90 | 1.14 | .87 | .63 | 1.05 | 2.21 | 3.32 | 1.13 | 1.86 | 1.57 |
| $Al_2O_3$ | 15.39 | 15.49 | 15.44 | 16.99 | 12.72 | 14.42 | 17.41 | 15.5 | 15.21 | 13.66 | 15.35 | 14.59 | 16.00 |
| TOTAL Fe as FeO | 8.58 | 8.58 | 8.58 | 10.78 | 10.08 | 10.22 | 7.08 | 11.30 | 9.90 | 11.75 | 8.19 | 8.22 | 9.60 |
| MgO | 7.66 | 7.15 | 7.41 | 8.76 | 5.67 | 5.81 | 4.35 | 6.85 | 4.18 | 4.55 | 8.94 | 7.90 | 4.18 |
| CaO | 7.51 | 8.52 | 8.02 | 8.24 | 10.60 | 10.61 | 4.81 | 7.65 | 8.64 | 6.89 | 8.24 | 6.89 | 8.64 |
| $Na_2O$ | 4.00 | 5.82 | 4.96 | .73 | 4.34 | 3.25 | 5.03 | 3.35 | 4.97 | 4.93 | 3.55 | 5.20 | 4.97 |
| $K_2O$ | .85 | .49 | .72 | .12 | .18 | 1.23 | 2.62 | .45 | .34 | .75 | .07 | .04 | .34 |

P.S. = Average of fifty-one patchy spilites from the Virgin Island Core (St. John).

N.S. = Average of twelve non-patchy spilites from the Virgin Island Core (St. John).

T.S. = Average of sixty-three patchy and non-patchy spilites from the Virgin Island Core (St. John).

B. = Average of eight Brecciated spilitic rocks from the Virgin Island Core (St. John).

TABLE 10 -- AVERAGE OF PARTIAL CHEMICAL ANALYSIS OF

SPILITE AND DIKE ROCKS FROM VARIOUS LOCALITIES. (CONT'D)

A.D. = Average of fourteen andesine-diabase dike rocks from the Virgin Island Core (St. John).

Al.D.= Average of four albite-diabase dike rocks from the Virgin Island Core (St. John).

A.P. = Average of three amphibole porphyry dike rocks from the Virgin Island Core (St. John).

D. = Average of four spilites from Concordia Bay (St. John), Virgin Island, (Donnelly, 1966).

W. = Average spilites of Wells (1923).

S. = Average spilites of Sundius (1930).

M.V. = Average analyses of five greenstones from the Mid-Atlantic Ridge (Melson and VanAndel, 1966).

C.V. = One spilite pseudomorphous after variolitic basalt from the Carlsberg Ridge, Indian Ocean, (Cann and Vine, 1967).

Vl. = Average of ninety-two spilites of Vallance (1960).

TABLE 11 -- PARTIAL CHEMICAL ANALYSIS OF SPILITES AND BRECCIATED ROCKS FROM THE CORE. (ST. JOHN, VIRGIN ISLAND).

| SAMPLE DEPTHS IN THE CORE | $SiO_2$ | $Al_2O_3$ | $TiO_2$ | Fe as FeO | MgO | CaO | $Na_2O$ | $K_2O$ | MnO |
|---|---|---|---|---|---|---|---|---|---|
| 26 | 44.51 | 18.43 | .97 | 10.50 | 10.30 | 7.40 | 1.43 | 1.00 | .18 |
| 60 | 51.60 | 13.82 | .55 | 7.50 | 8.85 | 7.25 | 2.70 | .70 | .14 |
| 84 | 55.69 | 13.53 | .45 | 5.45 | 5.00 | 13.70 | 1.85 | .11 | .23 |
| 92 | 50.71 | 17.60 | .57 | 7.55 | 8.40 | 3.10 | 5.00 | .19 | .15 |
| 101 | 45.10 | 16.92 | .64 | 11.55 | 13.25 | 2.25 | 4.05 | .11 | .18 |
| 110 | 53.21 | 13.27 | .67 | 9.25 | 11.10 | 2.35 | 1.20 | 1.18 | .18 |
| 140 | 56.90 | 14.72 | .42 | 7.00 | 8.15 | 7.30 | 1.80 | .54 | .12 |
| 150 | 56.80 | 13.75 | .50 | 7.35 | 7.80 | 6.40 | 3.95 | .34 | .13 |
| 163 | 60.13 | 13.94 | .39 | 6.25 | 5.15 | 6.22 | 3.90 | 1.78 | .12 |
| 173 | 46.60 | 13.60 | .76 | 9.21 | 8.53 | 10.90 | 4.85 | .84 | .22 |
| 234 | 52.21 | 16.00 | .56 | 7.50 | 8.35 | 9.60 | 4.65 | 1.50 | .20 |
| 242 | 53.30 | 14.75 | .50 | 9.37 | 3.55 | 9.60 | 2.55 | .81 | .14 |

TABLE 11 -- PARTIAL CHEMICAL ANALYSIS OF SPILITES AND BRECCIATED ROCKS FROM THE CORE. (ST. JOHN, VIRGIN ISLAND). (CONT'D)

| SAMPLE DEPTHS IN THE CORE | $SiO_2$ | $Al_2O_3$ | $TiO_2$ | Fe as FeO | MgO | CaO | $Na_2O$ | $K_2O$ | MnO |
|---|---|---|---|---|---|---|---|---|---|
| 251 | 53.49 | 15.25 | .43 | 8.15 | 7.3 | 6.70 | 4.80 | .99 | .12 |
| 258 | 53.20 | 16.63 | .66 | 8.50 | 8.30 | 6.60 | 2.30 | .77 | .16 |
| 264 | 47.80 | 16.25 | .56 | 10.86 | 9.95 | 5.70 | 2.45 | .75 | .17 |
| 271 | 45.00 | 15.69 | .51 | 7.97 | 5.97 | 9.50 | 4.95 | .98 | .10 |
| 281 | 53.68 | 15.00 | .54 | 8.65 | 5.95 | 4.87 | 4.60 | .39 | .14 |
| 297 | 52.23 | 15.70 | .38 | 5.30 | 7.92 | 3.35 | 5.45 | 1.25 | .13 |
| 302 | 45.10 | 14.45 | .42 | 14.55 | 7.70 | 8.25 | 6.35 | .16 | .13 |
| 316 | 53.70 | 14.83 | .46 | 7.33 | 7.18 | 7.25 | 6.60 | .13 | .16 |
| 345 | 47.20 | 17.50 | .49 | 10.15 | 5.60 | 9.20 | 5.45 | .46 | .13 |
| 349 | 50.60 | 15.76 | .44 | 8.55 | 4.60 | 7.60 | 5.85 | .99 | .14 |
| 358 | 54.45 | 15.25 | .53 | 9.45 | 6.00 | 10.25 | 3.32 | .13 | .18 |
| 373 | 49.98 | 15.00 | .52 | 8.88 | 4.50 | 6.65 | 5.90 | .63 | .19 |

TABLE 11 -- PARTIAL CHEMICAL ANALYSIS OF SPILITES AND BRECCIATED ROCKS FROM THE CORE. (ST. JOHN, VIRGIN ISLAND). (CONT'D)

| SAMPLE DEPTHS IN THE CORE | $SiO_2$ | $Al_2O_3$ | $TiO_2$ | Fe as FeO | MgO | CaO | $Na_2O$ | $K_2O$ | MnO |
|---|---|---|---|---|---|---|---|---|---|
| 379 | 46.70 | 17.23 | .63 | 11.20 | 8.90 | 7.25 | 1.80 | 1.55 | .22 |
| 396 | 47.90 | 15.43 | .68 | 10.72 | 7.10 | 7.40 | 3.10 | .39 | .19 |
| 406 | 51.94 | 15.05 | .48 | 9.42 | 7.30 | 5.14 | 3.55 | .63 | .13 |
| 417 | 50.22 | 15.56 | .58 | 9.25 | 7.30 | 7.15 | 3.56 | 1.51 | .14 |
| 425 | 45.60 | 16.04 | .48 | 9.80 | 8.25 | 6.87 | 5.70 | 2.04 | .16 |
| 437 | 49.90 | 16.22 | .53 | 9.72 | 8.70 | 6.54 | 3.90 | 1.22 | .13 |
| 446 | 53.50 | 13.17 | .56 | 7.87 | 6.50 | 5.95 | 3.75 | 1.89 | .13 |
| 454 | 48.97 | 15.59 | .61 | 8.80 | 7.80 | 5.00 | 3.73 | .93 | .14 |
| 473 | 51.22 | 13.92 | .54 | 6.80 | 6.10 | 9.75 | 4.70 | .76 | .12 |
| 503 | 47.10 | 16.39 | .74 | 10.13 | 10.00 | 8.25 | 3.65 | 1.36 | .14 |
| 521 | 46.13 | 15.23 | .50 | 8.00 | 5.70 | 10.25 | 5.80 | 1.61 | .18 |
| 542 | 46.20 | 14.21 | .56 | 8.77 | 7.71 | 10.10 | 2.35 | .89 | .18 |

TABLE 11 -- PARTIAL CHEMICAL ANALYSIS OF SPILITES AND BRECCIATED ROCKS FROM THE CORE. (ST. JOHN, VIRGIN ISLAND). (CONT'D)

| SAMPLE DEPTHS IN THE CORE | $SiO_2$ | $Al_2O_3$ | $TiO_2$ | Fe as FeO | MgO | CaO | $Na_2O$ | $K_2O$ | MnO |
|---|---|---|---|---|---|---|---|---|---|
| 560 | 46.90 | 15.25 | .34 | 6.65 | 6.85 | 10.80 | 3.67 | .78 | .18 |
| 564 | 44.28 | 16.75 | .72 | 11.07 | 8.50 | 7.60 | 4.00 | .54 | .20 |
| 573 | 46.73 | 14.00 | .55 | 7.10 | 8.55 | 9.05 | 1.85 | 1.55 | .18 |
| 581 | 40.90 | 15.89 | .61 | 9.80 | 9.45 | 10.20 | 1.60 | 1.05 | .19 |
| 590 | 44.20 | 12.98 | .47 | 7.55 | 7.60 | 9.50 | 3.57 | 1.50 | .19 |
| 592 | 47.69 | 15.19 | .79 | 9.12 | 7.60 | 7.00 | 2.75 | .37 | .20 |
| 596 | 53.20 | 15.71 | .59 | 7.90 | 6.80 | 4.99 | 5.75 | .45 | .14 |
| 604 | 49.63 | 17.35 | .67 | 8.75 | 9.30 | 6.00 | 2.60 | .58 | .19 |
| 607 | 43.00 | 15.70 | .74 | 7.38 | 9.40 | 9.70 | 3.25 | .95 | .21 |
| 632 | 42.69 | 15.18 | .65 | 8.80 | 8.75 | 9.50 | 4.25 | 1.93 | .19 |
| 654 | 43.10 | 15.18 | .57 | 9.15 | 7.60 | 8.90 | 6.60 | .31 | .22 |
| 665 | 49.63 | 14.45 | .49 | 6.95 | 4.30 | 9.90 | 4.85 | .63 | .18 |

TABLE 11 -- PARTIAL CHEMICAL ANALYSIS OF SPILITES AND BRECCIATED ROCKS FROM THE CORE. (ST. JOHN, VIRGIN ISLAND). (CONT'D)

| SAMPLE DEPTHS IN THE CORE | $SiO_2$ | $Al_2O_3$ | $TiO_2$ | Fe as FeO | MgO | CaO | $Na_2O$ | $K_2O$ | MnO |
|---|---|---|---|---|---|---|---|---|---|
| 668 | 43.10 | 17.65 | .47 | 8.92 | 8.80 | 8.45 | 5.65 | .16 | .22 |
| 673 | 50.05 | 16.00 | .64 | 9.65 | 8.30 | 4.25 | 4.50 | .96 | .24 |
| | | | | NON-PATCHY SPILITE | | | | | |
| 707 | 50.05 | 15.03 | .67 | 8.00 | 8.50 | 11.15 | 5.75 | .48 | .26 |
| 724 | 46.43 | 16.56 | .88 | 10.32 | 9.65 | 4.19 | 6.45 | .48 | .23 |
| 742 | 47.73 | 15.37 | .64 | 7.95 | 4.90 | 13.55 | 5.80 | .58 | .16 |
| 751 | 46.43 | 14.30 | .53 | 6.50 | 6.90 | 10.60 | 6.00 | .96 | .23 |
| 761 | 48.11 | 14.97 | .58 | 10.55 | 6.00 | 8.55 | 6.45 | .48 | .17 |
| 769 | 46.11 | 15.50 | .59 | 8.05 | 8.00 | 10.00 | 5.90 | .48 | .23 |
| 786 | 46.90 | 15.23 | .57 | 7.05 | 5.57 | 10.90 | 7.74 | .48 | .26 |
| 798 | 44.00 | 15.35 | .67 | 9.50 | 10.50 | 4.35 | 3.90 | .39 | .25 |
| 802 | 52.59 | 16.34 | .62 | 7.04 | 3.80 | 6.85 | 6.95 | .16 | .10 |

TABLE 11 -- PARTIAL CHEMICAL ANALYSIS OF SPILITES AND BRECCIATED ROCKS FROM THE CORE. (ST. JOHN, VIRGIN ISLAND). (CONT'D)

| SAMPLE DEPTHS IN THE CORE | $SiO_2$ | $Al_2O_3$ | $TiO_2$ | Fe as FeO | MgO | CaO | $Na_2O$ | $K_2O$ | MnO |
|---|---|---|---|---|---|---|---|---|---|
| 808 | 48.40 | 15.65 | .92 | 9.55 | 5.65 | 4.25 | 6.63 | .45 | .19 |
| 824 | 45.61 | 16.56 | .58 | 9.15 | 9.30 | 7.35 | 4.30 | .48 | .24 |
| 833 | 45.25 | 15.10 | .60 | 9.25 | 7.55 | 10.40 | 3.95 | .31 | .17 |
| | | | | BRECCIATED ZONE | | | | | |
| 1012 | 45.70 | 15.33 | 1.31 | 11.80 | 4.30 | 12.20 | 2.40 | .15 | .24 |
| 1028 | 42.50 | 18.20 | 1.03 | 11.15 | 10.20 | 13.25 | .05 | .19 | .27 |
| 1044 | 48.91 | 12.11 | .79 | 8.60 | 6.84 | 11.55 | .35 | .06 | .21 |
| 1045 | 51.82 | 14.09 | .79 | 11.75 | 8.90 | 9.80 | .10 | .06 | .25 |
| 1060 | 48.32 | 11.02 | .69 | 11.07 | 7.20 | 12.65 | 1.05 | .06 | .20 |
| R 1066 | 48.12 | 16.07 | .73 | 9.50 | 8.55 | 5.60 | 3.60 | .06 | .23 |
| 1074 | 57.20 | 17.85 | 1.26 | 6.28 | 3.30 | 11.50 | .04 | .06 | .16 |
| $R_1$ 1101 | 56.75 | 17.00 | .62 | 6.91 | 3.15 | 9.50 | 3.85 | .06 | .14 |

TABLE 11 -- PARTIAL CHEMICAL ANALYSIS OF SPILITES AND BRECCIATED ROCKS FROM THE CORE. (ST. JOHN, VIRGIN ISLAND). (CONT'D)

| SAMPLE DEPTHS IN THE CORE | $SiO_2$ | $Al_2O_3$ | $TiO_2$ | Fe as FeO | MgO | CaO | $Na_2O$ | $K_2O$ | MnO |
|---|---|---|---|---|---|---|---|---|---|
| 1129 | 44.80 | 16.82 | .80 | 10.97 | 10.65 | 7.05 | .43 | .06 | .17 |
| 1131 | 43.80 | 14.87 | .95 | 11.07 | 15.15 | 6.15 | .07 | .06 | .13 |
| 1147 | 46.60 | 16.60 | .85 | 9.82 | 6.35 | 6.47 | 1.40 | .09 | .14 |

R = Relic of Spilitic Rock rich in epidote.

$R_1$ = Relic of Amphibole Pseudomorphs Bearing Rocks.

TABLE 12 -- PARTIAL CHEMICAL ANALYSIS OF THE DARK PATCHES AND THE GREEN MATRIX OF THE SPILITE FROM THE CORE. (ST. JOHN, VIRGIN ISLAND).

| SAMPLE DEPTHS IN THE CORE | $SiO_2$ | $Al_2O_3$ | $TiO_2$ | Fe as FeO | MgO | CaO | $Na_2O$ | $K_2O$ | MnO |
|---|---|---|---|---|---|---|---|---|---|
| D 119 | 52.23 | 15.53 | .51 | 8.45 | 9.70 | 3.05 | 1.95 | 3.61 | .15 |
| G 119 | 47.10 | 13.47 | .56 | 10.73 | 10.10 | 9.80 | .10 | 2.59 | .24 |
| D 134 | 38.93 | 16.28 | .46 | 12.28 | 12.80 | 6.70 | 1.90 | .39 | .24 |
| G 134 | 36.30 | 16.12 | .66 | 11.07 | 10.80 | 12.60 | .40 | .13 | .28 |
| D 163 | 51.80 | 14.84 | .37 | 6.35 | 8.00 | 5.70 | 3.65 | 1.21 | .12 |
| G 163 | 46.13 | 13.60 | .34 | 9.72 | 11.80 | 8.45 | 2.85 | .26 | .19 |
| D 236 | 51.70 | 17.38 | .79 | 11.50 | 8.83 | 7.80 | 4.05 | .16 | .21 |
| G 236 | 47.50 | 16.00 | .95 | 12.50 | 10.70 | 8.60 | 1.85 | .26 | .19 |
| D 258 | 51.70 | 14.00 | .39 | 7.90 | 6.55 | 9.00 | 3.65 | .46 | .12 |
| G 258 | 51.22 | 16.25 | .56 | 10.10 | 8.85 | 8.75 | 1.50 | .58 | .16 |

TABLE 12 -- PARTIAL CHEMICAL ANALYSIS OF THE DARK PATCHES AND THE GREEN MATRIX OF THE SPILITE FROM THE CORE. (ST. JOHN, VIRGIN ISLAND). (CONT'D)

| SAMPLE DEPTHS IN THE CORE | $SiO_2$ | $Al_2O_3$ | $TiO_2$ | Fe as FeO | MgO | CaO | $Na_2O$ | $K_2O$ | MnO |
|---|---|---|---|---|---|---|---|---|---|
| D 325 | 57.22 | 11.32 | .39 | 9.80 | 8.00 | 5.45 | 4.95 | .58 | .12 |
| G 325 | 45.90 | 17.35 | .77 | 10.75 | 10.45 | 3.81 | 4.10 | .52 | .18 |
| D 345 | 49.90 | 16.78 | .38 | 9.30 | 8.92 | 5.45 | 7.15 | .52 | .16 |
| G 345 | 47.90 | 16.79 | .72 | 9.95 | 9.25 | 7.70 | 4.60 | .46 | .17 |
| D 379 | 43.30 | 15.76 | .37 | 13.70 | 15.32 | 7.10 | 3.30 | 1.37 | .18 |
| G 379 | 45.79 | 17.55 | .60 | 8.80 | 15.84 | 5.68 | 3.05 | 2.15 | .20 |
| D 406 | 51.60 | 12.58 | .34 | 10.50 | 7.30 | 5.75 | 4.65 | .39 | .12 |
| G 406 | 48.68 | 14.95 | .43 | 9.00 | 8.30 | 5.80 | 5.20 | 1.08 | .13 |
| D 439 | 42.91 | 13.84 | .37 | 10.60 | 7.90 | 6.78 | 2.85 | .53 | .12 |
| G 439 | 49.48 | 19.35 | .37 | 5.85 | 4.95 | 10.00 | 2.65 | 1.01 | .11 |

TABLE 12 -- PARTIAL CHEMICAL ANALYSIS OF THE DARK PATCHES AND THE GREEN MATRIX OF THE SPILITE FROM THE CORE. (ST. JOHN, VIRGIN ISLAND). (CONT'D)

| SAMPLE DEPTHS IN THE CORE | $SiO_2$ | $Al_2O_3$ | $TiO_2$ | Fe as FeO | MgO | CaO | $Na_2O$ | $K_2O$ | MnO |
|---|---|---|---|---|---|---|---|---|---|
| D 446 | 44.25 | 15.54 | .49 | 8.32 | 4.00 | 13.65 | 3.80 | .81 | .09 |
| G 446 | 53.50 | 15.20 | .67 | 9.28 | 9.87 | 6.02 | 4.45 | 2.82 | .10 |
| D 515 | 49.40 | 15.20 | .37 | 9.75 | 4.55 | 10.80 | 4.95 | .68 | .12 |
| G 515 | 51.54 | 14.43 | .52 | 9.00 | 7.80 | 9.95 | 4.10 | .82 | .17 |
| D 535 | 56.00 | 14.43 | .37 | 6.30 | 4.15 | 12.10 | 3.10 | .45 | .09 |
| G 535 | 44.67 | 12.76 | .45 | 6.65 | 5.90 | 13.20 | 1.70 | 1.67 | .16 |
| D 569 | 52.57 | 16.30 | .49 | 6.55 | 5.70 | 10.40 | 4.50 | 1.33 | .12 |
| G 569 | 48.81 | 11.35 | .52 | 6.10 | 6.35 | 8.05 | 2.15 | 1.55 | .15 |
| D 582 | 54.30 | 16.58 | .36 | 8.20 | 8.10 | 5.48 | 3.50 | 1.35 | .12 |
| G 582 | 49.00 | 13.92 | .56 | 5.70 | 6.40 | 7.25 | 2.05 | 2.25 | .14 |

TABLE 12 -- PARTIAL CHEMICAL ANALYSIS OF THE DARK PATCHES AND THE GREEN MATRIX OF THE SPILITE FROM THE CORE. (ST. JOHN, VIRGIN ISLAND). (CONT'D)

| SAMPLE DEPTHS IN THE CORE | $SiO_2$ | $Al_2O_3$ | $TiO_2$ | Fe as FeO | MgO | CaO | $Na_2O$ | $K_2O$ | MnO |
|---|---|---|---|---|---|---|---|---|---|
| D 607 | 53.06 | 16.77 | .36 | 7.72 | 7.30 | 6.65 | 3.75 | .84 | .12 |
| G 607 | 51.26 | 15.18 | .52 | 6.70 | 7.40 | 7.80 | 4.10 | 1.14 | .15 |
| D 624 | 52.00 | 15.70 | .37 | 7.00 | 8.43 | 4.40 | 4.95 | .63 | .12 |
| G 624 | 48.30 | 15.00 | .40 | 6.65 | 10.80 | 7.83 | 2.95 | .50 | .18 |
| D 634 | 46.50 | 17.55 | .61 | 9.62 | 9.30 | 5.55 | 3.75 | 1.26 | .15 |
| G 634 | 48.91 | 16.15 | .72 | 7.95 | 8.40 | 3.95 | 2.60 | 1.79 | .14 |

D = Dark patch.

G = Green matrix.

TABLE 13 -- PARTIAL CHEMICAL ANALYSIS OF DIKE ROCKS FROM THE CORE. (ST. JOHN, VIRGIN ISLAND).

| SAMPLE DEPTHS IN THE CORE | $SiO_2$ | $Al_2O_3$ | $TiO_2$ | Fe as FeO | MgO | CaO | $Na_2O$ | $K_2O$ | MnO |
|---|---|---|---|---|---|---|---|---|---|
| | | | | AMPHIBOLE PORPHYRY | | | | | |
| 129 | 51.82 | 18.08 | .60 | 8.15 | 4.20 | 6.30 | 4.85 | 2.70 | .09 |
| 134 | 61.14 | 16.29 | .42 | 4.90 | 3.45 | 2.85 | 5.10 | 4.20 | .10 |
| 732 | 52.59 | 17.88 | .84 | 8.20 | 5.40 | 5.58 | 5.15 | .96 | .17 |
| | | | | ALBITE DIABASE | | | | | |
| 177 | 47.57 | 15.31 | .69 | 10.16 | 5.30 | 8.69 | 3.45 | .89 | .19 |
| 192 | 50.93 | 14.95 | 1.02 | 10.55 | 5.40 | 10.30 | 3.10 | .84 | .19 |
| 220 | 50.60 | 15.83 | .90 | 10.90 | 5.05 | 10.80 | 3.50 | .72 | .18 |
| 226 | 49.99 | 15.10 | .88 | 9.25 | 7.50 | 9.65 | 2.95 | 2.50 | .18 |
| | | | | ANDESINE DIABASE | | | | | |
| 847 | 49.61 | 14.88 | 1.44 | 12.05 | 6.45 | 7.65 | 5.36 | .16 | .21 |
| 862 | 44.10 | 15.68 | 1.41 | 12.50 | 5.15 | 9.65 | 3.50 | .19 | .20 |

TABLE 13 -- PARTIAL CHEMICAL ANALYSIS OF DIKE ROCKS

FROM THE CORE. (ST. JOHN, VIRGIN ISLAND). (CONT'D)

| SAMPLE DEPTHS IN THE CORE | $SiO_2$ | $Al_2O_3$ | $TiO_2$ | Fe as FeO | MgO | CaO | $Na_2O$ | $K_2O$ | MnO |
|---|---|---|---|---|---|---|---|---|---|
| 872 | 51.80 | 15.71 | .92 | 10.00 | 3.30 | 10.30 | 4.75 | .31 | .19 |
| 879 | 49.95 | 15.88 | 1.16 | 8.46 | 4.60 | 8.95 | 4.20 | .06 | .20 |
| 891 | 51.80 | 15.30 | 1.28 | 10.15 | 4.27 | 10.40 | 1.55 | .16 | |
| | | | | ANDESINE DIABASE | | | | | |
| 895 | 49.10 | 15.08 | 1.44 | 12.30 | 5.30 | 10.20 | 4.10 | .31 | .25 |
| 905 | 51.41 | 13.84 | 1.33 | 11.15 | 3.30 | 13.00 | 4.23 | .16 | .20 |
| 909 | 53.90 | 16.08 | .99 | 9.80 | 3.20 | 6.95 | 5.90 | .39 | .18 |
| 921 | 50.00 | 16.10 | 1.29 | 11.75 | 6.37 | 6.95 | 3.55 | .19 | .20 |
| 936 | 51.00 | 15.54 | .96 | 9.25 | 3.95 | 10.95 | 4.30 | .16 | .19 |
| 945 | 51.26 | 11.52 | .98 | 9.45 | 6.10 | 10.15 | 4.98 | .06 | .18 |
| 965 | 51.19 | 14.10 | .99 | 9.35 | 5.00 | 12.58 | 4.60 | .19 | .19 |
| 980 | 51.00 | 14.06 | 1.24 | 11.86 | 3.90 | 12.00 | 3.85 | .13 | .20 |

TABLE 13 -- PARTIAL CHEMICAL ANALYSIS OF DIKE ROCKS

FROM THE CORE. (ST. JOHN, VIRGIN ISLAND). (CONT'D)

| SAMPLE DEPTHS IN THE CORE | $SiO_2$ | $Al_2O_3$ | $TiO_2$ | Fe as FeO | MgO | CaO | $Na_2O$ | $K_2O$ | MnO |
|---|---|---|---|---|---|---|---|---|---|
| 985 | 70.91 | 10.85 | .46 | 4.00 | 2.80 | 5.25 | 3.40 | .13 | .11 |
| 1003 | 49.20 | 15.58 | 1.41 | 12.10 | 8.21 | 9.18 | 3.20 | .13 | .25 |

TABLE 14 -- CHEMICAL COMPARISON BETWEEN OCEANIC BASALTS, SPILITIC ROCKS AND AMPHIBOLITES.

| | 60 | 71 | 26 |
|---|---|---|---|
| $SiO_2$ | 49.19 | 47.43 | 48.94 |
| $TiO_2$ | 1.54 | .74 | 1.95 |
| $Al_2O_3$ | 15.92 | 16.21 | 16.73 |
| Total iron vs. FeO | 9.81 | 9.58 | 13.13 |
| CaO | 10.72 | 8.33 | 8.84 |
| MgO | 7.88 | 8.12 | 7.60 |
| $Na_2O$ | 2.96 | 2.84 | 3.98 |
| $K_2O$ | .24 | .42 | .72 |

60 = Average of sixty oceanic basalts dredged from the Mid-Oceanic Ridges in the Atlantic and Indian Oceans. (Hekinian 1968).

71 = Average of sixty three spilite and twelve brecciated spilitic rocks from the core. (St. John, Virgin Island).

26 = Average of twenty six ortho-amphibolite from Connemara, Ireland (Evans and Leake (1960).